FORMULATION, OPTIMIZATION, AND EVALUATION OF RIVASTIGMINE TARTRATE LOADED SOLID LIPID NANOPARTICLE BY MICROEMULSION TECHNIQUE

A Dissertation Submitted to

THE TAMIL NADU DR. M.G.R. MEDICAL UNIVERSITY

CHENNAI – 600032

In partial fulfilment of the requirements for the award of the Degree of

MASTER OF PHARMACY
IN
PHARMACEUTICS

Submitted by

NITHISH. K

(Reg. No. 261810902)

Under the guidance of

DR. J. PADMAPREETHA., M. Pharm., Ph. D.,

Department of Pharmaceutics

KMCH COLLEGE OF PHARMACY

KOVAI ESTATE, KALAPPATTI ROAD

COIMBATORE - 641048

APRIL 2020

PROF. DR. A. RAJASEKARAN, M. Pharm., Ph.D.,

Principal,

KMCH College of Pharmacy,

Kovai Estate, Kalappatti Road,

Coimbatore – 641048

CERTIFICATE

This is to certify that the dissertation work entitled **"FORMULATION, OPTIMIZATION, AND EVALUATION OF RIVASTIGMINE TARTRATE LOADED SOLID LIPID NANOPARTICLE BY MICROEMULSION TECHNIQUE"** was carried out by **Mr. NITHISH.K (Reg. No. 261810902).** The work mentioned in the dissertation was carried out at the Department of Pharmaceutics, KMCH College of Pharmacy, Coimbatore, Tamil Nadu, under the guidance of **DR. J. PADMAPREETHA., M. Pharm., Ph. D.,** for the partial fulfilment for the Degree of Master of Pharmacy during the academic year 2019-2020.

Date: **Prof. DR. A. RAJASEKARAN, M. Pharm., Ph.D.,**

Place: Coimbatore **PRINCIPAL**

DR. J. PADMAPREETHA., M. Pharm., Ph. D.,
Associate Professor,
KMCH College of Pharmacy,
Kovai Estate, Kalapatti Road,
Coimbatore - 641 048

CERTIFICATE

This is to certify that the research work entitled **"FORMULATION, OPTIMIZATION, AND EVALUATION OF RIVASTIGMINE TARTRATE LOADED SOLID LIPID NANOPARTICLE BY MICROEMULSION TECHNIQUE"** was carried out by **Mr. NITHISH.K (Reg. No. 261810902).** The work mentioned in the dissertation was carried out at the Department of Pharmaceutics, KMCH College of Pharmacy, Coimbatore, Tamil Nadu, under my supervision and guidance for the partial fulfilment for the Degree of Master of Pharmacy during the academic year 2019-2020.

Date: **DR. J. PADMAPREETHA., M. Pharm.,Ph. D.,**

Place: Coimbatore

DECLARATION

I hereby declare that the dissertation work **"FORMULATION, OPTIMIZATION, AND EVALUATION OF RIVASTIGMINE TARTRATE LOADED SOLID LIPID NANOPARTICLE BY MICROEMULSION TECHNIQUE"** submitted to The Tamil Nadu Dr. M.G.R. Medical University, Chennai, in partial fulfilment for the Degree of **Master of Pharmacy** in **Pharmaceutics** was carried out under the guidance of **DR. J. PADMAPREETHA., M. Pharm., Ph. D.,** at the Department of Pharmaceutics, KMCH College of Pharmacy, Coimbatore, Tamil Nadu during the academic year 2019-2020.

This research work either in part or full does not constitute any of other thesis / dissertation.

Date: **NITHISH. K**

Place: Coimbatore (**Reg. No. 261810902)**

EVALUATION CERTIFICATE

This is to certify that the research work entitled **"FORMULATION, OPTIMIZATION, AND EVALUATION OF RIVASTIGMINE TARTRATE LOADED SOLID LIPID NANOPARTICLE BY MICROEMULSION TECHNIQUE"** was carried out by **Mr. NITHISH.K (Reg. No. 261810902).** To The Tamil Nadu Dr. M.G.R. Medical University, Chennai, in the partial fulfilment for the Degree of **Master of Pharmacy** at the Department of Pharmaceutics, is a bonafide work carried out by the candidate at KMCH College of Pharmacy, Coimbatore, Tamil Nadu during the academic year 2019-2020 and the same was evaluated.

Examination Centre: KMCH College of Pharmacy, Coimbatore

Date:

Internal Examiner **External Examiner**

Convener of Examination

Dedicated to Almighty,

My Beloved Parents,

Sister & Friends

ACKNOWLEDGEMENT

It would not have been possible to write my thesis without the help and support of the kind people around me, who made it possible with their ideas, encouragement and helping mentality directly or indirectly.

Above all, it is the supreme power, the ***God Almighty*** who strengthens and guided me to complete my thesis work within the stipulated time.

It is my pleasure to express my deep sense of thanks to my mentor, philosopher and above all my guide **DR. J. PADMAPREETHA., M. Pharm., Ph. D.,** Associate professor, Department of Pharmaceutics. His timely advice and scientific approach have helped me to a very great extent to fulfill this task.

I am grateful to express my sincere thanks to **DR. K.S.G. Arulkumaran, M. Pharm., Ph.D., HOD,** Department of Pharmaceutics. His support and encourage helped me to complete my work.

I would like to express my gratitude to **Chairman Dr. Nalla G. Palaniswami,** and **Managing Trustee Dr. Thavamani D. Palaniswami**, for providing the necessities required to finish my project work successfully.

I owe a deep sense of obligation to **Dr. A. Rajasekaran, M. Pharm, Ph.D., Principal,** KMCH College of Pharmacy for his suggestions, encouragement and support throughout my work. His prompt inspirations, timely suggestions have enabled me to conclude the work fruitfully.

I extent my heartfelt thanks to **Miss. Gayathri, M.Pharm, DR. N. Tamilselvan, M. Pharm., Ph.D., Mr. S. Muthukumar, M.Pharm, & DR. K. Selvaraju, M.Pharm, Ph.D.,** for their invaluable support and encouragement in completing my project successfully.

I am thankful to lab technicians **Miss. Jeeva, Miss. V. Sridevi, Mrs. Kamalaveni, Mrs. Akila, Mrs. Selvi,** and **Mrs. Sudha & Mr. Arjun** , computer lab technicians, library staffs and all those who have co-operated with me during my project work.

I would like to express my thanks to **Mohini organics private limited, Mumbai** for their help in my work.

It was a pleasure to share my master studies and life with wonderful people. I am greatly indebted to all of my classmates – **Sumitha, Sundarajan, Baskar, Sridevi** and batch mates – **Anu, Anitta, Jinu, Haritha, Dharshan, Rajesh, Balamurugan, Pavithra , Maharaja, Anjala Devi, Nithyakala, Palanichamy** without their appreciation that has willingly helped me out with their abilities, this work might not come out in the shortest time. I pay my sincere thanks to them.

I profusely acknowledge all my seniors **Treesa, Arya, Vishali, Reshma, Keerthana, Nayanthara, Nijathan, Suresh, Raj, Nivetha, Henna, Solly, Nishanth,** for the advice, affection and encouragement throughout this journey.

It gives me immense pleasure to express my heartfelt gratitude and love to my juniors **Shreya, Shalabha, Madhan, Hamesh, Sujithara, Kowsalya, Manimekalai, Kavin, Amar, Mani, Yogesh, Mani, Nazeeb** and all other juniors for the advice, affection and encouragement throughout this journey.

I am highly obliged in taking the opportunity to sincerely thank my friends the lifeline**, Prabha, Sudha, Mouli, Azar, Moni, Shine, John, Frank, Finny, Suvedhan** who all have cooperated and participated with my happiness, my problems and disappointments and rebuilding my confidence at appropriate stages.

I am grateful to my parents **Mr. Krishna Murthy. N, Mrs. Vijaya. N**, and my sister **Mrs. Chandhini, Mrs. Shivani** for standing beside me in my tough and ease, and guiding me to the right path. I am blessed and grateful for their unconditional love, encouragement and support without which I will not be able to finish up my thesis.

Last but not the least; I thank everyone who was important for the successful completion of this thesis.

NITHISH K

INDEX

LIST OF TABLES

LIST OF FIGURES

LIST OF ABBREVIATIONS

%	Percentage
α	Alpha
ºC	Degree Celsius
AD	Alzheimer's disease
BBB	Blood Brain Barrier
CCD	Central Composite Design
CMAs	Critical Material Attributes
Cmax,	Maximum Concentration
CPPs	Critical Process parameters
CQAs	Critical Quality attributes
DOE	Design of Expert
DSC	Differential Scanning Calorimetry
EE	Entrapment Efficiency
FTIR	Fourier Transform Infra Red
gm	Gram
GMS	Glyceryl mono stearate
GTS	Glyceryl tri stearate
hr	Hour
HSH	High Speed Homogeniser
m^2/g	Meter square per gram
mg	Milligram
min	Minute
MRT	Mean Residence Time
mV	millivolt
nm	Nanometre
NPS	Nanoparticles
PS	Particle Size
PI	Polydispersity index
QbD	Quality by Design
QTPP	Quality Target Product Profile
rpm	revolution per minute
RT	Rivastigmine Tartrate

SEM	Scanning Electron Microscopy
SLN	Solid Lipid Nanoparticle
$t_{1/2}$	Half life
TEM	Transmission Electron Microscopy
USP	United States Pharmacopoeia
UV	Ultra Violet
WHO	World Health Organization
ZP	Zeta potential
λ max	Lambda max (maximum absorption)
µg	Microgram
µl	Microliter

INTRODUCTION

Alzheimer's disease (AD) is a progressive neurodegenerative disease most often characterized by initial memory impairment and cognitive decline that can ultimately affect behavior, speech, visuo-spatial orientation and the motor system. [1] Also typically characterized by its histological findings of neurofibrillary tangles and amyloid plaque, by increased levels of oxidative stress, neuro-inflammation and by greatly reduced levels of acetylcholine. Chiefly identified in its early stages by a decline in recent memory and in it's later by a cognitive decline so profound that its victims lose the abilities, interests, and skills to perform even day to day activities. Long before these final stages, a person with AD can no longer recognize children, spouses, and siblings and lose the personality traits that had characterized them as individuals. These losses together with the appearance of other behavioral problems that include violent behaviors, depression, delirium, various psychoses, and loss of judgment and social skills means that many persons with Alzheimer's disease spend their last years institutionalized and in a mental exile from others.[2]

Alzheimer's disease (AD) and other forms of dementia are a growing public health problem among the elderly people in developed and developing countries, whose aging population is increasing. The aging population size is now bigger for all the countries due to sustainable development in health care system around the globe. AD is epidemic with an estimated 33.9 million people worldwide having the disease. The incidence rate increases exponentially with aging so that at age 90 about 12% of people have AD, but about 40% of those over age 100 have it. Factors that put persons at increased risk of AD are a history of head injury, obesity, histories of smoking, diabetes mellitus, hypertension, renal disease and traumatic brain injury, or depression. Since these factors are occurring more commonly, the incidence of AD may increase even more. Clearly, interventions that prevent, stabilize, remediate, or cure AD are desperately needed. [3]

1. Current Estimation and Future Projection

Alzheimer's disease (AD) is considered to be the most prevalent neurodegenerative disorder in the world. Current census of people affected includes approximately 5.5 million people in the United States and 47 million people worldwide. Thirteen percentage of people older than age 65 years and 45% of those older than age 85 years

have AD, and the prevalence is increasing. It is expected that by 2050, one new case of AD will develop every 33 seconds, amounting to nearly a million new cases per year.

The future predictions are assumed based on the assumption that the prevalence of dementia is stable over time, which may not be true. If there is an increase in the number of older people due to the incidence of dementia or with increasing life expectancy, the prevalence of dementia will increase. In India the number of people with AD and other dementias is increasing every year because of the steady growth in the older population and stable increment in life expectancy. It is estimated that there will be a two fold increase by 2030 and three fold by 2050 can be expected. By the year 2025 UK is estimated to have 1 million people with dementia (Dementia UK Report, 2007). [4]

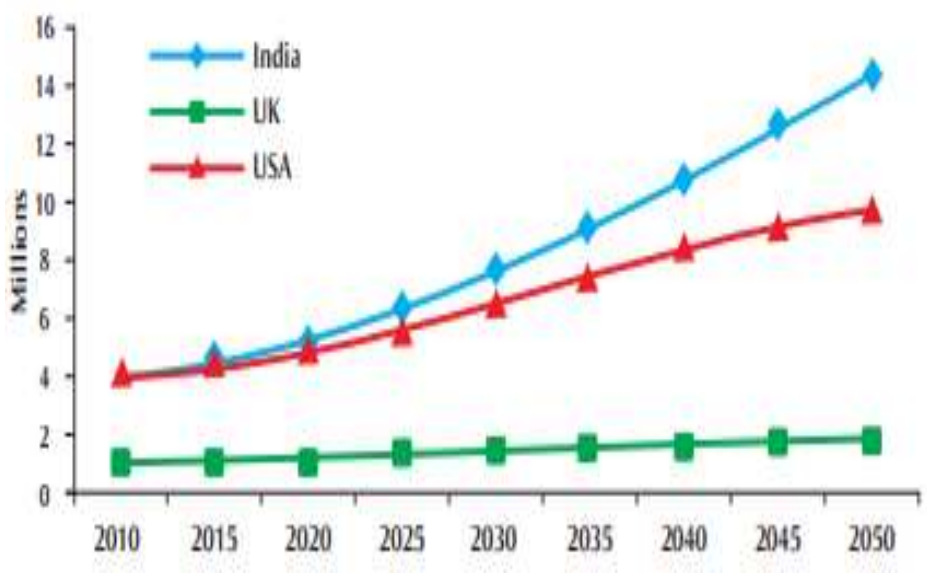

Figure 1: Estimated number of PwD (People with dementia) >60 years in India, UK and USA

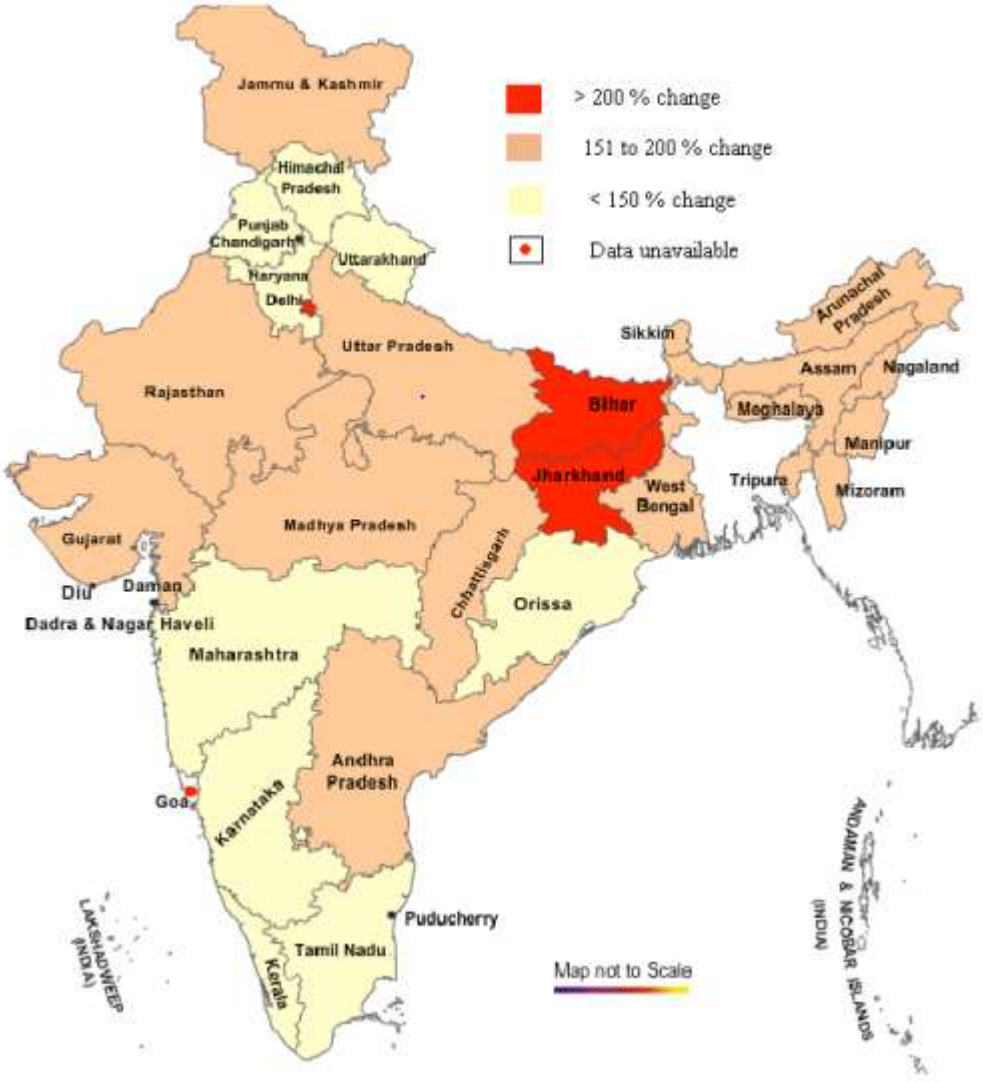

Figure 2: Projected changes between 2006 and 2026 in number of people living with dementia by State

2. PATHOPHYSIOLOGY OF ALZHEIMERS DISEASE

The etiology of AD is still not fully understood. Researchers suggest that signs signifying with AD can be found in the brain 20 or more years before the onset of symptoms. It may be possible that the initial changes in the brain can be compensated. When the changes are no longer reversible, symptoms gradually become significant. Initially cognitive decline occurs followed by memory loss will develop. Basic daily functions are affected in the most serious cases .The most popular hypothesis suggested on the pathophysiology are the amyloid hypothesis and the tau hypothesis.

2.1. Amyloid Hypothesis

The amyloid hypothesis suggests that the pathogenesis of AD is due to the extracellular accumulation and aggregation of Amyloid β (Aβ) peptides in the brain. Aβ is released because of the cleavage of the trans-membrane amyloid precursor protein (APP). The accretion of Aβpeptides leads to a series of neurotoxic issues. It leads to loss of mitochondrial function. It results in mitochondrial damage by localizing mitochondrial membranes and blocking the transport of proteins to mitochondria. It is also reported that Aβ peptides react with metal ions in the brain to produce reactive oxygen species (ROS) resulting in increased oxidative stress. Aβ peptide disrupts calcium homeostasis by changing the concentration of calcium ions and also triggers unregulated flux of calcium through the plasma membrane. At the same time, microglia release inflammatory of 26 mediators such as inflammatory cytokines and chemokines to cause neuro-inflammation due to the microglia activation by Aβ peptides. Production of Aβ peptides leads to neurotoxic responses, while such responses interfere with the metabolism of APP resulting in accumulation of Aβ peptides.

2.2. Tau Protein

According to the amyloid hypothesis, Aβ peptides accumulation initiates hyper phosphorylation of tau protein. Tau protein is a microtubule-associated protein (MAP) that is encoded by the microtubule-associated protein tau (MAPT) gene. It is a highly soluble protein to stabilize microtubules. Tau proteins, which are abundant in neurons of the CNS, exist as six isoforms in brain tissue .In the brain of AD patients, tau is hyper phosphorylated at least three folds (molar ratio) higher than that in the normal brain. The abnormal hyper phosphorylation of tau plays a potent role in neurofibrillary degeneration. During hyper phosphorylation, tau proteins miss fold and accumulate into paired helical filament (PHF) tau and also neurofibrillary tangles (NFTs). NFT may result in neuron degeneration by reducing normal tau function, compromise normal cellular functions and disrupt tau-mediated regulation of microtubule dynamics.

2.3. Others

According to the genome wide association studies (GWAS), there are at least 20 genes that contribute to the AD onset and evolution. Apo lipoprotein E (ApoE)

is one of the best well known genes in AD. ApoE isoforms regulate Aβ aggregation and clearance in the brain and participate in regulating glucose metabolism and neuronal signalling. It can also regulate the integrity of tight junctions and ApoE deficiency can lead to BBB leakage. Other genes that affect the BBB physiology and molecule exchanges across the BBB are ABCA7 gene, they are closely linked to excessive accumulation of amyloid peptides while ABCA7 gene down regulation might affect cholesterol and amyloid exchanges at the BBB.

3. SYMPTOMS OF ALZHEIMERS DISEASE

Alzheimer's disease begins with lapses of memory, difficulty in finding the right words for everyday objects or mood swings. As Alzheimer's progresses, the person may:

- Routine forgetting of recent events, names and faces and difficulty in understanding what is being said.
- Become confused while handling money or driving a car.
- Undergo personality changes
- Experience mood swings

3.1 Memory Loss

Declining memory or short-term memory is the most common early symptom of dementia. People with ordinary forgetfulness may briefly forget their next-door neighbour's name still they know the person they are talking to is their next-door neighbour but person with dementia will not only forget their neighbour's name but also the context.

3.2 Difficulty performing familiar tasks

People with dementia often find it hard to complete everyday tasks like they may not know in what order to put clothes on or the steps for preparing a meal.

3.3 Problems with language

A person with dementia often forgets simple words or substitutes unusual words, making speech or writing hard to understand compared to occasional forgetting in normal people.

3.4 Disorientation to time and place

People with dementia can become lost in familiar places such as the road they live in, forget where they are or how they got there, and not know how to get back home and may also confuse night and day.

3.5 Poor or decreased judgment

People with dementia may, wear several layers of clothes on a warm day or very few on a cold day showing poor judgemental senses.

3.6 Problems with keeping track of things

A person with dementia may find it difficult to follow a conversation or keep up with paying their bills.

3.7 Misplacing things

Anyone can temporarily misplace his or her wallet or keys but a person with dementia may put things in unusual places such as an iron in the fridge etc.

3.8 Changes in mood or behaviour

A person with dementia may experience rapid mood swings for no apparent reason. Alternatively they may show less emotion than was usual previously.

3.9 Changes in personality

A person with dementia may seem different from his or her usual self in ways that are difficult to pinpoint such as they may become suspicious, irritable, depressed, apathetic or anxious and agitated mostly in situations where memory problems are causing difficulties.

3.10 Loss of initiative

At times everyone can become tired of housework, business activities, or social obligations however a person with dementia have the chance of becoming very passive, sitting in front of the television for hours, sleeping more than usual, or appear to lose interest in hobbies.

If you are experiencing any of these symptoms or are concerned about a friend or relative, visit your doctor and discuss your concerns. [5]

4. FDA-approved treatments for Alzheimer's

While there is no cure for Alzheimer's disease, five prescription drugs are currently approved by the U.S. Food and Drug Administration (FDA) to treat the symptoms. Donepezil, galantamine and rivastigmine are from a class of drugs called "cholinesterase inhibitors which prevent the breakdown of a chemical messenger in

the brain that is important for learning and memory. The fourth drug is memantine that regulates the activity of a different chemical messenger in the brain that is also important for learning and memory. The fifth medication is a combination of the cholinesterase inhibitors (donepezil) with memantine.

4.1 At-a-glance treatment chart

Generic	Brand	Approved For	Side Effects
Donepezil	Aricept®	All stages	Nausea, vomiting, loss of appetite, muscle cramp ,increased frequency of bowel movements.
Galantamine	Razadyne®	Mild to moderate	Nausea, vomiting , loss of appetite and increased frequency of bowel movements.
Memantine	Namenda®	Moderate to severe	Headache, constipation, confusion and dizziness.
Rivastigmine	Exelon®	Mild to moderate	Nausea, vomiting, loss of appetite and increased frequency of bowel movements.
memantine + donepezil	Namzaric®	Moderate to severe	Nausea, vomiting, loss of appetite, increased frequency of bowel movements, headache, constipation, confusion and dizziness.

Table 1: FDA approved treatments for Alzheimers

4.2 Cholinesterase inhibitors

Cholinesterase inhibitors are prescribed to treat symptoms related to memory, thinking, language, judgment and other thought processes. Commonly prescribed inhibitors include:

- Donepezil (Aricept®), approved to treat all stages of Alzheimer's disease.
- Galantamine (Razadyne®), approved for mild-to-moderate stages.
- Rivastigmine (Exelon®), approved for mild-to-moderate Alzheimer's as well as mild to moderate dementia associated with Parkinson's disease.

4.2.1 Cholinesterase inhibitors mechanism

Cholinesterase inhibitors work by increasing levels of acetylcholine judgment and other thought processes. Certain brain cells release acetylcholine, which helps deliver messages to other cells. Once a message reaches the receiving cell, various other chemicals break acetylcholine down so it can be recycled.

Alzheimer's disease damages or destroys cells that produce and use acetylcholine, resulting in reduced amount available to carry messages. A cholinesterase inhibitor slows the breakdown of acetylcholine by blocking the activity of acetyl cholinesterase thereby by maintaining acetylcholine levels, the drug may help compensate for the loss of functioning brain cells.

Other benefits of cholinesterase inhibitors includes : Galantamine that stimulate the release of acetylcholine and strengthen the way certain message-receiving nerve cells respond to it and Rivastigmine that block the activity of another enzyme involved in breaking down acetylcholine.

Cholinesterase inhibitors can't reverse Alzheimer's and won't stop the underlying destruction of nerve cells, their ability to improve symptoms eventually declines as brain cell damage progresses.

4.2.2 Benefits of cholinesterase inhibitors

In clinical trials of all three cholinesterase inhibitors, people taking the medications performed better on memory and thinking tests than those taking a placebo, or inactive substance. However, the degree of improvement was small. In

terms of overall effect, cholinesterase inhibitors may delay or slow worsening of symptoms. The effectiveness of cholinesterase inhibitors, as well as how long they are effective, varies from person to person.

Combining the three drugs in fact, would result in greater frequency of side effects. The makers of Aricept (donepezil) released a 23 mg extended-release tablet of the medication intended for individuals with moderate-to-severe Alzheimer's who have been taking the more common 10 mg dose for at least three months. These individuals may have a better result with the extended-release form of Aricept, although both the extended-release and original forms can cause similar side effects.

4.2.3 Common side effects of cholinesterase inhibitors

Cholinesterase inhibitors are generally well tolerated still the common side effects include nausea, vomiting, loss of appetite and increased frequency of bowel movements. It is strongly recommended that a physician who is experienced in using these medications monitor patients who are taking them and that the recommended guidelines are strictly observed. [6]

The ChEI Rivastigmine (Exelon Novartis Pharmaceuticals Corporation, East Hanover, NJ, USA) has been available since 1997 and was approved for use by the FDA in 2006 in capsule and liquid form. It is available in many countries for the symptomatic treatment of mild to moderate Alzheimer's disease and, more recently, was approved for mild to moderate dementia associated with Parkinson's disease. Rivastigmine is a dual inhibitor of both acetyl cholinesterase and butyryl cholinesterase. The efficacy of Rivastigmine in Alzheimer's disease is dose related, with oral dosages ranging from 6mg/day to 12 mg/day being associated with greater efficacy. A benefit on cognitive performance, as assessed by MMSE scores, has been shown in patients with Alzheimer's disease who have taken Rivastigmine for up to 5 years. All ChEIs are associated with cholinergic gastrointestinal adverse effects, particularly during the titration phase. A rapid increase in brain acetylcholine levels after effective inhibition of target enzymes is believed to cause these adverse effects. The adverse effects of rivastigmine are most likely related to high maximal plasma concentrations (Cmax), the short time to Cmax (tmax) and large fluctuations in plasma concentrations.

Twice-Daily versus Three-Times-Daily

Administration of Rivastigmine in patients taking the rivastigmine capsule, strategies that prolong tmax and reduce fluctuations in plasma drug concentration have been shown to reduce the incidence of gastrointestinal adverse events. For example, administration of rivastigmine capsules with food reduced gastrointestinal adverse effects by delaying absorption, prolonging tmax by 1.5 hours and decreasing Cmax, despite the fact that the area under the plasma concentration-time curve (AUC) was increased by 30%.[53,54]. In a 26-week placebo-controlled study of rivastigmine capsules (2–12 mg/day) administered twice daily versus three times daily in 678 patients with mild to moderate Alzheimer's disease, superior tolerability for the three-time daily regimen over the twice-daily regimen was demonstrated. There was a reduction in nausea incidence and severity in the three-times-daily group compared with the twice-daily group. This improved tolerability was probably due to the reduced fluctuation and lower peaks in plasma rivastigmine concentrations observed in the three times- daily group, in whom more frequent administration of smaller doses of rivastigmine over the 24-hour period was possible. This study also reported that the improved tolerability of the three-times-daily dosage regimen over twice-daily administration of rivastigmine occurred even though three-times-daily patients took higher mean doses than those in the twice-daily group. This suggests that strategies that lower Cmax, such as three-times-daily versus twice-daily administration, help patients tolerate rivastigmine better, which in turn increases the likelihood of reaching optimal therapeutic doses. Greater exposure to rivastigmine may lead to greater efficacy, as was the case in this study. Treatment effects compared with placebo were significantly greater with respect to cognitive outcomes in patients treated three times daily compared with those in the twice-daily administration arm. The results of the three-times-daily versus twice-daily study, suggest that a reduction in fluctuations of plasma rivastigmine concentration can improve tolerability, allowing access to higher doses for patients who may require greater efficacy. [7]

5. Blood-Brain Barrier

The BBB is an active interface with an average surface area of about 12–18 m^2 for a human adult. Only a few regions, such as circum ventricular organs (CVO), lack the BBB. But it has to be noticed that a complicated system surrounding CVO preventing blood-borne compounds from entering the BBB-protected region. The total length of capillaries in a normal human adult brain is about 400 miles, that length is shorter in the brains of AD patients. Due to the degeneration of the capillaries, transportation of nutrients and essential substances across the BBB and the clearance of neurotoxins such as Aβ peptides from the brain are reduced. The BBB is a capillary wall mainly formed by brain endothelial cells and its basement membrane, with the presence of cell-cell junctions to keep the integrity of the brain microvasculature. Cell-cell adhesion can be categorized into adherens junctions and tight junctions. The tight junctions preclude the paracellular transport of movement of most of the molecules and ions. Therefore, the transport of most of the molecules between the vascular system and brain is mainly through the transcellular transport. There are also components that take part in the formation and functions of the BBB. The brain capillaries are surrounded by the end-feet of astrocytes, which are involved in the regulation of ion concentration and clearance of neurotransmitters. Pericytes are vascular mural cells locating on the abluminal aspect of endothelial cells and astrocyte end-feet wrap around the pericytes layer, which are able to regulate the blood flow by controlling capillary diameter. Pericytes are important for BBB formation and for down regulation of transcytosis activity when endothelial cells mature. Therefore, pericytes are also related to the transportation across the BBB. Other cellular components such as neurons and microglia also take part in forming the BBB. The functional interactions and signaling between the above-mentioned neurons and non-neuronal cells form a dynamic functional unit, which is called the neurovascular unit. All the components are essential for normal functions, stability of the BBB and the response of the BBB to pathophysiological stimuli. The dilemma for the treatment of AD and other brain diseases is not only due to the lack of effective therapeutic molecules but also due to their inability to penetrate the basement membrane of the BBB and reach the specific target site to treat the disease.

5.1 BBB Permeation Mechanisms

There are several transport routes for molecules to cross the BBB. A few small hydrophilic and lipophilic molecules can enter the brain by paracellular and transcellular diffusion. Other substances, such as amino acids, peptides and nucleosides, may enter the brain through carrier-mediated transport, receptor-mediated transcytosis and/or adsorptive-mediated transcytosis.

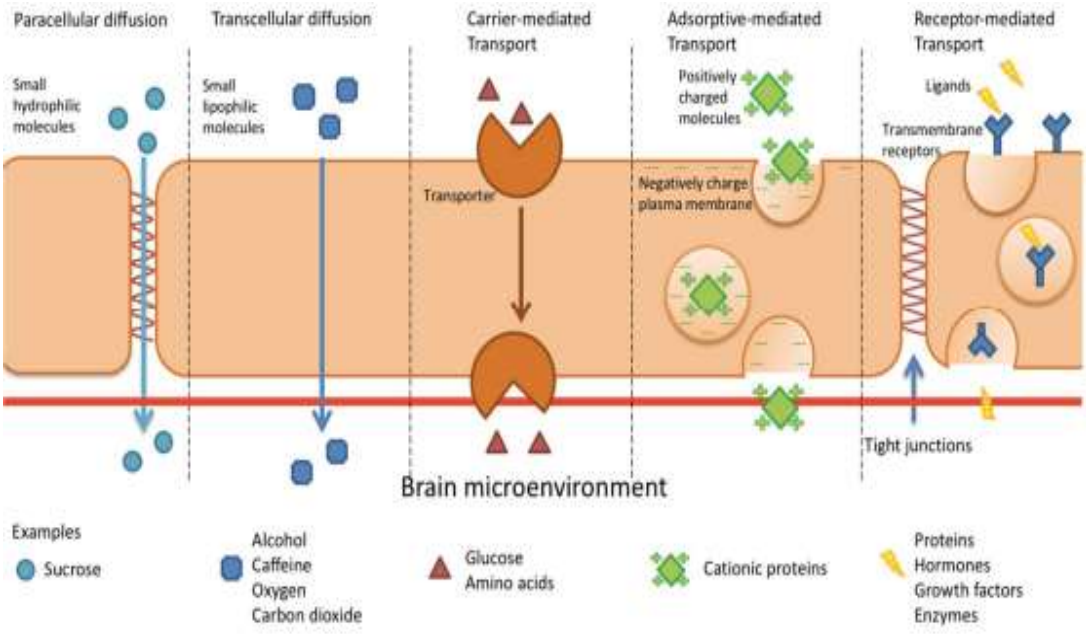

Figure 3: Pathways for BBB penetration

5.2 Role of the Blood-Brain Barrier in Drug Delivery

BBB serves as a physical barrier that can protect the CNS from exogenous substances and as a transport system, delivering chemicals to the CNS. In medicine, the BBB can be regarded as a target for DDSs that makes use of various types of receptors expressed on the endothelial cells to transport therapeutics across the BBB. Strategies for delivering molecules into the brain can be classified into two invasive and non-invasive. The invasive method is to directly administrate the drugs into brain that include temporarily opening the tight junctions by high osmolar solutions, injecting drugs intra cerebrally or guiding drug injection via catheter. However, invasive methods are inherently dangerous as there is risk of infection, potential damage to the brain tissue and possible uncontrolled drug distribution after administration. Therefore, non-invasive methods are generally preferred. In non-invasive approaches, the drugs can be administrated through intravenous injection or

intranasal administration. In the nasal pathway, the drugs are able to enter the brain once penetrating the nasal epithelium. And are delivered along olfactory and trigeminal neural pathways via extracellular route, which is the shortest path for molecules to reach the CNS. This approach does not require the drug to bind to any receptor for transcytosis. Nevertheless, the administration requires substances with high solubility as each dose is limited to about 20 to 30 µL. Both pH and salinity of the therapeutic formulation also influence the effectiveness of delivery. In extreme conditions, respiratory system may be damaged. Moreover, intranasal administration also requires skillful operations because improper injection may deliver the drug to lung or stomach. Another non-invasive strategy for brain delivery is the use of focused ultrasound (FUS) to open the BBB transiently. This is a promising strategy to achieve focal delivery of therapeutics including antibodies, nanoparticles and chemotherapies into the brain. It was reported in a study that the magnetic resonance-guided focused ultrasound applied to five patients with AD resulted in opening and restoration of the BBB. However, the sample size in the study was small and the efficacy to treat AD was not studied. More clinical data must be collected to verify the application of FUS in human.

Component	**Features in AD**
Capillaries	Total length is shorter
GLUT1	Down regulate, result in reduction of Aβ clearance
Transferrin receptor	Numbers of receptors in hippocampus are less than normal.
Insulin receptor	Brain insulin receptor density decreases with aging.
Lactoferrin	Expression is up regulated.
Melanotransferrin	Expression is up regulated.

Table 2: Features of blood-brain barrier dysfunction in AD.

In AD therapy, most of the compounds showing therapeutic efficacy are mostly lipophilic molecules with low water solubility which tend to be substrates for P-glycoprotein (ABCB1) and/or breast cancer resistance protein

(BCRP/ABCG2), which means that uptake through the BBB is restricted by the P-glycoprotein and BCRP efflux. In order to increase the uptake of drug molecules by the brain, different approaches are considered first, the structure of therapeutic molecules can be modified to adjust the physical and chemical properties. Synthesis of drug analogues is full of uncertainty because the activity site responsible for therapeutic effects and the properties of different functional groups have to be well studied. The synthesis usually requires several steps and sample loss is accumulated in each step. Conjugating the drug molecules with various cell penetrating peptides or antibodies is another strategy. This method can make use of the adsorptive-mediated transcytosis and receptor-mediated transcytosis pathways and facilitate the drug to cross the BBB. Although ligand-conjugated drugs bring improvements for drug to delivery into the brain, problems such as the rate of drug dissociation from ligands and the ratio of drug/ligand and ligand/receptors still need to be solved. To improve the mentioned problems, nanotechnology-based DDSs are potential alternative to be considered.

6. Colloidal carriers

Vesicular systems

- Liposomes
- Niosomes
- Pharmacosomes
- Virosomes
- Immunoliposomes

Micro particulate systems

- Micro particles
- Nanoparticles
- Magnetic microspheres
- Albumin microspheres
- Nano capsules
- Solid lipid nanoparticles

Cellular carriers

- Resealed erythrocytes

- Serum albumin
- Antibodies
- Platelet
- Leukocytes

Supra molecular delivery systems

- Micelles
- Liquid crystals
- Lipoproteins

Polymer based systems

- Signal sensitive
- Mucoadhesive
- Biodegradable
- Bioerodable
- Soluble synthetic polymeric carriers

Macro molecular carriers

- Proteins; Glycoproteins; Artificial viral envelops
- Glycosylated water soluble polymers
- Monoclonal antibodies
- Toxins
- Leptons
- Polysaccharides[8,9,10]

6.1 Nanotechnology

Nanoparticles are solid polymeric, submicron colloidal system range between 5-300 nm consisting of macromolecular substances that vary in size 1 nm to 1000 nm. The drug of concern is dissolved, entrapped adsorbed, attached or encapsulated into the nanoparticle matrix. Depending upon the method of preparation, nanoparticle, nanosphere or nanocapsule can be obtained with different properties and release characteristics for the encapsulated therapeutic agent.

Nanosphere are matrix system in which drug is physically and uniformly distributed throughout, then particles prepared by using different polymers such as

poly alkyl cyano acrylate & poly lactides or they can be solid lipid nanosphere prepared by using lipids like dipalmitoyl – phosphatidyl choline.

Nanocapsule are ultrafine vesicular system with a diameter less than 1 µm in which the drug is restrained to a cavity surrounded by a unique polymer membrane and having aqueous or oily core containing drug substances.

Nanoparticles holds much interest, since in this range materials can have different and enhanced properties compared with the same materials of a larger size due to the following two major principle factors. The increased surfaces are of quantum effect. These factors can enhance properties such as reactivity, strength, electrical characteristics & *in vivo* performance and a much greater surface area per unit mass compared with the larger particles leading to greater reactivity.

The advantages of using nanoparticles loaded with drugs, because of their small size can enter through small capillaries and are taken up by cells and allow the drug release at right rate and dose at specific sites in the body for a certain time to release the accurate delivery, which enhances the therapeutic effect and reduces the toxicity and side effects. The use of biodegradable resources for nanoparticles preparation allows sustained release within the target site over a period of days or even weeks.

Types of NPS as carrier for drug & diagnostic agents

- Polymeric NPS
- Nanosuspensions and nanocrystals
- Polymeric micelles
- Ceramic NPS
- Liposome's
- Fullerenes and dendrimers
- SLN (Solid lipid nanoparticles)
- Magnetic nanoparticle[11]

Nano drug delivery system	Carrier material	Active drug candidate	Investigation model	Molecular targets	Comments
Carbon nano tubes (CNT)	Pristine Multi-walled (MW)CNTs; Phospholipids and polysorbates	Berberine	beta-amyloid induced AD in wistar rats	BBB transcytosis Cholinergic systems	BRB-loaded MWCNT coated with phospholipids and polysorbates significantly restored the memory impairment and suppressed ACHE activity in AD rats, compare to its free form.
Dendrim-ers	Hydrophobic pyridyl phenyl-ene dendrimers	o-phenylene diamine	Inclusion bodies of ovine prion protein (PrP) representing amyloid protein aggregates	Amyloid cascades	The dendrimers form stable protein complexes, thereby resultantly disrupt the PrP amyloid aggregates at a physiological pH of 7.4, which can be adapted in reducing Aβburden. However further animal studies are required.
Gold (Au) NPs	AuNPs of 5 nm with PEG	Anthocyanin	Mouse brain endothelial cells/Aβ1–42Mouse Model	Amyloid cascades and tau hyper phosphorylat-ion	Anthocyanin-loaded PEG-AuNPs effectively exhibited neuro protective potential compared to its freeform, via regulation of p-PI3K/pAkt/pGSK3βpathway, inhibition of tau hyper phosphorylation and amyloid

					cascades in AD mice model.
Gold (Au) NPs	Gold colloids – rods (AuNR)and spheres (AuNS)	CLPFFD peptide	Porcine brain capillary endothelial cells	Amyloid cascades	PEGlyation of Au NPS, effectively stabilize the NPs by masking its Negative charge and facilitates BBB transport. Further functionalizing with CLPFFD peptide enhances their selective binding towards Aβ-amyloid fibrils.
Liposome NPs	Sphingo myelin, cholesterol functionalized with dimyristoyl phosphatidic acid (PA)or bi-functionalized with PA and modified Apo lipoprotein E-derived Peptide (mApo)	Curcumin derivative (CD)	Human blood plasma and cerebrospinal fluid (ex -vivo)	Amyloid cascades	MApo-PA-functionalized NPs effectively bind with Aβ1–42 in human biological fluid, which shall be adapted in promoting 'sink effect' in reducing Aβ burden.
Liposome NPs	PLGA [Poly (lactic-co glycolic	Peptide iAβ5	Porcine brain capillary	BBB transcytosis	Functionalized PLGA NPs safely and efficaciously transport iAβ5 peptides

	acid)] functionalized with anti-transferrin receptor monoclonal antibody (OX26)and anti-Aβ		endothelial cells	Amyloid cascades	across BBB cell models and can be targeted to Aβ burden.
Liposome NPs	Cholesterol, soyabean phosphatidyl-choline-functionalized with surface wheat germ agglutinin (WGA) and Cardiolipin	Curcumin and nerve growth factor	Human neuro blastoma cell Line/ADrat model	BBB transcytosis,Amyloid cascades and tau hyperph-osphorylatin	Curcumin-CL NPs inhibited phosphorylation of p38, JNK, and tau protein in Ab insulted neurons. WGA-curcumin-CL NPs substantially reduced Ab plaque deposition and lowered AChE activity in the Hippocampus of AD rats.
Mesoporous silica NPs(MSN)	N-Cetyl trimethyl ammonium	Rivastigmine hydrogen tartrate (RT)	Simulated gastric and body fluids and	Neuronal cell death/Choliner	RT-A-MSNs exhibited a sustained release profile of RT in gastric and body fluids.

	bromide functionalized with succinic anhydride (S) and 3-amino propyl triethoxy-silane		neuro blastoma SH-SY5Y cell line viability	gic systems	However, at higher dose concentrations, the bio-accumulation of RT-A-MSNs may be higher which resultantly shows toxicity to neuronal cells, compared to other functionalized MSNs. Thus, further extensive *in vivo* studies are required.
Mesoporous silica NPs (MSN)	N-Cetyl trimethyl ammonium bromide, Tetra ethoxysilane functionalized with gold(Au) nanoparticle	Metal chelator CQ (5-chloro-4-hydroxy-7-iodo quinoline)	PC12 rat adrenal medulla cells/endothelial cell line.	BBB transcytosis,Amyloid-cascades	MSN-AuNPs were reported to effectively cross in vitro model of the BBB and the metal chelator CQ loaded MSN-AuNPs significantly inhibits Cu2+-induced Aβ40 aggregation.
Metallic NPs	Iron crystal structure; functionalized with PEG	Iron oxide	Amyloid fibrillation experiments invitro	Amyloid cascades	Under magnetic field, the higher concentration of NPs accelerates Aβ fibrillation, whereby at lower concentration inhibits the same. Interestingly negative charged or uncharged NPs inhibits fibrillation more efficiently.

Polymeric NPs	Dendrigraft poly-l-lysines and poly ethelene glycol (PEG)	RVG29 peptide and BACE1-AS shRNA gene	Double transgenic AD mice/neuro-blastoma and brain capillary endothelial cell line	Amyloid cascades and tau-tangles	These multifunctional nanocarriers, successfully delivered dual therapeutic drug moieties and effectively suppressed Aβ plaque.
Polymeric NPs	Chitosan	Piperine	Colchicine induced AD rats	Cholinergic and oxidative stress systems	Compare to its free form, piperine NPs effectively alleviated the behavioral impairment in AD rat model via suppressing AChE and oxidative stress environment.
Polymeric NPs	Glycidyl methacrylate	Imino di acetic acid (IDA)	Zinc-mediated Ab42 aggregation human neuroblastoma SH-SY5Ycell line viability	Amyloid cascades	IDA-NPs effectively chelated zinc mediated Aβ42 aggregates, thereby proposed to strongly inhibit Aβ42 fibrillation pathway. However further animal studies are required to confirm the same.

Polymeric NPs	N-isopropyl acrylamide and N-t-butyl acrylamide – monomers; acrylic acid	Epigalloca-techin-3-gallate(EGCG)	Amyloid fibrillation experiments *invitro* and neuroblastoma SH-SY5Ycell line viability	Amyloid cascades	Negatively charged polymeric NPs loaded with EGCG synergistically suppressed Aβ (Aβ42 and Aβ40) fibrillation. However, further animal studies are required to confirm the same.
Solid Lipid NPs (SLNs)	Lipids and chitosan	RVG-9R/BACE1 siRNA	Human epithelial adenocarcinoma (Caco-2) cells	Amyloid cascades	SLNs formulation improvises the charge and muco adhesiveness of the system and relatively Enhanced its drug permeability. However, further confirmation through in vivo tests is highly essential.
Solid Lipid NPs (SLNs)	Cetyl palmitate and functionalized with monoclonal antibody (OX26 mAβ)	Resveratrol /grape seed extract	Human brain-like endothelial cells	BBB transcytosis and Amyloid cascades	Both the drug actively suppressed fibrillar formation, among them extracts shows higher activity. SLNs functionalized with OX-26 antibody shown higher transcytosis compare to un functionalized SLNs.
Solid lipid NPs (SLNs)	Glyceryl behe-nate lipids	Galantamine hydro bromide	Isoproterenol induced cognitive deficits in rats	Cholinergic systems	The SLNs loaded with galantamine, significantly restored the memory impairment.

Solid lipid NPs (SLNs)	Heparin-conjugated stearic acid; stearylamine-cationic lipid	Nerve growth factor (NGF)	Induced pluripotent mouse stem cells (iPSCs)	Neuronal cell death	NGF-loaded SLNs with EQ 1 induced differentiation of neuron-like cells, which projects that these SLNs can be further adapted for neuronal regeneration studies, with potential in vivo evidence.
Solid lipid NPs (SLNs)	Cetyl palmitate	Rapamycin (Rp)	SH-SY5Y neuroblastoma cell line	Mammalian target of rapamycin (mTOR) signaling pathway	Rp-SLNs effectively inhibited mTOR complex 1, with a sustained release profile in neuroblastoma cells, compare to its free form. However, further in vivo investigation is highly essential.

Table 3: A list of few potential Nano-drug delivery systems investigated in the field of AD therapeutic

7. SOLID LIPID NANOPARTICLE

Solid lipid nanoparticles (SLNs) were introduced in 1991 with the objective to provide biocompatibility, storage stability and to prevent the incorporated drug from degradation. SLNs that is colloidal carriers of nanoscopic size (50–1000 nm) are made up of solid lipids (high melting fat matrix) and are developed to conquer the weaknesses (e.g., polymer degradation and cytotoxicity, lack of a suitable large scale production method, inferior stability, drug leakage and fusion, phospholipid degradation, high production cost, and sterilization problems) of traditional colloidal carriers, like polymeric nanoparticles and liposomes. SLNs show various distinctive features such as low toxicity, large surface area, prolonged drug release, superior cellular uptake as compared to traditional colloidal carriers as well as capability to improve solubility and bioavailability of drugs. The release of drug from SLNs depends on matrix type and drug location in the formulation. The SLNs fabricated from biodegradable and biocompatible ingredients are able to incorporate both hydrophilic and lipophilic bioactive and thus turning out to be a viable option for controlled and targeted drug delivery. The solid core of SLNs is hydrophobic with a monolayer coating of phospholipids and the drug is usually dispersed or dissolved in the core (Figure 4).

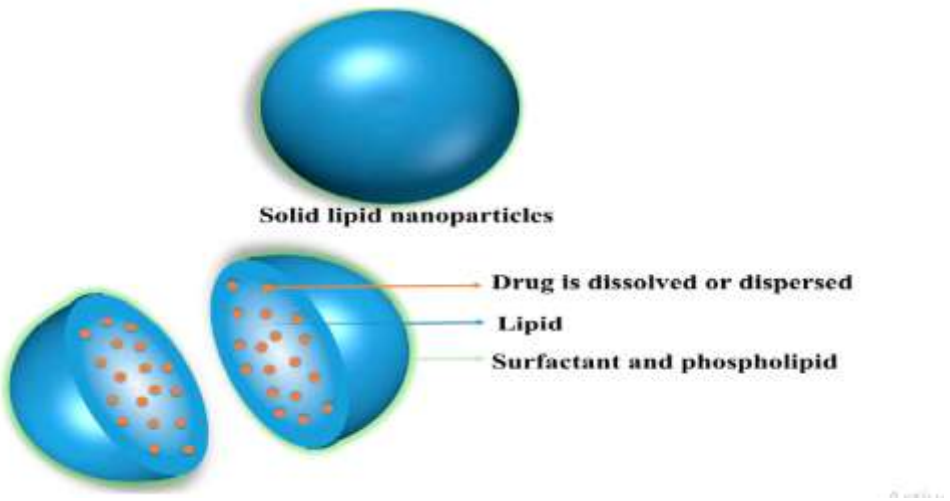

Figure 4: Structure of Solid lipid nanoparticles

7.1 Advantages of SLNs

- The cells of reticulo endothelial system (RES) are unable to take up SLNs because of their nano size range, thus enabling them to bypass spleen and liver filtration
- Provide high stability to incorporate drugs
- Feasibility of incorporating both hydrophilic and lipophilic drugs
- Improve bioavailability of poorly water soluble molecules
- Ease in sterilization and scale up
- Immobilizing drug molecules within solid lipids provides protection from photochemical, oxidative, and chemical degradation of sensitive drugs, with reduced chances of drug leakage
- Drying by lyophilization is achievable
- Provide opportunities for targeted and controlled release of drug
- Biocompatible and biodegradable compositional ingredients

7.2 Disadvantages of SLNs

- SLNs are compactly packed lipid matrix networks (ideal crystalline structure) having low space for drug encapsulation, leading to poor drug loading capacity
- Various factors affect the loading or encapsulation of drugs in SLNs, such as interaction of drug and lipid melt, nature or state of lipid matrix, drug miscibility with lipid matrix, and the drug being dispersed or dissolved in the lipid matrix
- Chances of drug expulsion following polymeric transition during storage
- The dispersions have a high (70–90%) water content

7.3 Compositional Profile of SLNs

Lipid and surfactant/stabilizer are the key components used to fabricate SLNs along with co-surfactant, preservatives, cryoprotectant, and charge modifiers (Table 4). By reducing the interfacial tension between the aqueous environment and the hydrophobic surface of the lipid core, surfactants help in stabilizing the SLN structure. [12]

INGREDIENTS	EXAMPLES
Lipid component	Beeswax, Stearic acid, Cholesterol, Caprylic/capric triglyceride, Cetyl palmitate, Glyceryl stearate (-mono, and -tri), Glyceryl tri laurate, Glyceryl tri myristate, Glyceryl behenate (Compritol), Glyceryl tr ipalmitate, Hardened fat (Witepsol E85, H5 and W35),Monostearate monocitrate, Solid paraffin, Behenic acid
Surfactant/Emul sifiers	Phosphatidyl choline, Soy and Egg lecithin, Poloxamer, Poloxamine, Polysorbate 80
Co-surfactant	Sodium dodecyl sulphate, Tyloxopol, Sodium oleate, Taurocholate sodium salt, Sodium glycocholate, Butanol
Preservative	Thiomersal
Cryoprotectant	Gelatin, Glucose, Mannose, Maltose, Lactose, Sorbitol, Mannitol, Glycine, Polyvinyl alcohol, Polyvinyl pyrrolidone
Charge modifiers	Dipalmitoyl phosphatidyl choline, Stearyl amine, Dicetyl phosphate, Dimyristoyl phophatidyl glycerol

Table 4: Ingredients used in SLNs-based formulations

7.4 METHODS OF PREPARATION

7.4.1 High shear homogenization (HSH)

Initially used for the production of solid lipid nano emulsions, this method is reliable. It involves high pressure homogenization which pushes the liquid with high pressure (100-2000 bar) through a narrow gap ranging a few microns. The fluid accelerates to a very short distance at very high viscosity of over 1000 km/h. Very high shear stress and cavitation forces disrupt the particles down to submicron range. As low as 5% to as high as of 40% lipid content has been investigated. Two general approaches to achieve HSH are hot homogenization and cold homogenization.

Hot homogenization is generally carried out at temperatures above the melting point of the lipid. A pre-emulsion of the drug loaded lipid melt and the aqueous emulsifier phase (same temperature) is obtained by high shear mixing device. The

resultant product is hot o/w emulsion and the cooling of this emulsion leads to crystallization of the lipid and the formation of SLNs. Smaller particle sizes are obtained at higher processing temperatures because of lowered viscosity of the lipid phase. However, high temperature leads to the degradation rate of the drug and the carrier. Increasing the homogenization temperature or the number of cycles often results in an increase of the particle size due to high kinetic energy of the particles. Generally, 3-5 homogenization cycles at a pressure of 500-1500 bar are used.

Cold homogenization has been developed to over-come the temperature related degradation problems, loss of drug into the aqueous phase and partitioning associated with hot homogenization method. Unpredictable polymeric transitions of the lipid due to complexity of the crystallization step of the nanoemulsion resulting in several modifications and/or super cooled melts. Here, drug is incorporated into melted lipid and the lipid melt is cooled rapidly using dry ice or liquid nitrogen. The solid material is ground by a mortar mill. The prepared lipid microparticles are then dispersed in a cold emulsifier solution at or below room temperature. The temperature should be regulated effectively to ensure the solid state of the lipid during homogenization. However, compared to hot homogenization, larger particle sizes and a broader size distribution are typical of cold homogenization samples.

7.4.2 Ultrasonication

Ultrasonication or high speed homogenization is another method for the production of SLNs. The advantage of this method is that the equipment used is commonly available at lab scale. However, this method suffers from problems such as broader size distribution ranging into micrometer range. Potential metal contaminations, physical instability like particle growth upon storage are other drawbacks associated with this technique

7.4.3 Microemulsion based SLN preparation

Gasco and coworkers (1997) developed SLNs based on the dilution of micro emulsions. These are made stirring an optically transparent mixture at 65-70°C which is typically composed of a low melting fatty acid like stearic acid, an emulsifier (e.g. polysorbate 20, polysorbate 60, soya phosphatydyl choline and tauro deoxy cholic

acid sodium salt), co-emulsifiers (e.g. butanol, sodium mono octyl phosphate) and water. The hot micro emulsion is dispersed in cold water (2-3°C) under stirring. Typical volume ratios of the hot micro emulsion to cold water are in the range of 1:25 to 1:50. The dilution process is critically determined by the composition of the microemulsion. The SLN dispersion can be used as granulation fluid for transferring in to solid product like tablets and pellets by granulation process, but in case of low particle content too much of water need to be removed. The nanoparticles were produced only with solvents which distribute very rapidly into the aqueous phase (acetone), while larger particle sizes were obtained with more lipophilic solvents.

7.4.4 Supercritical Fluid technology

This is a novel technique recently applied for the production of SLNs. A fluid is termed supercritical when its pressure and temperature exceed their respective critical value. The ability of the fluid to dissolve compounds increases. This technology comprises of several processes for nanoparticle production such as rapid expansion of supercritical solution (RESS), particles from gas saturated solution (PGSS), aerosol solvent extraction solvent (ASES), supercritical fluid extraction of emulsions (SFEE). The advantages of this technique includes avoidance of the use of solvents, particles obtained as a dry powder, instead of suspensions, requires mild pressure and temperature conditions. Carbon dioxide solution is the good choice as a solvent for this method.

7.4.5 Solvent emulsification/evaporation

For the production of nanoparticle dispersions by precipitation in o/w emulsions, the lipophilic material is dissolved in water-immiscible organic solvent (cyclo hexane) that is emulsified in an aqueous phase. Upon evaporation of the solvent nanoparticle dispersion is formed by precipitation of the lipid in the aqueous medium. The mean diameter of the obtained particles was 25 nm with cholesterol acetate as model drug and lecithin/sodium glycol cholate blend as emulsifier.

7.4.6 Solvent emulsification-diffusion

SLNs can also be produced by solvent emulsification-diffusion technique. The mean particle size depends upon lipid concentration in the organic phase and the emulsifier used. Particles with average diameters of 30-100 nm can be obtained by this technique. Avoidance of heat during the preparation is the most important advantage of this technique. Here, the lipid matrix is dissolved in water-immiscible organic solvent followed by emulsification in an aqueous phase. The solvent is evaporated under reduced pressure resulting in nanoparticles dispersion formed by precipitation of the lipid in aqueous medium.

7.4.7 Double Emulsion

In this method, the drug is encapsulated with a stabilizer to prevent drug partitioning to external water phase during solvent evaporation in the external water phase of w/o/w double emulsion. Prepared solid lipid nanoparticles loaded with bovine serum albumin (BSA) using double emulsion method.

7.4.8 Spray Drying

It is an alternative technique to lyophilization in order to transform an aqueous SLN dispersion into a drug product. This is a cost-effective method than lyophilization and recommends the use of lipid with melting point >70°C. This method causes particle aggregation due to high temperature shear forces and partial melting of the particle.

7.4.9 Solvent injection technique

Here, the solid lipid is dissolved in water miscible solvent. The lipid solvent mixture is injected into stirred aqueous phase with or without surfactant. Finally, the dispersion filtered to remove excess lipid. Emulsion within the aqueous phase helps to produce lipid droplets at the site of injection and stabilize SLNs until solvent diffusion gets completed. SLNs using Solvent injection method for delivery of Hepatitis B surface antigen for vaccination using subcutaneous route. [13]

7.5 Principle of Drug Release from SLN:

The general standards of medication discharge from lipid nanoparticles are as per the following:

- Higher surface territory because of little molecule measure in nanometer extent gives higher medication discharge.
- Slow medication discharge can be accomplished when the medication is homogenously scattered in the lipid framework. It depends on sort and medication entanglement model of SLN.
- Crystallization conduct of the lipid carrier and high portability of the medication lead to quick medication discharge.
- Fast initial drug release in the first 5 min in the drug –enriched shell model as a result of the outer layer of particle due to larger surface area of drug deposition on the particle surface.
- The burst release is reduced with increasing particle size and prolonged release could be obtained when the particles were sufficiently large, i.e., lipid macromolecules.
- The type of surfactant and its concentration, which will interact with the outer shell and affect its structure, should be noted as the outer factor which is important, because a low surfactant concentration leads to a minimal burst and prolonged drug release.
- The particle size affect drug release rate directly depends on various parameters such as composition of SLN formulation (such as surfactant, structural properties of lipid, drug) production method and conditions (such as production time, equipment, sterilization and lyophilization.

7.5.1 There are three drug incorporation models which describe drug release from SLN as shown in fig. 5

A) Homogenous matrix model

B) Drug enriched shell with lipid core

C) Drug enriched core with lipid shell [14]

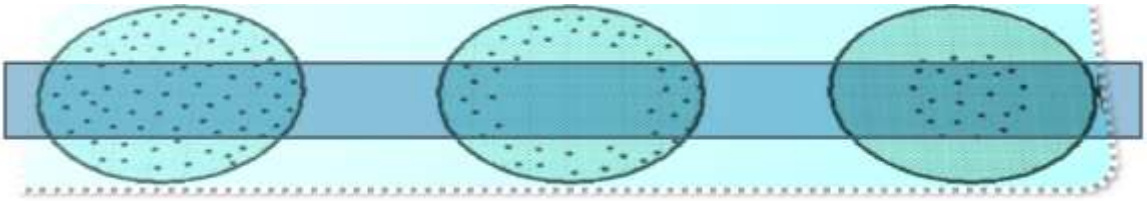

Figure 5: Drug release from SLN

A. Homogenous matrix model or solid solution model with drug being present in amorphous clusters or molecularly dispersed is mainly obtained when incorporating highly lipophilic drugs into SLN with using hot homogenization technique or applying cold homogenization method or by avoiding potentially drug solubilizing surfactants. In the cold homogenization technique the drug (in molecularly dispersed form) is dispersed in bulk of melted lipid, then the mechanical force of high pressure homogenization leads to the breakdown of molecular form to nanoparticles and giving rise to homogenous matrix model as shown in Figure 5. Etomidate SLN represents the homogenization matrix model.

B. The drug enriched shell with core shell model will be obtained when performing the production. During the production, the drug partitioned to water phase. Upon cooling, the lipid precipitates first, forming a practically drug free lipid core due to phase separation. At the same time, the drug re-partitions into the remaining liquid-lipid phase and drug concentration in the outer shell increasing gradually. Finally drug enriched shell crystallizes as depicted in Fig. 5. The amount of drug partitioning to the aqueous phase will increases with the increase of solubility of drug in the aqueous phase. Mainly two factors, increasing temperature of the aqueous phase and increasing surfactant concentration, are increasing the saturation solubility of drug in water phase. Tetracaine SLN were prepared by hot HPH shows drug enriched shell model.

C. A drug enriched core obtained when dissolving a drug (e.g. prednisolone) in the lipid melts at or close to its saturation solubility. In this model, cooling of the formed nanoemulsion will lead to super saturation of drug in melted lipid and it further leads drug precipitation prior to lipid precipitation. Further cooling will lead to precipitation of lipid surrounding the drug enriched core

as a membrane as indicated in Figure 3c. Due to increased diffusional distance and hindering effect of surrounding solid lipid shell, the carrier system shows sustained release profile. [14]

7.6 CHARACTERIZATION PARAMETERS:

7.6.1 Physiochemical Characterization of SLN's:

7.6.1.1 Particle Size and Shape

SLNs are submicron sized, particle size and shape is determined by:

a) Photon Correlation Spectroscopy (PCS)

It is an established method which is based on dynamic scattering of laser light due to Brownian motion of particles in solution/suspension. This method is suitable for the measurement of particles in the range of 3 nm to 3 mm. The PCS device consists of laser source, a sample cell (temperature controlled) and a detector. Photomultiplier is used as detector to detect the scattered light. The PCS diameter is based on the intensity of the light scattering from the particles.

b) Electron Microscopy

Electron Microscopy methods such as Scanning Electron Microscopy (SEM) and Transmission Electron Microscopy (TEM) are used to measure the physical characterization like overall shape and morphology of lipid nanoparticles. It permits the determination of particle size and distributions. SEM uses electrons transmitted from the surface of the sample while TEM uses electrons transmitted through the sample. TEM has a smaller size limit of detection.

7.6.1.2. Measurement of zeta potential

Zeta potential is used to measure the charge on the particles. It allows prediction about the storage stability of colloidal dispersion because of repulsion between particles. Malvern Zetasizer is most widely used instrument for measurement of Zeta potential. A zeta potential measurement can also be helpful in designing particles with reduced RES uptake. Zeta potential below -25 mV and above + 25mV are required for full electrostatic stabilization of the formulation.

7.6.1.3. Determination of Incorporated Drug

Amount of drug incorporated in SLNs influences the release characteristics; hence it is very important to measure the amount of incorporated drug. The amount of drug encapsulated per unit weight of nanoparticles is determined after separation of the free drug and solid lipids from the aqueous medium by ultracentrifugation, centrifugation filtration or gel permeation chromatography. The drug can be assayed by standard analytical technique such as Spectroscopy and HPLC methods.

7.6.1.4. Measurement of degree of crystallinity and lipid modification

Thermodynamic stability and lipid packing density increase while drug incorporation decrease in the following order:

Super cooled melt < α-modification < β'-modification < β-modification.

Due to the small size of the particles and the presence of emulsifiers, lipid crystallization and modification changes might be highly retarded. Differential scanning calorimetry (DSC) & X-ray scattering are used to investigate the status of the lipid. DSC uses the fact that different lipid modifications possess different melting points and melting enthalpies. By means of X-ray scattering it is possible to assess the length of the long and short spacing of the lipid lattice. It is highly recommended to measure changes of the SLN dispersion because solvent removal will lead to modifications.

7.6.1.5 Drug incorporation and loading capacity:

The crucial ingredients for SLNs contain lipids, and a single or a combination of emulsifiers. Depending on the lipid, emulsifier and the method of preparation the particle size, and the surfactant used for the preparation of SLNs is found to vary.

Factors that influence the loading capacity of a drug in the lipid are:

1. Drug solubility in the melted lipid.
2. Miscibility of lipid melt and the drug melt.
3. Chemical and physical arrangement of solid lipid matrix.
4. Polymorphic condition of lipid material.

7.6.2 EVALUATION PARAMETERS

Various methods used to study the in vitro release of the drug are:

In vitro drug release

Dialysis tubing:

In vitro drug release could be achieved using dialysis tubing. The solid lipid nanoparticle dispersion is placed in pre- washed dialysis tubing which can be hermetically sealed. The dialysis sac is then dialyzed against a suitable dissolution medium at room temperature, the samples are withdrawn from the dissolution medium at suitable intervals, centrifuged and analyzed for the drug content using a suitable analytical method.

Reverse dialysis:

In this technique a number of small dialysis sacs containing 1 ml of dissolution medium are placed in SLN dispersion. The SLN's are then displaced into the medium.

Franz Diffusion Cell:

The SLN's dispersion is placed in the donor chamber of Franz diffusion cell fitted with a cellophane membrane. The dispersion is then analyzed against a suitable dissolution medium; the samples are withdrawn from the dissolution medium at suitable intervals and analyzed for drug content using suitable methods like spectroscopy and HPLC methods.

7.7 Applications of Solid Lipid Nanoparticles

SLNs enhance the bioavailability of entrapped drugs via modification of the dissolution rate, and can be used to improve tissue distribution and targeting of drugs

. **Figure 6: Applications of SLNs**

7.7.1 Controlled Release of Drug

SLNs offer an advantage to modulate release of loaded drug either by varying drug loading approach or by altering surface properties or composition .In a recent study, SLN loaded with TNF-α siRNA was developed to achieve its prolonged release in treatment of rheumatoid arthritis. SLNs were prepared via a solvent displacement method using biocompatible lecithin and cholesterol, and a complex of siRNA with 1,2-dioleoyl-3-trimethylammonium-propane was encapsulated therein. In vitro release study of siRNA from SLNs demonstrates absence of burst release, and only 5% of siRNA was released in 30 days. This prolonged release property without burst release was attributed to the presence of cholesterol and complex of siRNA in formulation.

Cavallietal prepared inclusion complexes of hydrocortisone and progesterone with cyclodextrin by co-precipitation method. Inclusion complexes were later incorporated into different types of SLNs. The authors observed a delayed release of drug from SLNs of drug- cyclodextrin complex. Achieving controlled release of hydrophilic drugs using SLNs as a carrier is usually

challenging due to poor drug loading. However, controlled release of a hydrophilic peptide drug, gonadorelin, was achieved using SLN due to the ability of this carrier to load high amount of gonadorelin (up to 69.4%) by solvent diffusion technique. Drug release behavior from this monostearin SLNs exhibited a biphasic pattern. After burst release (24.4% during first 6 h), a distinctly prolonged release for over 12 days was observed.

Formulated an anti-acne SLN-based hydrogel for topical delivery of adapalene for treatment of acne. Novel formulation based on a pH-sensitive system. In this system, curcumin loaded SLNs, which act as depot, were coated with mesoporous silica matrix, to control the release of curcumin. A pH dependent release was observed from this complex, which could be attributed to the interaction between silanols of them spore surface and curcumin.

7.7.2 SLNs for Targeted Brain Drug Delivery

SLNs can improve the ability of the drug to penetrate through the blood-brain barrier (BBB). Abbas et al. targeted clonazepam to brain via intranasal olfactory mucosa utilizing nanolipid carriers that were co-loaded with super paramagnetic iron oxide nanoparticles (SPIONs), both for the guidance of nanocarrier and holding in external magnetic field. The nanolipid carriers are incorporated in situ in thermo-sensitive mucoadhesive gels, resulting in the enhanced delivery of clonazepam. This study raises the light on new intranasal management of epilepsy with reduction in clonazepam peripheral harmful effects.

7.7.3 SLNs for Anticancer Drug Delivery

Recently, SLNs bearing anti-neoplastic drug have been investigated for breast cancer treatment, and results showed a sustained release of tamoxifen with good therapeutic activity. Surface modified SLNs can be fabricated for tumor targeting purposes with help of a suitable targeting ligand for effective delivery of some anticancer drugs like methotrexate(MTX) and camptothecin.

Lipid core nanoparticles (LDE) containing anti proliferative agent PTX and reported the reduction in atherosclerosis lesions induced in rabbits through cholesterol feeding. After withdrawal of feeding of cholesterol, as compared to

LDE-single group, the LDE-PTX and LDE-PTX+LDE-MTX managements has the ability to rise by 49 and 59% plaque areas regression, respectively. The tumor necrosis gene expression factor α was decreased by 65 and 79% using LDE-PTX and LDE-PTX+LDE-MTX, respectively. This result showed the action of combined chemotherapy for achieving higher effects on strongly atherosclerotic inflamed lesions.

Distearoyl-floxuridine loaded SLN. In vitro cytotoxicity study performed on human cancer cell lines like HT-29, MDA-MB231 and M14 cells suggested the superior activity of distearoyl-floxuridine SLN towards cancer cell killing. The distearoyl floxuridine SLNs were found to be 100 times more efficient as compared to free floxuridine. Furthermore, clono genic assay suggested higher cytotoxicity of distearoyl-floxuridine SLN as compared to free drug.

7.7.4. SLNs for Antimicrobial Drug Delivery

SLNs release antimicrobial payloads for the effective elimination of infectious microbes harbored at lymphatic sites. Nanoparticles and the nanostructured surfaces oppose the growth of bacteria and infections, which is an effective solution regarding difficulties related to biofilm and antibiotic resistance. SLNs are manufactured for delivery of antimicrobial agents and act against microbes by encapsulating the antimicrobial drugs, disruption of microbial adherence, and receptor-based binding to cellular surfaces.

7.7.5. SLNs as Gene Carrier

Several studies have been carried out on SLN bearing genetic materials such as plasmid deoxyribonucleic acid (p-DNA), DNA, and other nucleic acids. SLN based vectors could act as a beneficial system of gene delivery for management of corneal diseases and inflammation.

7.7.6. SLNs for Topical Use

SLNs are used topically to deliver various drugs such as vitamin A, sisotretinoin, and flurbiprofen. The flurbiprofen-loaded SLN gel can be applied directly to the site of action, to induce higher tissue concentrations of the drug in controlled fashion.

SLN loaded diflunisal (DIF), a non-steroidal anti-inflammatory drug, has also been developed for effective management of rheumatoid arthritis. SLNs formulated by hot homogenization method (based on microemulsification technique) were spherical in shape with a mean size of 124.0 ± 2.07 nm (PDI 0.294 0.15). These SLNs showed significant decrease in fluid volume, granuloma tissue weight, leukocyte count/mm^3 in mice air pouch model. Similarly, in mice ear oedema and rat paw oedema model, 2.30 and 1.29 times increase in percentage inhibition of oedema was observed respectively, using SLN formulation compared to conventional cream.

7.7.7. SLN in Cosmetics

SLNs are novel nanocarriers that can replace the conventional delivery systems such as creams, gels, ointments usage in cosmetics. Curcumin (CUR) has therapeutic properties against skin disorders (SD). The cationic SLNs (CSLN) loaded with CUR were developed and analyzed physic-chemically for SD. It was suggested that the surface charge of CSLN (zeta potential, +23.1 to +30.1 mV) played a major role in selective accumulation of drug to the diseased tissue.

Lipid nano-based systems and traditional cosmetic products compared on account of occlusiveness. The film formed via lipid nanoparticles on skin was smooth in comparison to film formed using a traditional paraffin product. SLNs based products showed great activity of UV-blocking and photo protection.

7.7.8. SLNs as Adjuvant for Vaccines

Immunologic adjuvants are substances that are used to augment the degree, stimulation, or robustness of vaccines. In this sequence, Squalene containing steam sterilized SLNs based adjuvant system for a yeast-based vaccine. Size of squalene loaded SLN measured by static and DLS technique was found to be in the range of 120–170 nm. Evaluation of the developed vaccine adjuvant on a mouse model showed excellent efficacy against the harm fulbursal virus disease. Squalene-based adjuvants represented high biocompatibility and also demonstrated immune stimulation properties, which is comparable with Freund's adjuvant.

7.7.9. SLNs in Anti-tubercular Chemotherapy

In the current scenario, SLNs and other nanocarriers are utilized to eradicate Mycobacterium tuberculosis completely. SLNs could work as efficient drug delivery system for the natural anti-oxidants derived from seed of grape in oxidative stress model in airway epithelial cells. The authors pointed long-term persistence and stability inside cells and liberation of pro antho cyanidins. The IR results create a path for novel anti-inflammatory and anti-oxidant therapies for chronic respiratory diseases.

7.7.10 SLNs in Bio imaging

The detection and removal of lipopolysaccharides (LPS) from pharmaceutical preparations and food is vital for safe administration and to prevent septic shock. An abiotic system prepared using SLNs aim at reversible capture, detection, and removal of LPS in aqueous solutions. Furthermore, the regenerated particles also act as colorimetric labels in the dot blot bioassays for basic and prompt evaluation of the LPS elimination.

In the advanced field of nanomedicine, diverse approaches for rheumatoid arthritis (RA) therapy are available. Albuquerque et al. developed anti-CD64 antibody anchored SLN based the ranostic system consisting of SPIONs and MTX (co-encapsulated in the SLNs) for targeting them acrophages in RA. The formulations have sizes lower than 250nm and -16mV zeta potential with suitable features for intravenous administration. TEM photographs showed that SPIONs were encapsulated within SLN matrix and obtained values of MTX association efficiency were greater than98%.In-vitro studies demonstrated that all formulations exhibited low cytotoxicity 500µg/mL concentration in THP-1 cells. The SLN based formulations are, therefore, promising candidates for both therapeutic and imaging purposes.

REVIEW OF LITERATURE

Maria Inês Teixeira *et al.*, 2020 stated that main reason for the failure of promising neuro therapeutic candidates is the existence of selective and impermeable cellular interfaces such as the BBB. In fact, the BBB is a double-edged sword, since while it helps maintain an optimal and constant milieu for neuronal function, it also restricts most drugs passing from the circulatory system to the brain. Consequently, there is a significant demand for clinically effective and harmless drug delivery systems that can facilitate the crossing of molecules through the BBB. Lipid-based nano systems, such as SLN, NCL, liposomes or micro and nano emulsions, have emerged as an efficient and promising tool to enhance the delivery of neurotherapeutics to the CNS. [16]

Hossein Derakhshankhah *et al.*, 2019 commented on conventional as well as novel therapeutic approaches with an emphasis on stem cell and nano-based therapies for improvement and management of AD pathogenesis. In recent years, investigators have studied the use of NPs to treat human diseases such as Alzheimer's disease. Among nano-materials, lipids NPs have received the most attention as drug carriers due to their low toxicity. The most important of those that have been investigated as drug delivery systems for the treatment of Alzheimer's include phospholipid compounds such as liposomes and non-phospholipid compounds such as solid lipid nanoparticles (SLNs) and nanostructured lipid carriers (NLCs). The SLNs have a globular morphology with a diameter of between 40-1000 nm and are composed of solid fats in a water phase. SLNs may be used as carriers for both hydrophilic and hydrophobic drugs. SLNs can be produced without solvent and exhibit a higher biodegradability, easier preparation, more efficient mass production, greater physical stability, higher freedom of release, lower toxicity, better degradability, and lower cost. [17]

Meenakshi Kanwar Chauhan *et al.*, 2019 developed nano lipid carrier (NLC) loaded transdermal system of rivastigmine for bioavailability enhancement. NLC was optimized using Box-Behnken Design (BBD). Mean size, poly dispersity index (PDI), zeta potential and entrapment efficiency were evaluated. In vitro release studies showed there was more sustained release of drug from NLC loaded

transdermal patches in comparison to Exelon® patch. Pharmacokinetic parameter of optimised rivastigmine- NLCs patches and Exelon® patch in rat plasma after transdermal application were determined. Skin irritation studies proved the non-irritant nature of developed NLC based transdermal patch. From pharmacokinetic studies it was observed that there was increased Cmax and AUC0–72 in plasma treated with NLC loaded transdermal patches as compared to conventional patch. It was concluded from animal studies that RV-NLCs loaded patches showed more bioavailability in comparison to conventional dosage. These experimental results indicate that NLC based transdermal patch could be utilized as a potential carrier for enhancing bioavailability of rivastigmine for the better treatment and management of dementia. [18]

Tahereh Dara *et al.*, 2019 denoted Erythropoietin (EPO), a hematopoietic factor, as one of the promising neuroprotective candidates in neurodegenerative disorders such as Alzheimer's disease (AD). Due to the high molecular weight, hydrophilicity and rapid clearance from circulation, EPO could not completely pass the blood-brain555 barrier in the case of systemic administration. To overcome this limitation, they developed EPO-loaded Solid Lipid Nanoparticle (EPO-SLN) using a double emulsion solvent evaporation method (W1/O/W2). Glycerin mono stearate (GMS), span®80/span®60, Dichloromethane (DCM) and tween®80 were chosen as lipid, internal phase surfactants, solvent, and external aqueous phase surfactant, respectively. After physicochemical evaluations, the effect of EPO-SLN on the beta-amyloid-induced AD-like animal model was investigated. In vivo evaluations, it was demonstrated that the memory was significantly restored in cognitive deficit rats treated with EPO-SLN compared to the rats treated with native drug using the Morris water maze test. In addition, EPO-SLN reduced the oxidative stress, ADP/ATP ratio, and beta-amyloid plaque deposition in the hippocampus more effectively than the free EPO. The results suggested that new EPO-loaded solid lipid nanoparticle can successfully protect the memory in an animal model of AD, and can be considered as a promising approach in the treatment of neurodegenerative disorders and subsequent pharmacodynamics and pharmacokinetics studies. Hence, the designed SLN can be regarded as a promising system for safe and effective delivery of EPO in the AD. [19]

Kathleen Oehlke *et al.*, 2019 stated that when carrier systems like solid lipid nanoparticles (SLN) are added to a protein rich food matrix adsorption of protein to the particles alters the surface properties of SLN which in turn can alter the properties of the whole system. Thus, the effect of the SLN composition on the protein layer (protein corona) is important to understand. The adsorption of βLG at SLN surfaces was studied by centrifugation, AF4 and ultrafiltration. They studied the adsorption of β-lactoglobulin (βLG) to unloaded SLN and SLN loaded with ferulic acid or tocopherol. The formed layer was removable and incomplete at the concentrations and βLG: SLN ratios studied here. Covalent and non-covalent binding between βLG and the co-emulsifiers and FA could be experimentally excluded. However, as revealed by fluorescence quenching, Toc bound to the surface of βLG molecules under the given conditions. We therefore propose that Toc presented an additional binding patch for βLG at the surface of Toc-SLN. In addition, the surface hydrophobicity of SLN could have been increased by Toc or decreased by the ionic FA, thereby non-specifically affecting the hydrophobically driven protein adsorption. The amount of bound βLG was increased by the presence of tocopherol and decreased by the presence of ferulic acid. The adsorbed protein layer thus depends on SLN characteristics governed by encapsulated compounds. [20]

Anubhav Anand *et al.*, 2019 used Sucrose stearate as a bio surfactant for develop and assess the efficacy of rivastigmine hydrogen tartrate (RHT) loaded nanostructured lipid carrier (RHT-NLCs) for the cure of dementia. RHT-NLCs were developed by a modified solvent emulsification- diffusion method. Box-Behnken design was used for optimization of the developed formulation. Quantitative RT-PCR of RHT-NLCs displayed acetyl cholinesterase expressing enzymes (AChE 1 and AChE 2) down-regulation, responsible for the expression of acetyl cholinesterase In accordance with the present results, it can be concluded that RHT-NLCs formulated with Compritol 888 ATO, Triacetin and Ryoto Sugar could be a better option for the treatment of Alzheimer's disease. [21]

Md. Faheem Haider *et al.*, 2018 aimed to develop nanoemulsion of RHC that can improve its brain delivery through nasal route, avoid first pass metabolism and distribution to non-targeted sites. For the preparation of nanoemulsion, selection of excipients was done on the basis of solubility and miscibility studies. They formulated

RHC-loaded nano emulsion and optimized using Box-Behnken statistical experiment design which gives the optimum concentration of oil and water. The release of RHC from NEs was significantly higher than RHC solution and the release mechanism was found to be diffusion controlled (Higuchi model). The results of permeation study demonstrated great potential of developed NEs formulation for enhancing the permeation of RHC across nasal mucosa in contrast to RHC solution. Significantly high level of RHC was achieved in brain via NEs as evident in result of pharmacokinetic studies in comparison of RHC solution. Further optimized formulation was non-toxic and safe as demonstrated by nasal ciliotoxicity studies. The present study clearly demonstrated that i.v. administration of optimized NEs is highly efficient for attaining the higher brain concentration of RHC which could be of great benefit for enhancing its therapeutic prospect. [22]

S. Scioli Montoto *et al.*, 2018 described Solid lipid nanoparticles (SLN) and nanostructured lipid carriers (NLC). Four different nano formulations of the antiepileptic drug Carbamazepine (CBZ) were designed and prepared by the homogenization/ ultrasonication method, with encapsulation efficiencies ranging from 82.8 to 93.8%. The formulations remained stable at 4ºC for at least 3 months. Physicochemical and microscopic characterization were performed by particle size analysis using photon correlation spectroscopy (PCS), transmission electron microscopy (TEM), and atomic force microscopy (AFM); thermal properties by differential scanning calorimetry (DSC), thermogravimetry (TGA) and X-ray diffraction analysis (XRD). The results indicated the presence of spherical shape nanoparticles with a mean particle diameter around 160 nm in a narrow size distribution; the entrapped CBZ displayed an amorphous state. The *in vitro* release profile of CBZ fitted into a Baker-Lonsdale model for spherical matrices and almost the 100% of the encapsulated drug was released in a controlled manner during the first 24 h. The apparent permeability of CBZ-loaded nanoparticles through a cell monolayer model was similar to that of the free drug. *In vivo* experiments in a mice model of seizure suggested protection by CBZ-NLC against seizures for at least 2 hours after intra peritoneal administration. The developed CBZ-loaded lipid nanocarriers displayed optimal characteristics of size, shape and drug release and possibly represent a promising tool to improve the treatment of refractory epilepsy linked to efflux transporters up regulation. [23]

Nancy Abdel Hamid Abou Youssef *et al.*, 2018 designed efficient safe delivery system for intranasal (IN) brain targeting of the water-soluble anti- migraine drug Almotriptan malate (ALM). Solid lipid nanoparticles (SLNs) were prepared by w/o/w double emulsion-solvent evaporation method, selectively chosen for entrapping hydrophilic drugs in SLNs. Selection of the optimized SLNs formula was based on evaluating particle size (PS), poly dispersity index (PDI) and entrapment efficiency (%EE). The selected SLNs formula with highest %EE and small PS, was air-dried and dispersed in an optimized mucoadhesive thermo-sensitive *in-situ* gel, after extensive studies, to enhance nasal residence time and hence its bioavailability. Pharmacokinetic and bio-distribution evaluation revealed that intranasal *in-situ* gel-based formulae, NF (SLNs based) is a good candidate for ALM nose to brain targeting, as it showed obvious fast ALM brain delivery; Tmax/brain was 10 min., Cmax/brain was double that of ND (Free ALM based) and I.V. The calculated targeting indices (DTE% and DTP%) confirmed the capability of both NF and ND for ALM nose to brain targeting. Biomarkers' evaluation and histopathological examination results indicated the higher safety profile of NF (*in-situ* gel based SLNs) for nasal administration. It didn't show any signs of cell necrosis, mucosal damage or cilia loss, with safe biomarker levels. Finally, the designed NF of Pr-SLNALM in C4 *in-situ* gel, combined a well reputed vector that preferentially targets receptors in the olfactory region, enhancing ALM absorption and its targeting to brain, bypassing the BBB, using a safe delivery system with a rapid onset even faster than in case of intravenous route, and a preferentially greater amount. [24]

Giulia Graverini *et al.*, 2018 stated that Novel nano formulations based on drug delivery systems offer significant promise in overcoming the limitations of Andrographis.SLN were prepared using Compritol 888 ATO as solid lipid and Brij 78 as surfactant and applying emulsion/ evaporation/solidifying method as preparative procedure. Nanoparticles have a spherical shape, small dimensions, and narrow size distribution. Encapsulation efficiency of AG-loaded SLN was found to be 92%. Nanoparticles showed excellent physical and chemical stability during storage at 4 ◦C for one month. The lyophilized product was also stable at 25 ◦C during the same period. SLN remained unchanged also in the presence of human serum albumin and plasma. In vitro release at pH 7.4 was also studied. The release of AG was prolonged and sustained when the compound was entrapped in SLN. The ability of SLN to cross

the blood-brain barrier (BBB) was evaluated first in vitro by applying a permeation test with artificial membrane (parallel artificial membrane permeability assay, PAMPA) to predict passive and transcellular permeability through the BBB, and then by using hCMEC/D3 cells, a well-established in vitro BBB model. In vitro results proved that nanoparticles improved permeability of AG compared to free AG. Fluorescent nanoparticles were then prepared for in vivo tests in healthy rats. After intravenous administration, fluorescent SLN were detected in brain parenchyma outside the vascular bed, confirming their ability to overcome the BBB. [25]

Yuan Ding *et al.*, 2018 incorporated nicotine in lipid nanoparticles as an effective tool to minimize its irritation potential and to use the particles as intermediate to produce final products. However, as a hydrophilic active, it was a challenge to prepare nicotine loaded lipid nanoparticles with high drug loading. They formed lipid-drug-conjugates (LDC) by nicotine and different fatty acids to enable the production of sufficiently loaded nicotine lipid nanoparticles. The encapsulation efficiency of nicotine in LDC-containing SLN was about 50%, which increased at least fourfold compared to the non-LDC formulations (around 10%) due to the increased lipophilicity of nicotine by strong interactions between positively charged nicotine and negatively charged fatty acids (formation of LDCs). The z-average of all formulations (150 to 350 nm) proved to be in the required submicron size range with a narrow size distribution. In case loading with nicotine itself (not conjugate) is desired, the option of further increasing the pH of SLN nanosuspensions exists, which will be unproblematic when incorporating these SLN into nicotine chewing gum or lozenges.[26]

Rasha Shtay *et al,* 2018 were motivated by the development of solid lipid nanoparticles (SLNs) for food applications. A focus of the study is the use of a factorial design to optimize the preparation variables. SLNs were prepared by hot homogenization at 60 °C. Cocoa butter was used to form the lipid core and the surfactant blend used to emulsify and stabilize the system was a mixture of sodium stearoyl-2-lactylate (SSL) and mono and di-glycerides of fatty acids (MDG). The main purpose of the experimental design is to establish a causal relationship between independent and dependent process variables. A two levels full factorial design with three center points was employed to investigate the influence of four variables in

order to optimize the solid lipid nanoparticle preparation. The required number of experiments for an experimental design with two levels is in general 2k, where k is the number of variables. Four variables were used in the present study, therefore the necessary number of experiments was 24 ¼ 16. The particle size, PI and ZP values obtained from the 20 experiments including four experiments at the center points. The particle characteristics and stability of obtained SLN-suspensions were investigated. Moreover, the effect of various cooling conditions on the properties of SLNs and the storage stability during a period of three months were examined. Results proved that cocoa butter is suitable to prepare SLNs with a food-grade quality where the optimized preparation variables resulted in a particle size of 112.7 nm. [27]

Aleksandra Zielińska *et al.*, 2018 mention that Two mono-terpenes (citral and geraniol) were firstly tested for their anti-inflammatory activity in a RAW 264.7 cell line, demonstrating citral to have enhanced capacity to inhibit NO production (ca. 84% for citral and 52% for geraniol at the lowest tested concentration of 5 μg/ml). As citral showed higher NO inhibitory activity than geraniol, to measure the level of cytotoxicity of citral. Citral exhibited a strong cytotoxic effect in both cell lines. An optimized solid lipid nanoparticles (SLNs) formulation for citral was further developed by design of experiments (22 factorial design), followed by accelerated stability testing (LUMiSizer®). A factorial design approach was applied to maximize the experimental efficiency requiring a minimum of experiments to optimize the SLN production. The influence of the surfactant ratio (Poloxamer 188) and lipid ratio (Imwitor® 900 K) on citral loaded SLNs was evaluated by using a 22 factorial design composed of 2 independent variables (surfactant and lipid concentrations) which were set at 2-levels each. An optimal SLN composed of 1 wt.% of citral, 4 wt.% of lipid and 2.5 wt.% surfactant were successfully produced by hot high-pressure homogenization (hot HPH) showing a mean particle size (Z-Ave) of 97.7 nm and polydispersity index of 0.249. The produced formulations were analysed in a high-end dispersion analyser LUMiSizer® to characterize any de-mixing phenomena, demonstrating to be long-term stable at room temperature (25ºC), exhibiting very low instability indices. [28]

Fabiano Yokaichiya *et al.*, 2017 developed alternative drug delivery carriers, with a focus on cancer treatment with reduced side effects, is a primary goal of recent cancer research. They observed that sodium tetra decyl sulfate (STS) containing and

soybean-oil based carriers are more efficient in reducing the viability of HeLa cells tumor cells in comparison to their respective counterparts. They performed structural analysis of soybean oil or Mygliol 812 solid lipid nanoparticle (SLN) based drug delivery systems using the combination of complementary scattering techniques: small angle neutron scattering (SANS) and small angle X-ray scattering (SAXS). Combining both scattering techniques revealed structural characteristics of these systems, such as the cubic structure and the surface fractality via SAXS measurement, and also observe a strongly polydisperse non-fractal objects that varies with the concentration of the Dox in these systems (via SANS measurement) in a large q range, as a complementarily technique to SAXS data. Indications of an unusual orthorhombic structure (observed via SAXS) and the presence of an extrapeak that may indicate the thickness of the lamellae (VSANS), as well as the behaviour of the systems as a function of temperature, still need to be confirmed with other techniques (like WAXS and PDF analysis). Moreover, in order to obtain a more accurate model for these SLN systems, further analysis also needs to be performed combining SANS and SAXSdata of the SLN systems for soybean oil and Mygliol 8126. [29]

Mitali Patel *et al.*, 2017 implement Quality by Design (QbD) concept to Solid Lipid Nanoparticles (SLN) containing Asenapine maleate (AM) in order to identify critical process and formulation variables which can affect product quality such as particle size (PS) and entrapment efficiency (EE). Initially, risk assessment using Ishikawa diagram and preliminary investigation of critical variables was carried out. Two statistical designs were used to optimize critical variables which can affect product quality attributes i.e. PS and EE. PBD and CCD were useful to fully understand influence (main, interactive and quadratic effect) of various variables of high-speed homogenization followed by ultrasonication method and their relative influence on product quality attributes. Plackett Burman Design (PBD) was used to screen 8 variables and results showed that lipid concentration, surfactant concentration and sonication time had significant effect on PS and EE. These critical factors were further optimized using Central Composite Design (CCD), a type of response surface methodology, to assess its effect on PS and EE. Design space was identified and implementation of control strategy for responses generated quality of the desired product. Design space was generated for SLN for reducing intra-batch and inter-batch variability in formulation development process. Analysis of robustness of

design space predicted that the formulation must be prepared in established design space to reduce batch variations. The results conclusively demonstrated the potential of QbD concept to build quality in SLN formulation. [30]

Christos Tapeinos *et al.*, 2017 mentioned Solid Lipid Nanoparticles (SLNs) and Nanostructured Lipid Carriers (NLCs) comprise a category of versatile drug delivery systems that have been used in the biomedical field for >25 years. SLNs and NLCs have been used for the treatment of various diseases including cardiovascular and cerebrovascular, and are considered a standard treatment for the latter, due to their inherent ability to cross the blood brain barrier (BBB). They described basic fabrication techniques of SLNs and NLCs. A detailed description of the reported studies of the last seven years, of active and passive targeting SLNs and NLCs for the treatment of glioblastoma multiforme and of other brain cancers, as well as for the treatment of neurodegenerative diseases are also carried out. Finally, a brief description of the advantages, the disadvantages, and the future perspectives in the use of these nanocarriers is reported, aiming at giving an insight of the limitations that have to be overcome in order to result in a delivery system with high therapeutic efficacy and without the limitations of the existing nano-systems. [31]

Dalia M.N. Abouhussein *et al.*, 2017 promoted the bioavailability and the brain delivery of rivastigmine tartarate (RV) through optimization of muco-adhesive thermo sensitive *in situ* gel via intranasal (IN) route. The muco-adhesive in situ gels were developed using pluronic F127 (PF127) as thermo gelling agent and different muco-adhesive polymers. A full factorial design was implemented to study the influence of three factors; pluronic type at two levels (PF127, PF127/PF68), muco-adhesive polymer type at four levels (HPMC, Chitosan, Carbopol 934 and NaCMC) and muco-adhesive polymer concentration at two levels. They studied responses were sol-gel temperature, consistency, gel strength, adhesion work and T50% of drug release. In vivo pharmacokinetic and bio distribution studies of the selected formula were investigated using radiolabelling approach using normal albino mice. The optimal RV *in situ* gel (PF127 and 1% Carbopol 934) showed significant transnasal permeation (84%) which was reflected in better distribution to the brain (0.54 %ID/g), when compared to RV IN solution (0.16 % ID/g) and RV IV intravenous solution (0.15 %ID/g). In conclusion, the investigated results showed the potential use of

muco-adhesive *in situ* gel as a promising system for brain targeting of RV via the trans nasal delivery system.[32]

Preeti Wavikar *et al.*, 2017 explores the potential of Nanostructured Lipid Carriers (NLCs) for nose to brain delivery of Rivastigmine (RV), which is further enhanced by incorporating into an *in-situ* gelling system, increasing retention in nasal cavity. NLC was fabricated by a scalable method. Pharmacokinetics showed sustained release of intranasal (IN) and intravenous (IV) NLC's compared to RV solution by same route, with significantly higher AUC. Bio distribution indicated blood brain barrier (BBB) penetrating potential of IV NLCs and IN NLCs) with 4.6 and 5.3-fold enhancement in brain concentrations compared to IV and IN solution of RV solution. Similar results reflected in pharmacodynamics, indicating faster regain of memory loss in amnesic mice with 5-fold decrease in escape latency with NLC's compared to plain RV solution by IV and IN routes respectively. Sub-acute toxicity studies demonstrated safety of developed formulations to vital organs without any hematological and biochemical changes compared to control group. Moreover, nasal toxicity studies of NLC's showed no signs of inflammation, maintaining the integrity of ciliary epithelial cell, thus confirming safety of the formulation for its intended nasal application [33]

Patrícia Severino *et al.*, 2017 assumed development of new drug entities via biotechnological processes is however expensive and time-consuming. Polymyxin is known for its serious adverse side effects, such as nephrotoxicity, neurotoxicity and promotion of skin pigmentation. To overcome these limitations, the use of biodegradable nanoparticles has been proposed to allow site-specific targeting, increasing the drug's bioavailability and decreasing its side effects. development of an optimized pharmaceutical formulation composed of solid lipid nanoparticles (SLN) loading polymyxin B sulphate (PLX) for the treatment of bacterial infections. The PLX-loaded SLN were produced by a double emulsion method (w/o/w), obtaining particles with a mean size of approximately 200 nm, polydispersity of 0.3 and zeta potential of -30 mV. The encapsulation efficiency reached values above 90% for all developed formulations. SLN remained stable for a period of 6 months of storage at room temperature. The occlusive property of the SLN was shown to be dependent on the type of lipid, while the antimicrobial properties of PLX-loaded SLN were effective against resistant strains of *Pseudomonas aeruginosa*. Results from the

differential scanning calorimetry (DSC), wide angle x-ray diffraction (WAXD) and small angle x-ray scattering (SAXS) analyses confirmed the crystallinity of the inner SLN matrices, suggesting the capacity of these particles to modify the release profile of the loaded drug. [34]

Ahmed M Fatouh *et al.*, 2017 prioritized to enhance its absolute bioavailability, and second to increase its brain delivery. To achieve that, the nasal route was adopted to exploit first its avoidance of the hepatic first-pass metabolism to increase the absolute bioavailability, and second the direct nose-to-brain pathway to enhance the brain drug delivery. Solid lipid nanoparticles were selected as a drug delivery system to enhance agomelatine permeability across the blood–brain barrier and therefore its brain delivery. The optimum solid lipid nanoparticles have a particle size of 167.70 nm ±0.42, zeta potential of -17.90 mV ±2.70, polydispersity index of 0.12±0.10, entrapment efficiency % 91.25%±1.70%, the percentage released after 1 h of 35.40%±1.13% and the percentage released after 8 h of 80.87%±5.16%. The pharmacokinetic study of the optimized solid lipid nanoparticles revealed a significant increase in each of the plasma peak concentration, the AUC (0–360 min) and the absolute bioavailability compared to that of the oral suspension of Valdoxan® with the values of 759.00 ng/mL, 7,805.69 ng·min/mL and 44.44%, respectively. The optimized solid lipid nanoparticles gave a drug-targeting efficiency of 190.02, which revealed more successful brain targeting by the intranasal route compared with the intravenous route. The optimized solid lipid nanoparticles had a direct transport percentage of 47.37, which indicates a significant contribution of the direct nose-to-brain pathway in the brain drug delivery. The intranasal administration of agomelatine solid lipid nanoparticles has effectively enhanced both the absolute bioavailability and the brain delivery of agomelatine. [35]

Yung-Chih Kuo Shih-Jue Cheng *et al.*, 2016 Solid lipid nanoparticles (SLNs) conjugated with tamoxifen (TX) and lecto ferrin (Lf) were applied to carry anticancer carmustine (BCNU) across the blood–brain barrier (BBB) for enhanced anti-proliferation against glioblastoma multiforme (GBM). BCNU-loaded SLNs with modified TX and Lf (TX-Lf-BCNU-SLNs) were used to penetrate a monolayer of human brain-micro vascular endothelial cells (HBMECs) and human astrocytes and to target malignant U87MG cells. The surface TX and Lf on TX-Lf-BCNU-SLNs

improved the characteristics of sustained release for BCNU. When compared with BCNU-loaded SLNs, TX-Lf-BCNU-SLNs increased the BBB permeability coefficient for BCNU about ten times. In addition, TX-BCNU-SLNs considerably promoted the fluorescent intensity of intracellular aceto methoxy derivative of calcein (calcein-AM) in HBMECs via endocytosis. However, the conjugated Lf could only slightly increase the fluorescence of calcein-AM. Moreover, the order of formulation in the inhibition to U87MG cells was TX-Lf-BCNU-SLNs > TX-BCNU-SLNs > Lf-BCNU-SLNs > BCNU-SLNs. TX-Lf-BCNU-SLNs can be effective in infiltrating the BBB and delivering BCNU to GBM for future chemotherapy application. [36]

Eameema Muntimadugu *et al.*, 2016 noticed the poor brain penetration of tarenflurbil (TFB) was one of the major reasons for its failure in phase III clinical trials conducted on Alzheimer's patients. Thus, there was a tremendous need of developing efficient delivery systems for TFB. They designed a study with the aim of improving drug delivery to brain through intranasally delivered nanocarriers. TFB was loaded into two different nanocarriers i.e., poly (lactide-co-glycolide) nanoparticles (TFB-NPs) and solid lipid nanoparticles (TFB-SLNs). Particle size of both the nanocarriers (<200 nm) as determined by dynamic light scattering technique and transmission electron microscopy, assured transcellular transport across olfactory axons whose diameter was ≈200 nm and then paving a direct path to brain. *In vitro* release studies proved the sustained release of TFB from TFB-NPs and TFB-SLNs in comparison with pure drug, indicating prolonged residence times of drug at targeting site. Pharmacokinetics suggested improved circulation behavior of nanoparticles and the absolute bio availabilities followed this order: TFB-NPs (i.n.) > TFB-SLNs (i.n.) > TFB solution (i.n.) > TFB suspension (oral). Brain targeting efficiency was determined in terms of %drug targeting efficiency (%DTE) and drug transport percentage (DTP). The higher %DTE (287.24) and DTP (65.18) were observed for TFB-NPs followed by TFBSLNs (%DTE: 183.15 and DTP: 45.41) among all other tested groups. These encouraging results proved that therapeutic concentrations of TFB could be transported directly to brain via olfactory pathway after intranasal administration of polymeric and lipidic nanoparticles. [37]

Kalpana Nagpal *et al.*, 2015 formulated brain targeted nanoparticles (NP) of Rivastigmine (RT) to improve its therapeutic potential and to verify its safety profile. The NP were optimized using a two factor three level (32) central composite design aiming to minimize particle size; maximize zeta potential and drug entrapment efficiency of NP. The optimized formulation (cRTNP) was evaluated using in vitro drug release study; in vivo behavioural, and biochemical and maximum tolerated dose (MTD) study. The optimized formulation evidenced a significant reversal of scopolamine-induced amnesia by Tween 80® coated nanoparticles as compared to both pure RT as well as uncoated nanoparticles. T80 coated RTNP of CS were prepared u sing ionotropic gelation method with narrow size distribution. The MTD of RT was increased by 10% by formulating them as cRTNP. Thus, formulation of RT as cRTNP improved the therapeutic and safety profile of RT. [38]

Sara Laserra *et al.*, 2015 described the preparation, physicochemical characterization, release, and in vitro cytotoxicity of stealth SLNs as innovative approach to improve solubility and absorption through the gastrointestinal tract of lipoyl–memantine (LA–MEM), a potential anti-Alzheimer codrug. They prepared SLNs according to a slight modification of the emulsification–evaporation–solidifying method. The new nanoparticulate delivery system loaded with LA–MEM was successfully prepared and characterized in terms of physico-chemical properties, entrapment efficiency, and release profile in simulated gastrointestinal fluids. The data obtained from preliminary in vitro biological tests revealed that SLNs–LA–MEM could be tested as a suitable DDS for the brain since they resulted safe from toxicological point of view. [39]

Brijesh Shah *et al.*, 2015 Quality by Design (QbD) approach were applied on the development and optimization of solid lipid nanoparticle (SLN) formulation of hydrophilic drug rivastigmine (RHT). RHT SLN was formulated by homogenization and ultra-sonication method using Compritol 888 ATO, tween-80 and poloxamer-188 as lipid, surfactant and stabilizer respectively. The effect of independent variables (X1 – drug: lipid ratio, X2 – surfactant concentration and X3– homogenization time) on quality attributes of SLN i.e. dependent variables (Y1 – size, Y2 – PDI and Y3 - %entrapment efficiency (%EE)) were investigated using 33 factorial design. Multiple linear regression analysis and ANOVA were employed to indentify and estimate the 2

main effect, 2FI, quadratic and cubic effect. Optimized RHT SLN formula was derived from an overlay plot on which further effect of probe sonication was evaluated. Final RHT SLN showed narrow size distribution (PDI- 0.132 ± 0.016) with particle size of 82.5 ± 4.07 nm and %EE of 66.84 ± 2.49. DSC and XRD study showed incorporation of RHT into imperfect crystal lattice of Compritol 888 ATO. In comparison to RHT solution, RHT SLN showed higher *in-vitro* and *exvivo* diffusion. The diffusion followed Higuchi model indicating drug diffusion from the lipid matrix due to erosion. Histopathology study showed intact nasal mucosa with RHT SLN indicating safety of RHT SLN for intranasal administration. [40]

Mirza Salman *et al.*, 2015 developed and optimized levofloxacin loaded solid lipid nanoparticles for the treatment of conjunctivitis. Box-Behnken experimental design was applied for optimization of solid lipid nanoparticles. The independent variables were stearic acid as lipid (X1), Tween 80 as surfactant (X2) and sodium deoxycholate as cosurfactant (X3) while particle size (Y1) and entrapment efficiency (Y2) were the dependent variables. Further in vitro release and antibacterial activity in vitro were also performed. Results demonstrate that using stearic acid as lipid, Tween 80 and sodium deoxycholate as surfactant and co-surfactant respectively increases levofloxacin entrapment, and produces SLN with the desired size, size distribution, and morphological properties. The levofloxacin-SLN obtained in vitro release experiments exhibited a biphasic release pattern with burst release at the initial phase followed by sustained release. The optimized formulation of levofloxacin provides particle size of 237.82 nm and showed 78.71% entrapment efficiency and achieved flux 0.2493 μg/cm2/h across excised goat cornea. In vitro release study showed prolonged drug release from the optimized formulation following Korsmeyer- Peppas model. Antimicrobial study revealed that the developed formulation possesses antibacterial activity against *S. aureus*, and *E. coli* equivalent to marketed eye drops. HET-CAM test demonstrated that optimized formulation was found to be non-irritant and safe for topical ophthalmic use. Their results concluded that solid lipid nanoparticles are an efficient carrier for ocular delivery of levofloxacin and other drugs. [41]

Balaram Gajra *et al.*, 2015 intended to develop and optimize sustained release of biodegradable chitosan nanoparticles (CSNPs) as delivery vehicle for sodium cromoglicate (SCG) using the circumscribed Box–Behnken experimental design (BBD) and evaluate its potential for oral permeability enhancement. The 3-factor, 3-level BBD was employed to investigate the combined influence of formulation variables on particle size and entrapment efficiency (%EE) of SCG-CSNPs prepared by ionic gelation method. The generated polynomial equation was validated and desirability function was utilized for optimization. Optimized SCG-CSNPs were evaluated for physicochemical, morphological, in-vitro characterizations and permeability enhancement potential by ex-vivo and uptake study using CLSM. SCG-CSNPs exhibited particle size of 200.4 ± 4.06nm and %EE of 62.68 ± 2.4% with unimodal size distribution having cationic, spherical, smooth surface.Physicochemical and *invitro* characterization revealed existence of SCG in amorphous form inside CSNPs without interaction and showed sustained release profile. Ex-vivo and uptake study showed the permeability enhancement potential of CSNPs. The developed SCG-CSNPs can be considered as promising delivery strategy with respect to improved permeability and sustained drug release, proving importance of CSNPs as potential oral delivery system for treatment of allergic rhinitis. Hence, further studies should be performed for establishing the pharmacokinetic potential of the CSNPs. [42]

Andjelka B *et al.*, 2013 develop solid lipid nanoparticles (SLN) stabilized with poly hydroxy surfactants varying in the chemical structure and to investigate the influence of the surfactants on the characteristics of the particles. Particles were produced by hot high-pressure homogenization and the physico-chemical properties, e.g. contact angle, particle size, size distribution, zeta potential and crystallinity were determined. Results showed that the chemical structure of the surfactants influences the contact angle, particle size and crystallinity. Furthermore, the low surfactants concentration used (1% (w/w)) allowed the formation of the particles with a mean size below 200 nm, polydispersity index lower than 0.1 and sufficient physical stability for at least 6 months. As postulated by the zeta potential analysis stabilization ability of the surfactants was attributed to the superposition of electrostatic and steric effect which complements each other. All SLN formulations consisted of the same lipid matrix, but were found to possess different crystallinity indices. These differences are obviously created by the differences in the chemical structure of the

surfactants. Polyhydroxy surfactants investigated were proven to be suitable stabilizers for SLN. The stabilizers were also found to influence the crystalline state of the particles. A more crystalline matrix of the particles was obtained with the solid lipid tail surfactants with a relatively high contact angle on the solid lipid used as particle matrix, low HLB values and a melting point above the melting point of the SLN matrix. Due to the promoting effect on the crystallinity of the particles these so called "solid lipid" tail surfactants might be used for the development of the lipid nanoparticles with high oil content and thus improved loading capacity. On the other side, the "liquid lipid" tail stabilizers and sucrose palmitate, with a fatty acid chain length similar to the lipid matrix and melting point below the melting point of the SLN did not influence the crystallinity. [43]

Vandita Kakkar *et al.*, 2013 defined a significant bioavailability of curcumin by its incorporation into SLNs (C-SLNs) during pharmacokinetic (32–155 times) and pharmacodynamic (3–4 times) studies, their intent was to proof their targeting to brain. Hence, fluorescent/confocal microscopy, biodistribution and gamma scintigraphy techniques were explored to observe the presence of C-SLNs in the brain. 1 h post p.o administration of C-SLNs/free curcumin (C-S) to rats, blood was withdrawn, following which the animals were sacrificed and their harvested brains were frozen at −80 ◦C. The obtained plasma and brain cryosections were observed for fluorescence under fluorescent/confocal microscope. Biodistribution study was performed using 99mTc-labeled C-SLNs and C-S in Balb/c mice after p.o. and i.v. administration and % radioactivity/g organ was recorded. Subsequent to this gamma scintigraphs of the New Zealand rabbits following similar treatments were performed. Presence of yellow fluorescent particles in plasma and brain indicated effective delivery of C-SLNs across the gut wall and the BBB. Blood AU Coral value for C-SLNs was 8.135 times greater than that for C-S, confirming a prolonged circulation of former. The ratio of blood AUC i.v. C-SLN/C-S in blood is ≤1 while the ratio in brain promisingly indicates 30 times higher preferential distribution of C-SLNs into brain confirming their direct delivery. [44]

Jeetendra Singh Negi *et al.*, 2012 prepared Solid lipid nanoparticles (SLNs) of poor orally bioavailable drug lopinavir using hot self nano-emulsification (SNE) technique. Hot isotropic mixture of stearic acid, poloxamer and polyethylene glycol was spontaneously self nano-emulsify in hot water and SLNs were formed with

subsequent rapid cooling. Self nano-emulsification ability of stearic acid, poloxamer and polyethylene glycol mixture was assessed by ternary phase diagram study. Only hand shaking was good enough for rapid formation of SLNs. The particle size, shape, entrapment efficiency and stability of optimized SLNs were found appropriate for drug delivery. The good EE and drug loading were observed for LOP due to good miscibility of LOP in SA. The oral bioavailability of LOP was also improved due to higher intestinal lymphatic uptake of LOP-SLNs. This avoids both p-GP efflux transport as well as CYP450 3A mediated first pass metabolism of LOP. SLNs were evaluated by transmission electron microscopy (TEM) and atomic force microscopy (AFM) for morphological study. Further, Differential scanning calorimetry (DSC) and X-ray diffraction (XRD) of SLNs were also performed for checking solid state characterization. Higher oral bioavailability was found for lopinavir loaded SLNs in comparison to bulk lopinavir due to higher lymphatic drug transport ($p < 0.05$). Thus, SLNs can be prepared by a low cost and energy efficient hot SNE technique for oral bioavailability enhancement. [45]

Panakanti Pavan Kumar *et al.*, 2012 stated that Homogenization followed by ultrasonication method is suitable to produce SLN of 50–125 nm size ranges. They described the formulation of Atorvastatin (ATRS) loaded solid lipid nanoparticles by hot homogenization fallowed by ultrasonication technique, and optimization of formulation and process parameters to formulate preferred SLN dispersions. The effects of composition of lipid materials, surfactant mixture and sonication time on particle size, PDI, zeta potential, drug entrapment efficiency, and in vitro drug release behaviour were investigated The mean particles size, PDI, zeta potential and entrapment efficiency of optimized formulation (A5) was found to be 50.0± 6.12 nm, 0.08±0.011,10.40± 4.68mV, 88.7± 6.08 % respectively. To characterize the state of drug and lipid modification in ATRS loaded solid lipid nanoparticles, differential scanning calorimetry analysis was performed. Shape and surface morphology were determined by Transmission Electron Microscopy (TEM) which revealed fairly spherical shape of nanoparticles. The results of the in-vitro drug release studies demonstrated, significantly low release of ATRS (40.68%) from ATRS-SLN as compared to dispersion of pure drug (98.4 %). In vitro release of ATRS followed Higuchi and Weibull equations better than first-order equation. This system is most suitable for exploiting lymphatic transport pathway for improving oral bioavailability of ATRS. The in-vitro drug release study demonstrated that ATRS-SLN formulation

(A5) possessed controlled drug release over a period of 24 hourrs than dispersion of pure drug. Stability studies performed on the selected formulations revealed that there was no physical instability of the developed formulation for a period of 3 months at room and refrigerated temperatures. These data collectively support that SLNs are the promising delivery systems for poorly water-soluble drugs, such as ATRS. [46]

Mohammad Fazil *et al.*, 2012 prepared rivastigmine (RHT) loaded chitosan nanoparticles (CS-RHT NPs) by ionic gelation method to improve the bioavailability and enhance the uptake of RHT to the brain via intranasal (i.n.) delivery. CS-RHT NPs were characterized for particles size, particle size distribution (PDI), encapsulation efficiency, zeta potential and in vitro release study. The results indicated that with an increase in the concentration of either CS or TPP particle size increased. Nose-to-brain delivery of placebo nanoparticles (CSNPs) was investigated by confocal laser scanning microscopy technique using rhodamine-123 as a marker. The biodistribution and pharmacokinetic study in Wistar rats, in which the DTE% and DTP% are more indicative of direct nose to brain transport bypassing the BBB there by proving the superiority of CS-RHT NPs over RHT solution i.v. The qualitative biodistribution study by CLSM also demonstrated the existence of nose to brain transport of CS-RHT NPs as compared to RHT solution i.v. and i.n. On the basis of these research findings, it was concluded that CSRHT NPs could be a novel colloidal drug delivery system for the treatment of Alzheimer's disease via nose to brain. [47]

Carla Vitorino *et al.*, 2011 investigated the role of different factors affecting the size of solid lipid nanoparticles (SLN), prepared by the emulsification–solvent evaporation method. A double factorial design was conducted so as to cover a wide range of sizes, highlighting zones with different behaviour with respect to changes in the controlled variables: lipid concentration, solvent: lipid ratio and emulsifier concentration. The solvent: lipid ratio constituted the main factor influencing particle size. Increasing the amount of solvent induced a decrease in the size. This was a general trend, essentially independent from solvent and lipid type. The amount of emulsifier had a non-trivial impact on size, depending on whether systems were located below, above or close to the optimal surface coverage. The amount of lipid had a limited influence upon particle size, being more relevant for lower lipid concentrations. An optimal formulation was selected for intermediate levels of the

three variables. Sonication reduced both particle size and polydispersity. These particles were also tested as drug carriers using simvastatin as a model of lipophilic drug. SLN were able to entrap a high amount of simvastatin, with little effect upon size and zeta potential, constituting a promising carrier for lipophilic drugs. [48]

Sanju Dhawan *et al.*, 2010 formulated solid lipid nanoparticles (SLNs) of quercetin, a natural flavonoid with established antioxidant activity, for intravenous administration in order to improve its permeation across the blood–brain barrier into the CNS, and eventually to improve the therapeutic efficacy of this molecule in Alzheimer's disease. The SLNs of quercetin were formulated using Compritol as the lipid and Tween 80 as the surfactant through a microemulsification technique, and optimized employing a 32 central composite design (CCD). Selection of the optimized SLN formulation, using brute force methodology and overlay plots, was based on its efficiency of entrapping quercetin inside the lipophilic core, particle size, surface charge potential and ability of the SLNs to release the entrapped drug completely. The optimized formulation was subjected to various in-vivo behavioural and biochemical studies in Wistar rats. The optimized formulation exhibited a particle size of less than 200 nm, 85.73% drug entrapment efficiency and a zeta potential of 21.05 mV. In all the in-vivo behavioural and biochemical experiments, the rats treated with SLN-encapsulated quercetin showed markedly better memory-retention vis-à-vis test and pure quercetin-treated rats. Besides, the maintenance of lipid peroxidation, glutathione and nitrite levels in the brain homogenates of these rats also corroborated successful targeting of quercetin-loaded SLNs into the CNS. Hence, the significant reversal of aluminium induced neurotoxicity achieved by employing quercetin loaded SLNs indicates the immense potential of SLNs as a platform technology to target various natural and synthetic molecules to the brain to improve their efficacy in various CNS disorders. The studies demonstrated successful targeting of the potent natural antioxidant, quercetin, to brain as a novel strategy having significant therapeutic potential to treat Alzheimer's disease. [49]

Sanjay Singh *et al.*, 2010 developed solid lipid nanoparticles (SLN) of a hydrophilic drug Zidovudine (an anti-human immunodeficiency viral agent) and improve the entrapment efficiency of the drug in SLN. The SLN were prepared with stearic acid by process of w/o/w double-emulsion solvent-evaporation method using

3^2 factorial design. Different triglycerides alone and in different combinations, with/without stearic acid were used to prepare SLN using similar procedure. Two operating variables, polyvinyl alcohol concentration and amount of lipid were found to have significant effect on the particle size and entrapment efficiency (EE) of the SLN. The maximum EE was found to be ca. 27% with particle size of 621 nm which was significantly higher than that reported earlier. A comparative study of the fabricated SLN using fatty acid (SA) and TG and their combinations clearly shows the superior capacity of the fatty acids over TGs to encapsulate the model hydrophilic drug. The optimized batch was also analyzed for its morphological, physiochemical and drug release properties. EE of batches with triglycerides were significantly less than that achieved with stearic acid alone. It indicated the possible advantage of fatty acids over triglycerides in the entrapment of hydrophilic drugs in SLN.[50]

Maria Luisa Bondì *et al.*, 2010 prepared nanoparticulate systems as drug carriers for riluzole, with sufficiently high loading capacity and small particle size, to a reach therapeutic drug level in the brain. Solid lipid nanoparticles containing riluzole have great potential as drug-delivery systems for amyotrophic lateral sclerosis and were produced by using the warm oil-in-water microemulsion technique. The resulting systems obtained were approximately 88 nm in size and negatively charged. Drug-release profiles demonstrated that a drug release was dependent on medium pH. Bio distribution of riluzole blended into solid lipid nanoparticles was carried out after administration to rats and the results were compared with those obtained by riluzole aqueous dispersion administration. Rats were sacrificed at time intervals of 8, 16 and 30 h, and the riluzole concentration in the blood and organs such as the brain, liver, spleen, heart and kidney were determined. It was demonstrated that these solid lipid nanoparticles were able to successfully carry riluzole into the CNS. Moreover, a low drug biodistribution in organs such as the liver, spleen, heart, kidneys and lung were found when riluzole was administered as drug-loaded solid lipid nanoparticles. Riluzole-loaded solid lipid nanoparticles showed colloidal size and high drug loading, a greater efficacy than free riluzole in rats, a higher capability to carry the drug into the brain and a lower indiscriminate biodistribution. [51]

Sagar D. Mandawgade *et al.*, 2008 developed solid lipid nanoparticles (SLNs) from indigenous, natural solid lipids by using a simple microemulsion technique. Furthermore, they characterized the SLNs and evaluated its potential in the topical delivery of a lipophilic drug, tretinoin (TRN). The developed SLNs were characterized for particle size, polydispersity index, entrapment efficiency of TRN and morphology. TRN-loaded SLN-based topical gels were formulated and the gels were evaluated comparatively with the commercial product with respect to primary skin irritation, in vitro occlusivity and skin permeation. The results of the study showed mean particle size <100nm of the SLN dispersions with the novel lipids. Up to 46% of drug entrapment in the lipids was attained. Lesser skin irritancy, greater skin tolerance, occlusivity and slow drug release was observed with the developed TRN-loaded SLN-based gels than the commercial product. The research work could be concluded as successful production of SLNs using highly purified stearine fraction of natural solid lipids. The results of the characterization and evaluation established the safety for use, suitability and compatibility of indigenous natural lipids as a novel excipient. [52]

Celeste Roney *et al.*, 2005 stated that targeted drug delivery to the central nervous system (CNS), for the therapeutic advancement of neurodegenerative disorders such as Alzheimer's, is complicated by restrictive mechanisms imposed at the blood–brain barrier (BBB). Opsonization by plasma proteins in the systemic circulation is an additional impediment to cerebral drug delivery. They conclude that Polymeric nanoparticles are the promising candidates to deliver drugs beyond the BBB for the scrutiny of the central nervous system. There are challenges ahead of us to resolve the question of binding of the drugs (loaded onto nanoparticles) to amyloid plaques. [53]

3. AIM AND OBJECTIVES

AIM

The aim of the present study is to develop, optimize and evaluate Rivastigmine tartrate loaded solid lipid nanoparticle (RT SLN) by using central composite design.

OBJECTIVES

- To study solubility of RHT in different solid lipids
- To formulate RHT loaded SLN
- To perform preliminary screening of lipids and HSH time and rpm
- To formulate SLN by using microemulsion technique
- To optimize the factors affecting the formulation
- Characterization of RHT loaded SLN
- To perform *in vitro* drug release study and kinetics

PLAN OF WORK

1. Literature survey
2. Characterization of active ingredient
    - Description and Solubility
    - FT-IR spectroscopy
    - DSC
3. Standard calibration curve
    - Estimation of absorption maximum (λ_{max})
    - Preparation of standard curve
4. Formulation Development and optimization
    - Preparation of RT-loaded solid lipid nanoparticles
    - Risk Analysis
    - Screening of lipids, surfactants, HSH rpm and time
    - Compatibility study of selected excipients with drug
    - Central composite design
5. Evaluation of optimized Rivastigmine tartrate SLN
    - Particle size, PDI and Zeta potential
    - Scanning electron microscopy (SEM)
    - Differential scanning calorimetry (DSC)
    - Entrapment efficiency
    - *In vitro* drug release study
    - *In vitro* drug release kinetics

DRUG PROFILE [54, 55, 56, 57]

Drug name : RIVASTIGMINE TARTRATE

Structure :

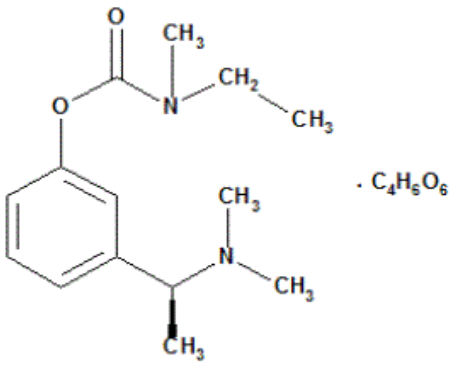

IUPAC Name :(2*R*,3*R*)-2,3-dihydroxybutanedioicacid;[3-[(1*S*)-1(dimethylamino) ethyl] phenyl] *N*-ethyl-*N*-methyl carbamate

Empirical formula : $C_{18}H_{28}N_2O_8$

Molecular weight : 400.4 g/mol

Color : White to off white

Odour : Odourless

Solubility :Very soluble in water, soluble in ethanol and acetonitrile, slightly soluble in n-octanol and very slightly soluble in ethyl acetate

Biological half-life : 1.5 hours

BCS Class : Class I (High Solubility, High permeability)

Bioavailability : 60 to 72%

Log p : 2.45

Density : 145g/ml

Melting point : 123-125°C

Boiling point : 316.2^0C

T_{max} : 2-4 hours

PHARMACOKINETICPARAMETERS:

Route of administration	:	Oral
Elimination half-life	:	5–9 hours in healthy subjects aged 20 to 45
Protein binding	:	40%
Absorption	:	Rivastigmine tartrate is rapidly and completely absorbed. Peak plasma concentrations are reached in approximately 1 hour.
Distribution	:	Rivastigmine tartrate is weakly bound to plasma proteins (approximately 40%) over the therapeutic range. It readily crosses the blood-brain barrier, reaching CSF peak concentrations in 1.4 to 2.6 hours. It has an apparent volume of distribution (VD) in the range of 1.8 to 2.7 L/kg
Metabolism	:	Rivastigmine is rapidly metabolized by cholinesterase mediated hydrolysis.
Excretion	:	Rivastigmine is extensively metabolized primarily via cholinesterase-mediated hydrolysis to the decarbamylated metabolite NAP226-90. Renal excretion of the metabolites is the major route of elimination. Less than 1% of the administered dose is excreted in the feces.

Mechanism of action:

Rivastigmine Tartrate is the tartrate salt form of rivastigmine, a phenyl carbamate derivative exhibiting cognitive stimulating property. Although the mechanism of action has not been fully elucidated, rivastigmine tartrate may bind reversibly to cholinesterase, thereby decreasing the breakdown of acetylcholine and enhancing cholinergic function.

BRAND NAME:

Exelon

DOSAGE FORMS:

Capsules administered through oral route.

- 1.5 mg
- 3 mg
- 4.5 mg
- 6 mg

Oral solution administered through oral route

- 2mg/ml

SIDE EFFECTS:

Common side effects are:

- Diarrhea
- Dizziness
- Hallucinations
- Indigestion
- Nausea
- Vomiting

In frequent side effects

If experienced, these tend to have a severe expression

- Fainting
- High blood pressure
- Slow heartbeat

If experienced, these tend to have a less severe expression

- Anxious feelings
- Decreased appetite
- Depression
- Difficulty sleeping
- Drowsiness

- Excessive sweating
- Generalized weakness
- Head pain
- Low energy
- Stomach cramps
- Urinary tract infection
- Weight loss

Rare side effects

If experienced, these tend to have a severe expression

- A skin disorder with blistering and peeling skin called Stevens-Johnson syndrome
- A type of abnormal movement disorder called Dyskinesia
- Abnormal liver function tests
- Abnormal liver function tests
- Abnormal muscle movements
- An Ulcer from too much stomach acid
- Atrial fibrillation
- Atrio ventricular block, a type of slow heart rhythm disorder
- Bloody vomit
- Dehydration
- Fast heartbeat
- Hepatitis
- Inflammation of skin
- Pancreatitis
- Seizures

If experienced, these tend to have a less severe expression

- A reaction at the site of administration
- Skin rash
- Abnormal manner of walking
- Aggressive behavior
- Agitation
- An acute skin rash
- Blurred vision
- Chest pain
- Contact dermatitis
- Excessive saliva production
- Extrapyramidal disease
- Gastro esophageal reflux disease
- Hives
- Involuntary leakage of urine
- Itching
- Muscle tremors
- Nightmares
- Sensation of spinning or whirling
- Throat irritation
- Trouble breathing

CONTRA INDICATIONS:

- A type of movement disorder called parkinsonism
- Extrapyramidal disease
- Sick sinus syndrome

- Slow heartbeat
- Abnormal heart rhythm
- Asthma
- Stomach or intestinal ulcer
- Bleeding of the stomach or intestines
- A blockage in the urinary tract
- Seizures
- Decreased appetite
- Weight loss
- Vomiting
- Diarrhea
- A chronic lung disease where the airways become partially blocked with mucus called COPD

EXCIPIENT PROFILE

POLOXAMER 188[58, 59]

Synonym : Pluronic F68, Vepoloxamer, Polyethylene-propylene glycol, Poly(ethylene oxide-co-polypropylene oxide) block

IUPAC name : 2-(2-propoxypropoxy) ethanol

Chemical formula : $C_8H_{18}O_3$

Structural formula:

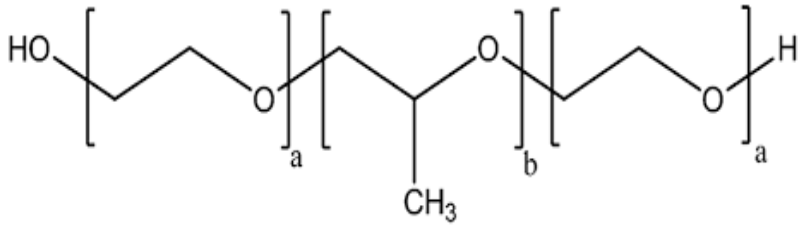

(a=80, b=27)

Molar Mass : 162.23 g/mol

Melting Point : 52-57ºC

Description : White, waxy, odourless, free-flowing prilled granules

Solubility : Freely soluble in 95% ethanol, cold water

Storage : Store in a well-closed container

Functional category:

- Stabilizing agent
- Co-emulsifying agent
- Solubilizing agent
- Tablet lubricant
- Wetting agent

TWEEN 80[60, 61]

Synonym : Polyoxyethylene-sorbitan-20 mono-oleate, Polysorbate 80

IUPAC name : 2-[2-[3, 5-bis (2-hydroxyethoxy)oxolan-2-yl]-2-(2 hydroxy ethoxy) ethoxy] ethyl (E)-octadec-9-enoate

Chemical formula : $C_{32}H_{60}O_{10}$

Structural Formula:

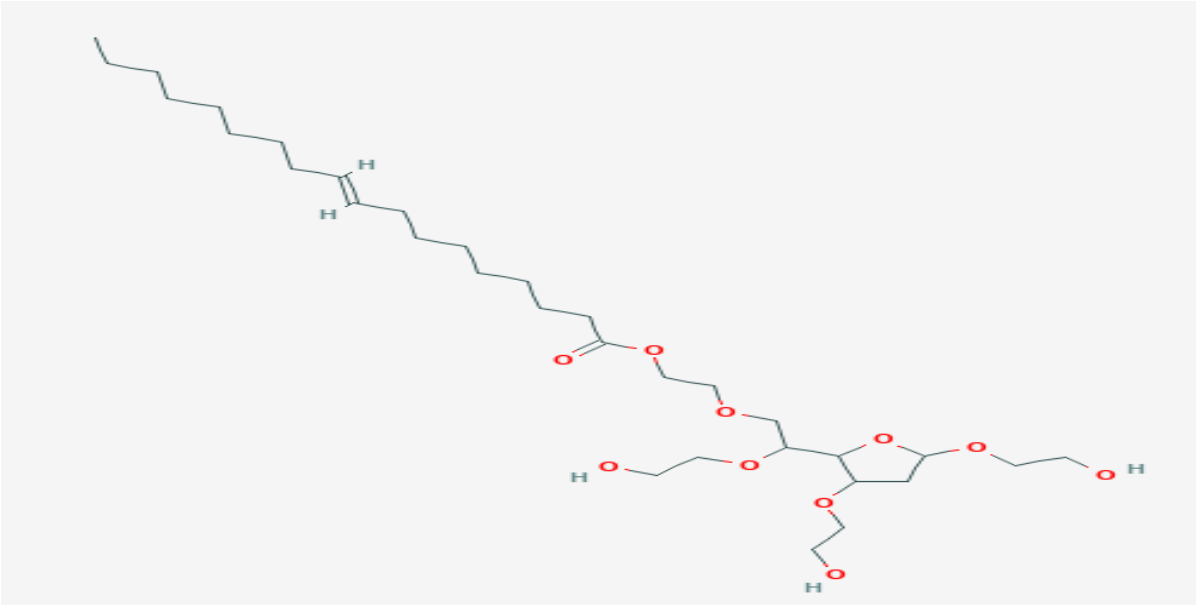

Molar Mass : 604.8 g/mol

Melting Point : 52-57ºC

Description : Yellow to orange colored, oily liquid

Solubility : Very soluble in water, soluble in alcohol, ethyl acetate, methanol

Storage : Store in a well-closed container

Functional category:

- Foaming agent
- Emulsifying agent
- Dispersing agent

GLYCERYL MONOSTERATE [62, 63]

Synonym : Glycerin monostearate, Glycerol monostearate, Glyceroli monostearas, Glyceryl monooctadecanoate, Glyceryl monopalmitostearate, Glyceryl stearate, Monoglyceryl stearate, Monostearate (glyceride), Monostearin,, monoester with glycerol and Stearoylglycerol.

IUPAC Name : 2,3-dihydroxypropyl octadecanoate

Chemical formula : $C_{21}H_{42}O_4$

Structural Formula:

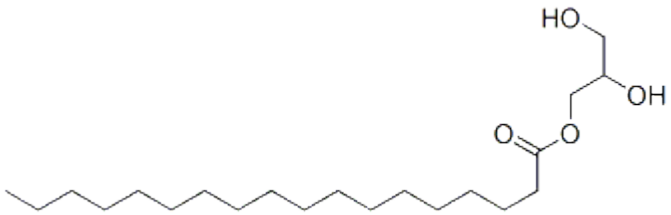

Molecular weight : 358.6 g/mol

Melting Point : 78 - 81ºC

Description : Dry Powder

Solubility : Soluble in hot ethanol, ether, chloroform, practically insoluble in water, but may be dispersed in water with the aid of a small amount of soap or other surfactant.

Functional category:

- Emulsifier
- Thickening agent
- Anti-caking agent
- Antistaling

STERIC ACID [64]

Synonym : n-Octadecanoic acid, Stearophanic acid, Cetyl acetic acid

IUPAC name : Octadecanoic acid

Chemical formula : $C_{18}H_{36}O_2$

Structural formula :

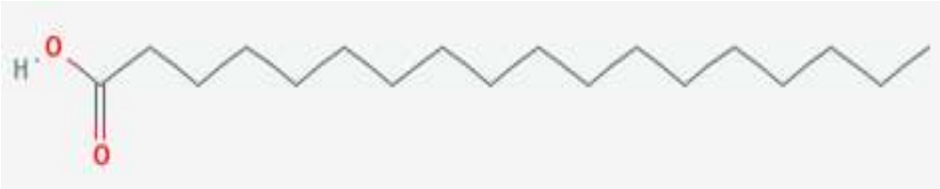

Molar Mass : 284.5g/mol

Melting Point : 69-71ºC

Description : White solid with a mild odour

Solubility : Slightly soluble in ethanol, benzene, soluble in acetone and chloroform

Storage : Store in a well-closed container

Functional category:

- Binding agent
- Emulsifying agent
- Detergent agent
- Tablet lubricant
- Solubilizing agent

GLYCERYL TRI STERATE [65]

Synonym : Tristearin, Glyceryl tristearate, Trioctadecanoin, triacylglycerol

IUPAC name : 2,3-di (octadecanoyloxy) propyl octadecanoate

Chemical formula : $C_{57}H_{110}O_6$

Structural formula :

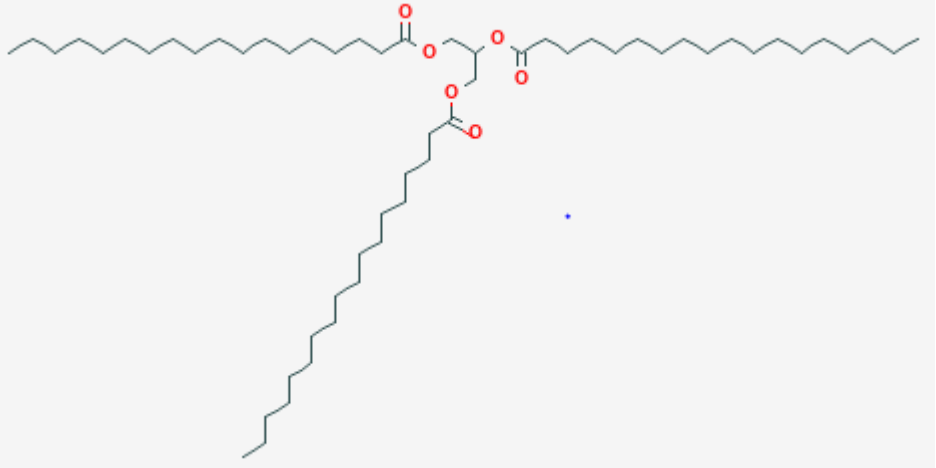

Molar Mass : 891.5 g/mol

Melting Point : 72-75 °C

Description : Solid White powder odorless Tasteless

Solubility : Insoluble in water. Soluble in chloroform, carbon disulfide Insoluble in ethanol; very soluble in acetone, benzene

Storage : Store in a well-closed container

Functional Category:

- Glyceryl Tristearate is a formulation aid, lubricant, and release agent. The additive is used as a crystallization accelerator in cocoa products; a formulation aid in confections; a formulation in fats and oils; and a winterization and fractionation aid in fat and oil processing
- Emollient

COCO MONO ETHANOLAMIDE [66]

Synonym : Coconut fatty acid mono ethanol amide; Cocoyl mono ethanol amine; N-(2-Hydroxyethyl) coco fatty acid amide; Coconut oil fatty acid ethanol amide

IUPAC name : N-(2-hydroxyethyl)dodecanamide

Chemical formula : $CH_3(CH_2)_nCONHCH_2CH_2OH$

Structural formula :

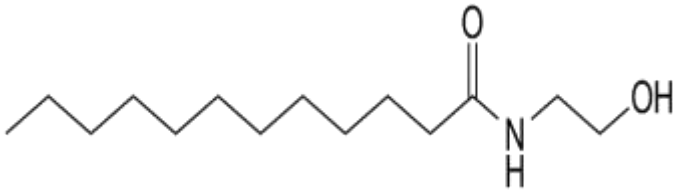

Molar Mass : 284.5g/mol

Melting Point : 60-63ºC

Description : Waxy solid flakes, slight yellow color

Solubility : Slightly soluble in ethanol, benzene, soluble in acetone and chloroform

Storage : Store in a well-closed container

Functional category:

- Foaming agent
- Emulsifying agent
- Detergent agent
- Non-ionic surfactant

MATERIALS AND EQUIPMENTS USED

Sl. NO.	MATERIALS	MANUFACTURES
1	Rivastigmine Tartrate	Gift sample from Alembic pharmaceuticals limited
2	Poloxamer 188	Sigma Aldrich
3	Tween 80	RFCL Ltd
4	Stearic acid	FINAR
5	Glceryl monosterate	Mohini organics Private limited
7	Glyceryl tristerate	Mohini organics Private limited
8	Coco mono ethanolamide	Mohini organics Private limited

Table 5: Materials used in the study

Sl. NO.	EQUIPMENTS	MODEL	MANUFACTURES
1	Digital weighing balance	AX200	Shimadzu Corporation, Japan
2	pH meter	Cyber scan	Eutech Instrument, Singapore
3	UV-Visible Spectrophotometer	UV-1700	Pharmaspec, Shimadzu
4	High speed homogenizer	RO-127A	Cole Parmer
5	Probe sonicator	VT- PROBE 250	V- Tech
6	Bath sonicator	2200MH	LIFE CARE
7	Magnetic stirrer	MLH	REMI
8	Cooling centrifuge	C-30BL	REMI
9	FTIR Spectrophotometer	4100	JASCO
10	Zeta sizer	MAL 1021384	Malvern Instruments Ltd
11	Scanning electron microscopy	JSM 6390	Jeol
12	Differential scanning calorimetry	DSC 60	Shimadzu
13	Glass wares	Borosilicate	Mumbai, India

Table 6: Equipment used in the study

EXPERIMENTAL PROTOCOL

1. CHARACTERIZATION OF ACTIVE INGREDIENT

Drug characterization is one of the essential steps of any formulation development. Drug characterization step involves identification (confirmation) of drug by infra-red spectroscopy and Differential scanning calorimetry.

Description and solubility

The drug substance Rivastigmine tartrate was tested for description and solubility as specified in United States Pharmacopoeia (USP 2014a)

FT-IR Spectroscopy

Fourier Transform Infrared (FT-IR) is an important complementary tool for the solid-state characterization of pharmaceutical solids. IR spectra obtained compared with standard spectrum of pure drug and checked for any shifting in functional peaks and non-involvement of functional group. The samples were studied using FTIR JASCO 4100 in the wavenumber range from 500 to 4,000 cm^{-1}.

Differential scanning calorimetry

The physical state of RT was characterized by Differential Scanning Calorimetry (DSC-60, Shimadzu, Japan). Sample was sealed in standard aluminium pans with lids and purged with air at a flow rate of 40 ml/min. A temperature ramp speed was set at 20 C/min, and the heat flow was recorded in the range of 30–300 C under inert nitrogen atmosphere.

2. ANALYTICAL METHOD FOR RIVASTIGMINE TARTRATE

Calibration curve in phosphate buffer pH7.4

Preparation of Primary Stock Solution:-

Stock solution of RT in distilled water was prepared by accurately weighing 50mg RT and transferred to 50 ml volumetric flask. 50 ml phosphate buffer of pH7.4 was measured accurately and then transferred to volumetric flask. The drug was dissolved properly to produce 1000µg/ml RT. The primary stock solution was stored at 2°C to 8°C.

Preparation of Test solution:-

Suitable aliquots of the standard stock solution of RT were measured accurately using graduated pipette and transferred into 10ml volumetric flasks. The volume was made up to phosphate buffer of pH7.4 to give final concentrations of 10, 20, 30, 40, 50 and 60µg/ml. Determination of UV absorbance maxima of Rivastigmine tartrate:- RT test solution of 10µg/ml was scanned for determination of absorbance maxima on a UV- Visible spectrophotometer. The scanning was carried out in a range of 200- 400nm.

Calibration Curve of Rivastigmine Tartrate:-

The calibration curve of RT was prepared in distilled water. Prepared test solutions were shaken well and the absorbance was measured at 264nm against distilled water as a solvent blank. The above procedure was repeated three times and the mean absorbance was determined. [67]

3. FORMULATION DEVELOPMENT, OPTIMIZATION AND EVALUATION of SOLID LIPID NANOPARTICLES (SLNS) FOR RIVASTIGMINE TARTRATE

Formulation Development

Solid lipid nanoparticles were developed by using strategy of quality by design (QBD) which includes steps of preliminary screening of lipid, surfactant, homogenization speed and time followed by optimization of nano formulation.

Design of Experiment

Design of Experiments (DoE) is the main component of the statistical toolbox to deploy Quality by Design in both research and industrial settings. It should be noted that there are numerous mathematical modelling techniques, for addressing pharmaceutical development and more specifically within the QbD and Process Analytical Technology (PAT) concept.

Quality by Design (QbD) is defined as a systematic approach to development that begins with predefined objectives and emphasizes product and process understanding and process control, based on sound science and quality risk

management. Experimental design is a structured, organized method for determining the relationships between factors affecting a process and the output of that process. It is also known as "Design of Experiments" (DoE). In other words, the latter is the means of achieving process knowledge, through the establishment of mathematical relationships between process inputs and its outputs. [68]

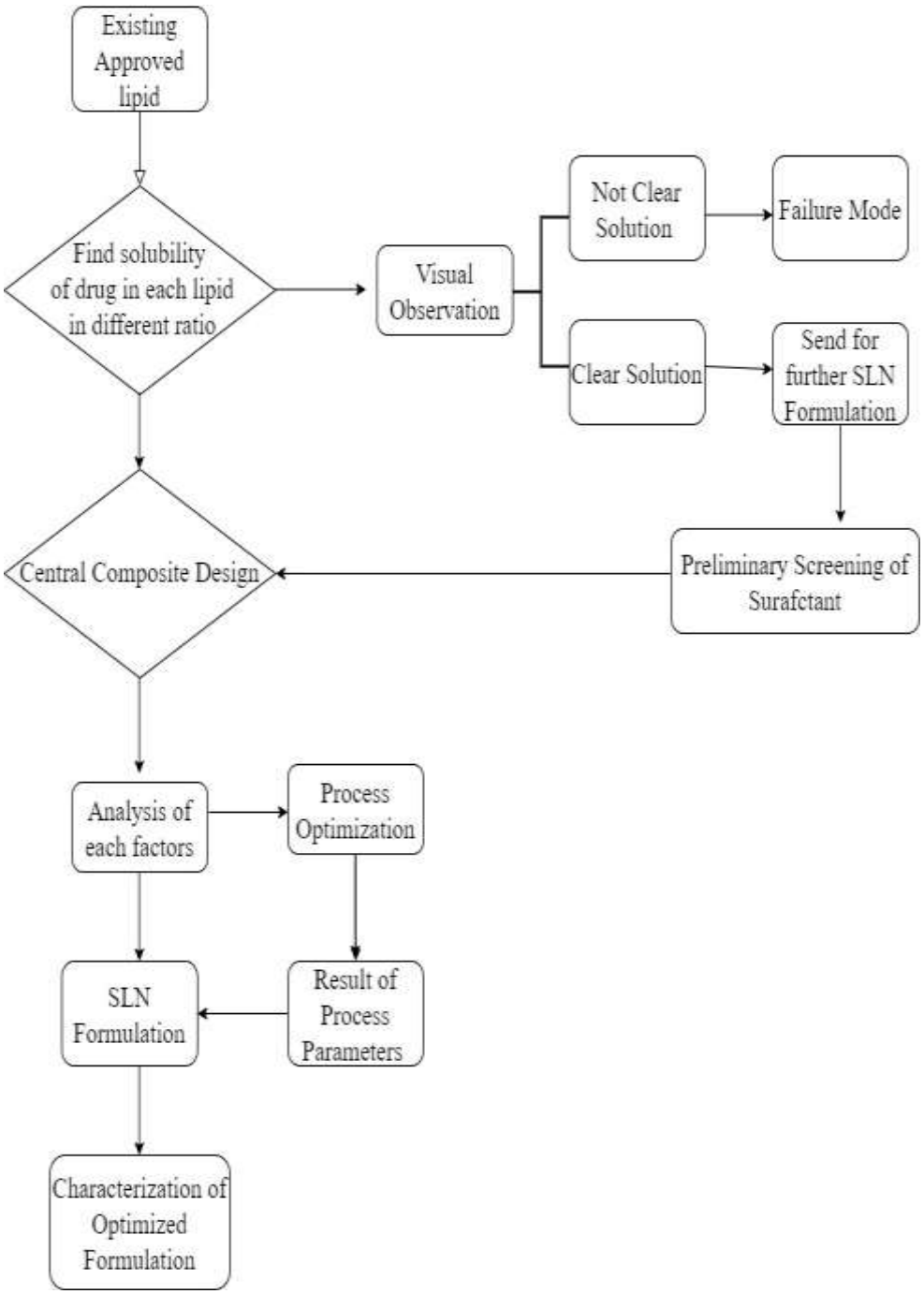

Figure 7: Strategical overview of methodology

Various elements of quality by design as described in ICH Q8 (R2) for pharmaceutical development include Target product profile, Identification of quality attributes, Risk assessment to identify process/product risk, Design space development and Control strategies. [69]

In the present work, various preformulation investigations were performed like identification of drug, selection of different materials, compatibility studies, etc. followed by formulation and optimization of various parameters by Central composite design to achieve minimize particle size and maximum encapsulation efficiency of the drug in SLN. [70]

4. FORMULATION STRATEGY

Preparation of RT-loaded solid lipid nanoparticles

The solid lipid nanoparticle was prepared using the microemulsion technique. A microemulsion was spontaneously obtained as recognized by a clear solution after adding the heated water phase into the oil phase of the same temperature. Addition of a hot microemulsion to cold water led to precipitation of the lipid phase forming fine particles. High-temperature gradients facilitate rapid lipid crystallization and prevent lipid aggregation. Briefly, the drug (10mg) was dispersed in melted lipid, and then the mixture was dispersed in a hot aqueous solution with surfactant concentration ranging from 50 to 150mg, by high speed stirring, using a High speed homogenizer at 15000 rpm for an appropriate period of time. The resulting dispersion was then cooled and each sample was diluted with water before the particle size was measured. [71]

Risk analysis of SLN

Risk variables were categorised in initial drug and excipient related risk, processing equipment related risk, processing variable risk and product profile related risk. Justification of all variables was studied based on literature survey and further it was defined with low, medium and high level with possible justification. These factors were studied from past published data and implemented with aim to implement at each stage of formulation preparation. However, it is purely related to multiple trials based on suitable conditions.

S.No	Variable	Risk category
1	Drug particle distribution	Drug and excipient related risk
2	Drug and lipid solubility	Drug and excipient related risk
3	High speed homogenizer	Processing equipment related risk
4	Dissolution of lipid	Processing variable related risk
5	Homogenization speed	Processing variable related risk
6	Drug and lipid ratio	Processing variable related risk
7	Surfactant concentration	Processing variable related risk
8	Homogenization time	Processing variable related risk
9	Particle size	Product profile related risk
10	Encapsulation efficiency	Product profile related risk

Table 7: Process variable and associated category of risk

SCREENING OF COMPONENTS FOR THE PREPARATION OF SLNS

For the SLNs development, selection of suitable excipients (lipid and surfactant) is vital. Excipients should be pharmaceutically acceptable, non-irritant and non-sensitizing in nature. They should be generally regarded as safe.

Screening of Lipids

As equilibrium solubility study was not possible due to the solid nature of the lipids, an alternative method was adopted to measure solubility of drug in the solid lipids. Briefly, 10 mg Rivastigmine Tartrate was weighed accurately and placed in a screw capped glass bottle covered with aluminum foil. About 100 mg of lipid was added in the bottle and heated at 80 ◦C under continuous stirring. Then additional lipid was added in portions under continuous stirring and heating at 80 ˚C until a clear solution was formed. Total amount of lipid added to get a clear solution was recorded.[72]

Screening of Surfactants

In 1949, William C. (Bill) Griffin developed the Hydrophilic-lipophilic Balance (HLB) System. According to the HLB system, all lipids, surfactants, fats and oils have a required HLB. The lipid selection was made on the basis of solubility of drug in lipid. The surfactant was selected here on the basis of HLB value of selected lipid i.e. GMS. GMS has the HLB value 3.8 and therefore the HLB value of surfactant needed to emulsify the GMS for a stable emulsion should be around or more than 3.8. Hence surfactant or co-surfactant or solvent should be chosen in such a concentration as to have a required combined value of 3.8 or more than 3.8. In this research work several surfactants like tween 80 and poloxamer 188 alone or in combination were applied for the preparation of SLNs. Surfactants were tried in concentration 1.5 % w/v, decided on the basis of literature survey (Singh et al., 2012). The stability of prepared SLN dispersion was observed visually after 24 h. [73]

Screening of High Speed Homogenizer rpm and time

During the process of stirring, organic solvents diffuse into the aqueous phase, leading to the synthesis of SLNs. The speed and the time of stirring may influence the particle size as well as the drug entrapment. In the present study, the stirring speed was kept constant at 15000 rpm, and the time of stirring was optimized. Three points of time were used for the optimization 5, 10 and 15 minutes along with screened surfactant and lipid. .

Compatibility study of selected excipients with drug

FT-IR Spectroscopy

FTIR spectral studies lies more in the qualitative identification of substances either in pure form or in combination with polymers and excipients and acts as a tool in establishment of chemical interaction. Since FT-IR.is related to covalent bonds, the spectra can provide detailed information about the structure of molecular compounds. In order to establish this point, comparisons were made between the spectrum of the substances and the pure compound.

Infrared spectroscopy is one of the most powerful analytical tools for elucidation of the molecular structures of inorganic and organic compounds. Infrared spectroscopy, IR radiation is passed through a sample. The functional groups present

in the pure and metal ions doped samples are analysed using FTIR spectroscopy. Some of the infrared radiation is absorbed by the sample and a portion is transmitted. The resulting spectrum represents the molecular absorption and transmission, creating a molecular fingerprint of the sample. In the present study, FTIR spectra are recorded with JASCO 4100 model spectrophotometer equipped with ATR.

Infrared spectroscopic analysis was performed to check out the compatibility between the selected carriers, drug and mixtures IR spectrum of the pure drug and the physical mixtures of drug with lipids, and excipients of optimized formulation were studied.

IR spectra was compared and checked for any shifting in functional peaks and non-involvement of functional group. The samples were studied using FTIR JASCO 4100 in the wavenumber range from 500 to 4,000 cm^{-1}.

Central composite design

Central composite design (CCD) was used to estimate the contribution and coefficient of parameters and their interactions that screened by ANOVA following conduction of minimum number of runs and minimizing the cost and errors. Present experimental design is based on variables including the Lipid concentration (A) and Surfactant concentration (B) (Table 8). In this model, 13 random experiments were selected to minimize the effect of uncontrolled variables.

An experimental design is a statistical technique used to simultaneously analyse the influence of multiple factors on the properties of the system being studied. The purpose of an experimental design is to plan and conduct experiments in order to extract the maximum amount of information from the collected data in a minimal number of experimental runs. Central composite design, based on the response surface method, is applied to design formulations. [74]

Factor	Name	Units	Type	Minimum	Maximum	Coded Low	Coded High
A	Lipid concentration	mg	Numeric	100.00	300.00	-1 ↔ 129.29	+1 ↔ 270.71
B	Surfactant concentration	mg	Numeric	50.00	150.00	-1 ↔ 64.64	+1 ↔ 135.36

Table 8: Factors used in formulation design

5. Characterization of Optimized Rivastigmine tartrate SLN

Particle size, PDI and zeta potential analysis

The surface charge on the particles can play an important role in the storage stability of nanoparticles and predict the fate of nanoparticles *in vivo.* RT SLN (1 ml) was dispersed in distilled water (10 ml), and then its particle size range was determined using Malvern Mastersizer (MAL 1021384 Malvern Instruments, Worcestershire, UK). The mean particle size, polydispersity index (PI) and zeta potentials were determined.

Encapsulation efficiency

Entrapment efficiency was determined by determining the amount of free drug spectrophotometrically at 264 nm in the supernatant after centrifugation of the known amount of nanoparticulate dispersion at 10000 rpm using REMI centrifuge for 15minutes.The entrapment efficiency was calculated using the equation. [75]

$$\text{Drug entrapment efficiency (\%)} = \frac{\text{Total drug taken} - \text{Free drug}}{\text{Total drug taken}} \times 100$$

Scanning electron microscopy (SEM)

The surface morphology of drug substance and prepared formulations of RT SLN were examined using scanning electron microscopy (Jeol, JSM 6390). [76]

Differential scanning calorimetry (DSC)

The physical state of RT entrapped in the NPs was characterized by Differential Scanning Calorimetry (DSC-60, Shimadzu, Japan). Each sample was sealed in standard aluminium pans with lids and purged with air at a flow rate of 40

ml/min. A temperature ramp speed was set at 20 C/min, and the heat flow was recorded in the range of 30–300 C under inert nitrogen atmosphere. Thermograms were taken for RT, GMS, physical mixture, Blank SLN and RT-loaded SLN. [77]

In vitro drug release studies

In vitro release studies were performed using the dialysis bag method, modified to maintain a sink condition and achieve satisfactory reproducibility. The dialysis bag (molecular weight cut off 12000–14000) was soaked in deionised water for 12h before use. 1mL of RT loaded SLN dispersion was first poured into the dialysis bag with the two ends fixed by thread and placed into the preheated dissolution media (phosphate buffer pH 7.4) placed in beaker. The beaker was placed on a magnetic stirrer. At fixed time intervals of 0.5,1,2,3,4,6, and 8hrs a sample was removed for analysis and equal volume of fresh dissolution medium was added. The sample was analyzed by using a UV Spectrophotometer at a λmax of 263nm against a blank of phosphate buffer of pH 7.4. [78, 79]

In vitro drug release kinetics

In order to understand the kinetic and mechanism of drug release, the result of *in vitro* drug release study of nanoparticles were fitted with various kinetic equation like zero order (cumulative % release vs. time), first order (log % drug remaining vs time), Higuchi's model (cumulative % drug release vs. square root of time). r^2 and k values were calculated for the linear curve obtained by regression analysis of the above plots. [80]

RESULTS AND DISCUSSIONS

1. CHARACTERIZATION OF ACTIVE INGREDIENT

DESCRIPTION AND SOLUBILITY

The drug substance Rivastigmine tartrate was examined in-order to explain its description and solubility as per United States pharmacopeia (USP 2014a) as test for identification. The results are tabulated in Table 9

Test	Specification	Result
Description	White to off-white, fine crystalline powder	Complies
Solubility	Very soluble in water and in methanol, very slightly soluble in ethyl acetate.	Complies

Table 9: Description and solubility of Rivastigmine tartrate

FT-IR spectroscopy

Various functional groups present in the powder drug sample was determined by fourier-transform infrared (FT-IR) spectroscopic and compared with the standard spectra of RT for confirmation. The observed and reported IR spectra of RT are shown in Figure 8 and 9.

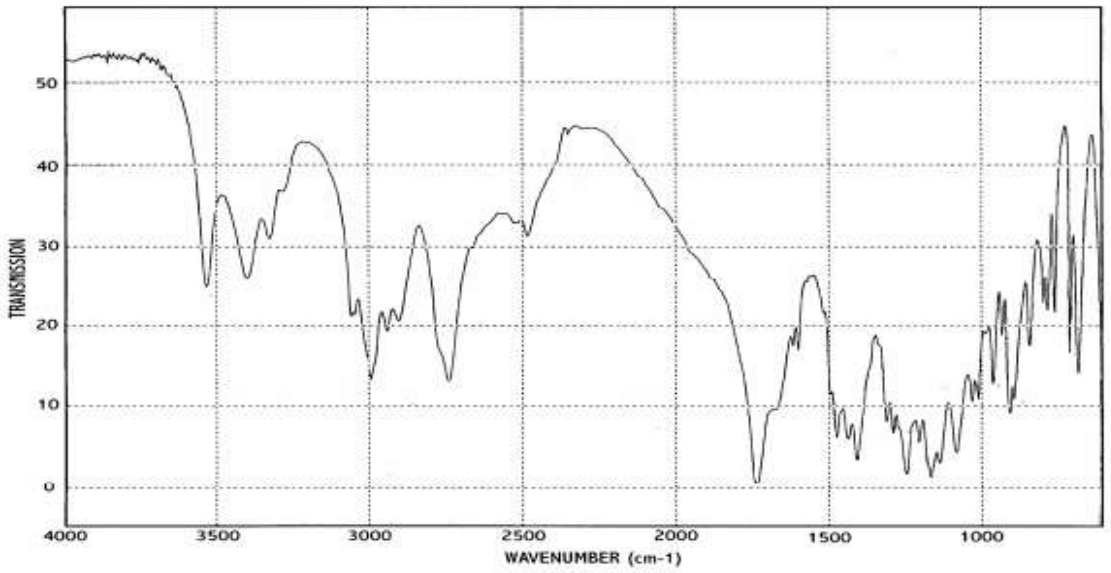

Figure 8: FT-IR spectra of Standard Rivastigmine tartrate

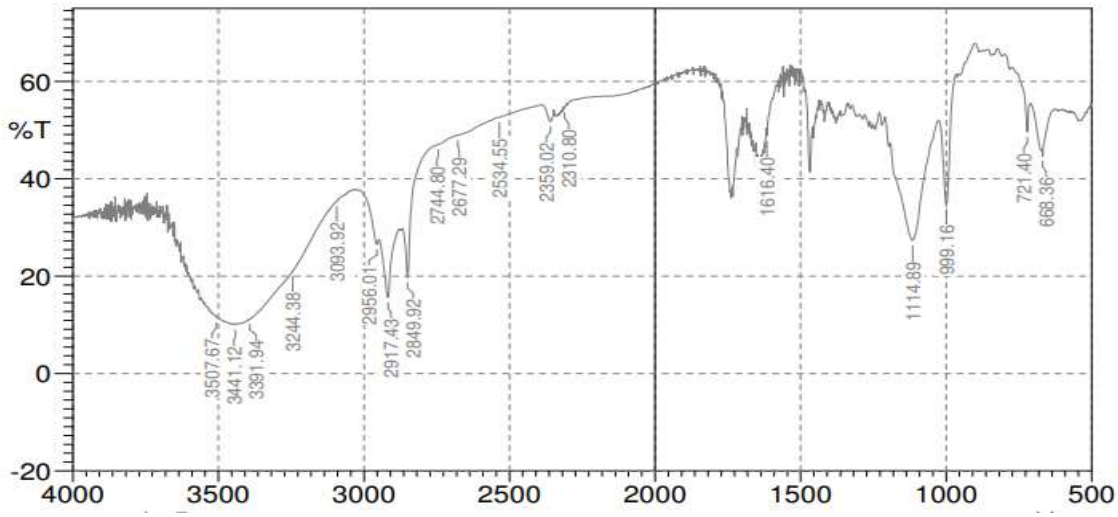

Figure 9: FT-IR spectra of Test Rivastigmine tartrate

The infrared absorption spectrum was found to be comparable with the reference IR spectrum as disclosed in the patent US20080255231A1. The Figure 8 and 9 show the IR spectra of test and standard reference sample. The IR absorbance peaks (Wave number) of rivastigmine tartrate were 3530, 3397, 2736, 1728, 1399, 1280 and 755 cm-1. The 3500-3410 corresponds to N–H stretch, 2962–2853 corresponds to C-H, 1675-1600 corresponds to carbon double bond stretch, 1200-1050 corresponds to carbonyl functional group. The 3050 - 3100 corresponds to aromatic ring CH stretch, 3507 represents OH functional group.

Differential scanning calorimetry

For RT sharp peak was obtained at 128.5˚C which indicates the melting point of RT.

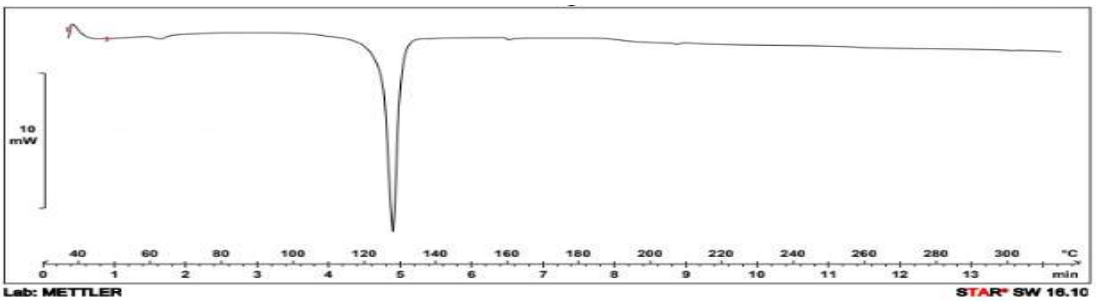

Figure 10: DSC of Rivastigmine tartrate

2. ANALYTICAL METHOD FOR RIVASTIGMINE TARTRATE

2.1. Determination of absorption maximum

The sample Rivastigmine tartrate at a concentration of 10 µg/ml was scanned under UV-VIS Spectrophotometer in the range of 200-400 nm using blank and the wavelength corresponding to maximum absorbance (λ max) was recorded. The sample showed maximum absorbance at wavelength 263 nm**.**

2.2 Preparation of calibration curve

Aliquots of 10, 20, 30, 40,50 and 60 µg/ml RT standard solution were accurately transferred into a series of 10 ml calibrated flask and made up to the mark with phosphate buffer pH 7.4. The absorbance of the resulting solution was measured at 264 nm against blank **(Table 10).** Calibration curve was prepared by plotting the absorbance against concentration of RT **(Figure 11).** The standard concentrations of RT (10-60 µg/ml) showed good linearity with R^2 value of 0.999 which suggests that it obey Beer-Lamberts law.

Sl. No.	Concentration (mcg/ml)	Absorbance
1	0	0
2	10	0.1213
3	20	0.2537
4	30	0.3731
5	40	0.4963
6	50	0.6244
7	60	0.753

Table 10: Absorbance of Rivastigmine tartrate in phosphate buffer pH 7.4

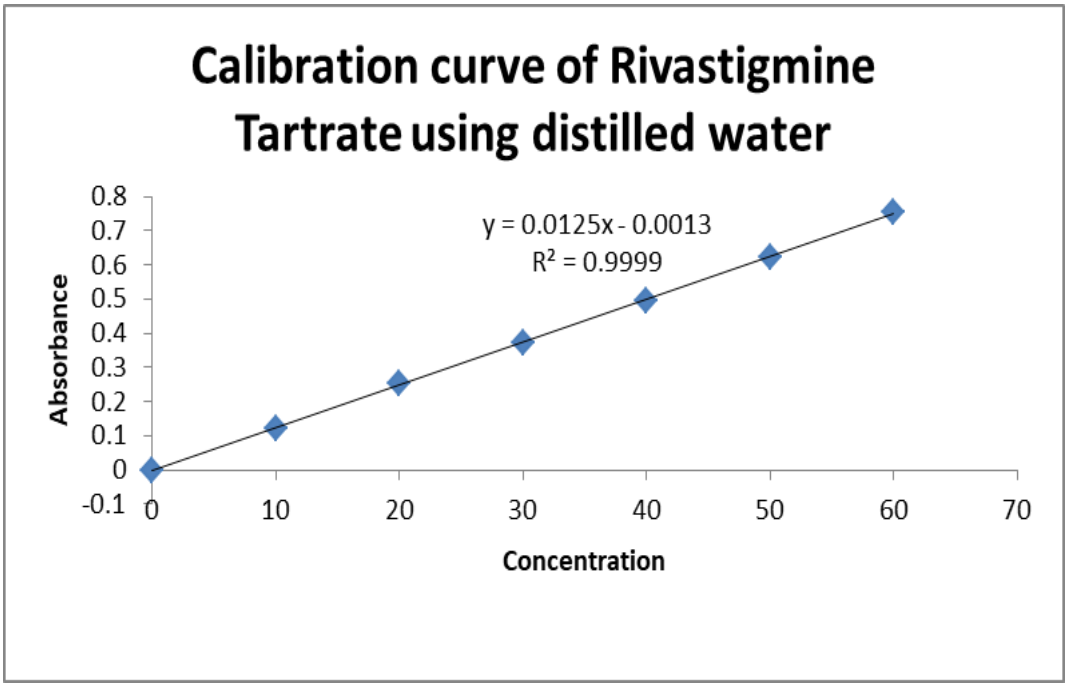

Figure 11: Calibration curve of Rivastigmine tartrate in phosphate buffer 7.4

3. FORMULATION DEVELOPMENT AND OPTIMIZATION OF SOLID LIPID NANOPARTICLES (SLNS) FOR RIVASTIGMINE TARTRATE

Literature survey was done to identify and determine the QTPP, CQAs, CPPs, CMAs and manufacturing procedures for SLN, various process and formulation attributes having effect on product CQAs. For better absorption of the drug, minimum average size of the nanoparticles is required. Hence, minimum particle size is one of the most important CQA along with minimum PDI (monodispersity), maximum entrapment efficiency, maximum drug loading, minimum zeta potential of ± 30 mV for stability and no residual solvent for avoiding toxicity and ensuring safety. A CQA is a physical, chemical, biological, or microbiological property or characteristic that should be within an appropriate limit, range, or distribution to ensure the desired product quality. In the present investigation, risk analysis and different preliminary experiments were carried out on the basis for selection of suitable excipients/materials which may directly or indirectly influence critical quality attributes. The compatibility of the drug-excipient was checked before the optimization of various process and formulation variables. Risk analysis data was implemented in to the formulation preparation. CQA importance level was derived from risk analysis data which will be discuss in further section. With the selected excipients and CQA identified through

literature survey and preliminary experiments and those were optimized sequentially as per the steps involved in the formulation. Finally, the formulation variables were optimized using central composite design in design expert software further analyzing the data statistically and graphically using response surface plots.

3.1. RISK ANALYSIS

The initial risk assessment of the overall formulation process is shown in table 11 and possible justifications are provided is given based on literature survey. Existing experience with these process steps was used to determine the degree of risk associated with each process step and its potential to impact the CQAs of the finished product in form of nano formulation. Process variables that could have potentially impact on product CQAs were identified and their associated risk was evaluated. Categorisation of variable (i.e.: drug and excipient related risk, processing equipment related risk, processing variable risk and product profile related risk) were defined with low, medium and high level with possible justification.

SI.NO	VARIABLE	RISK ASSESSMENT	JUSTIFICATION
DRUG AND EXCIPIENT RELATED RISK			
1	Drug particle distribution	Low	SLN processing step involves the solubilisation of drug in solvent and ultimately in lipid. There is no direct effect in any response. Hence this can be categorised as low risk factor.
2	Drug and lipid solubility	High	This variable is directly related to solubility of drug in lipid which is an important step in formulation as well as in drug loading. So this falls under the category of high risk.

PROCESSING EQUIPMENT RELATED RISK			
3	High speed homogeniser	Low	HSH is selected based on the accessibility and easiness. This can be categorised under low risk.
PROCESSING VARIABLE RELATED RISK			
4	Dissolution of lipid	High	It is an initial step of SLN preparation undissolved or partially dissolved in lipid fraction and may directly effect the product yield.
5	Homogenisation speed	Medium	Lower or higher speed may result inappropriate drug encapsulation. However, this variable is controllable.
6	Drug and lipid ratio	Medium	This factor indirectly effect on encapsulation efficiency as well as PDI and particle size.
7	Surfactant concentration	Medium	This factor indirectly effect on encapsulation efficiency as well as PDI and particle size.
8	Homogenization time	Medium	Particle aggregation may form due to static force for prolonged time of homogenisation. However this variable is controllable.
PRODUCT PROFILE RELATED RISK			
9	Particle size and PDI	Medium	Homogenously distributed particles provides a uniform drug release from the entire formulation .
10	Encapsulation efficiency	High	Encapsulation efficiency is accepted with maximum level upto 90 to 95%. This variable directly affects the drug content.

Table 11: Variable related risk assessment

3.2 SCREENING OF COMPONENTS FOR THE PREPARATION OF SLNS

Screening of Lipids

RT is highly hydrophobic and lipophilic drug. Solubility study was performed to evaluate the solubility profile of drug against various lipids as it is one of the essential steps for formulation development. The selection of the lipid was primarily based on the solubility of the drug in lipid since higher the solvent capacity, higher will be the drug loading potential and entrapment efficiency. The solubility of the drug was determined in four different lipids – Glyceryl mono stearate, Glyceryl tri sterate, Stearic acid, and Coco mono ethanolamine. The results obtained are as shown in Table 12 and Figure 12.

Solid lipids	Amount of lipid required to solubilise 10mg of RT (mg)
GMS	48
GTS	55
Coco mono ethanolamide	67
Stearic acid	83

Table 12: Selection of lipid based on solubility of drug in lipid

Among them, GMS (48 mg) showed highest solubilisation capacity followed by GTS (55 mg). Amount of coco mono ethanolamide (67 mg) and Stearic acid (83 mg) required to solubilize 10 mg tretinoin was significantly higher than GMS (48 mg). This study indicated that Rivastigmine tartrate loading capacity along with GMS is found to be higher than GTS, coco mono ethanolamide, and Stearic acid. GMS is selected as lipid for formulation.

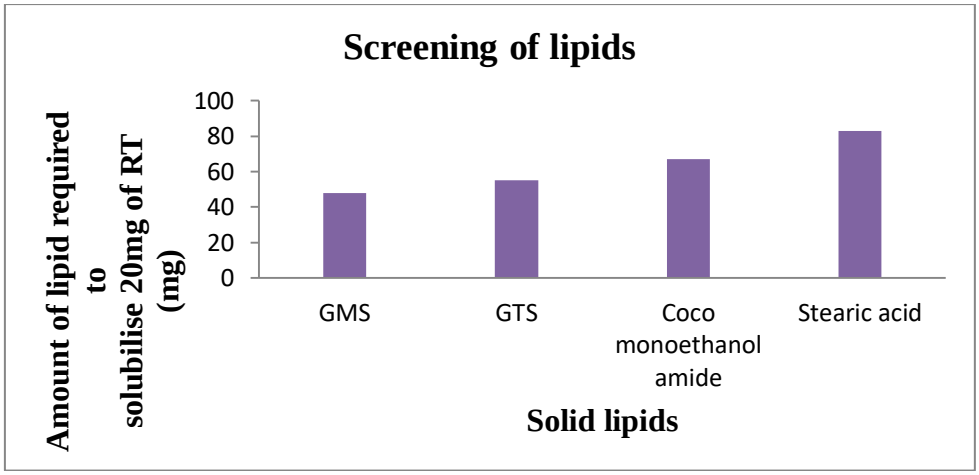

Figure 12: Solubility of Rivastigmine tartrate in different lipids

Screening of surfactants

The surfactant was selected here on the basis of HLB value. SLN was prepared with two different surfactants alone or combination using GMS as lipid and were evaluated for particle size and PDI. The results obtained are as shown in Table 13 and figure 13,14,15,16

Surfactants	Particle size (nm)	PDI
Poloxamer 188	381.1	0.056
Tween 80	458.3	0.013
Poloxamer 188/ Tween 80	498.8	1.000

.

Table 13: Selection of Surfactant on the basis of Particle size and PDI

This study indicates that Poloxamer 188 (381.1) having smaller particle size and stable when compared to Tween 80 (458.3) and combination of poloxamer 188/Tween 80 (498.8)

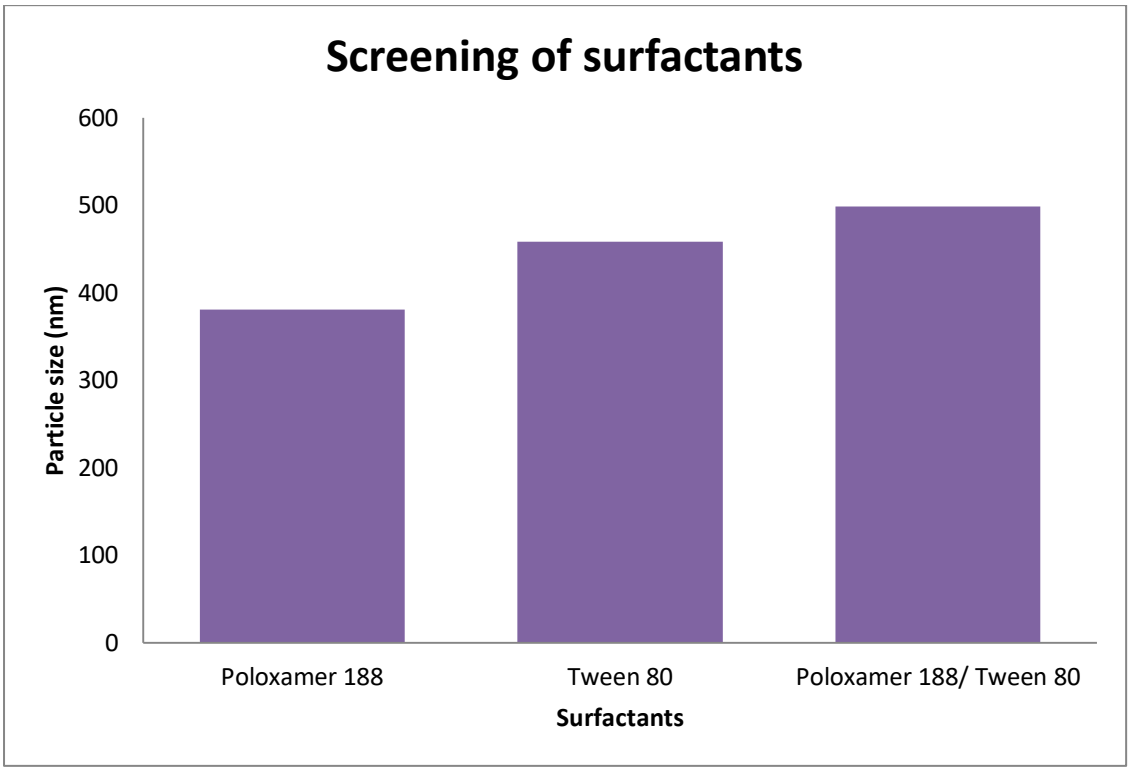

Figure 13: Screening of surfactants

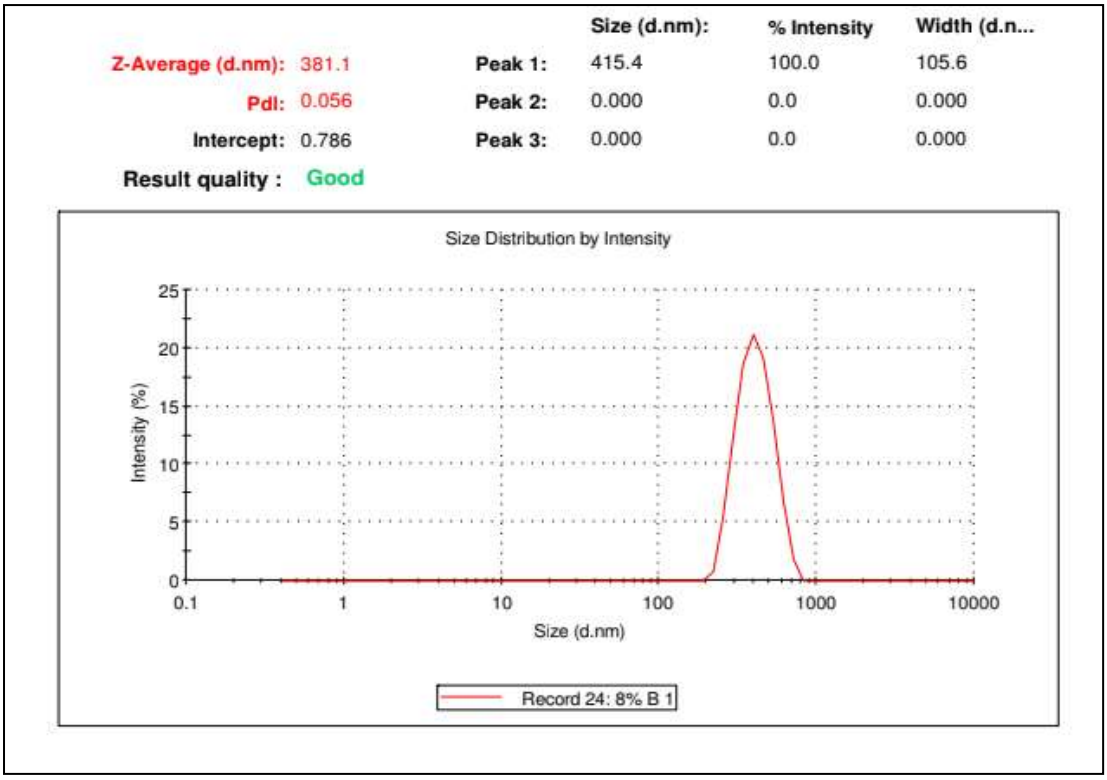

Figure 14: Particle size distribution of RT SLN using poloxamer 188

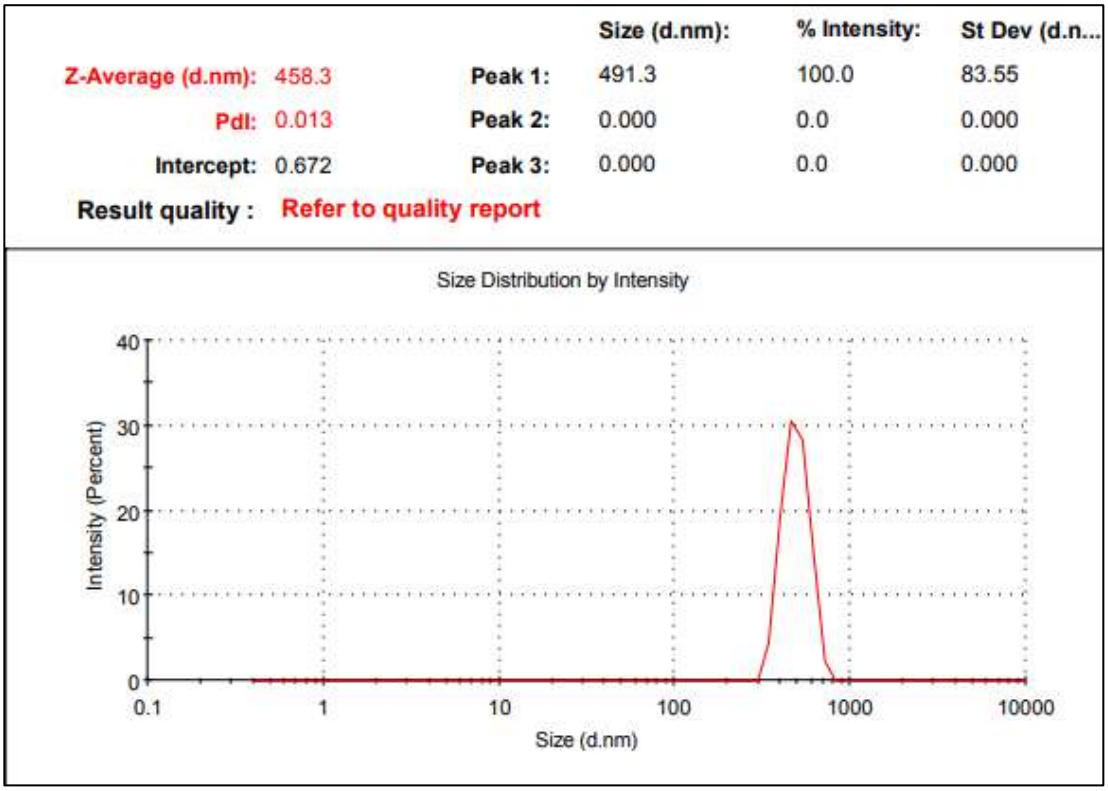

Figure 15: Particle size distribution of RT SLN using Tween 80

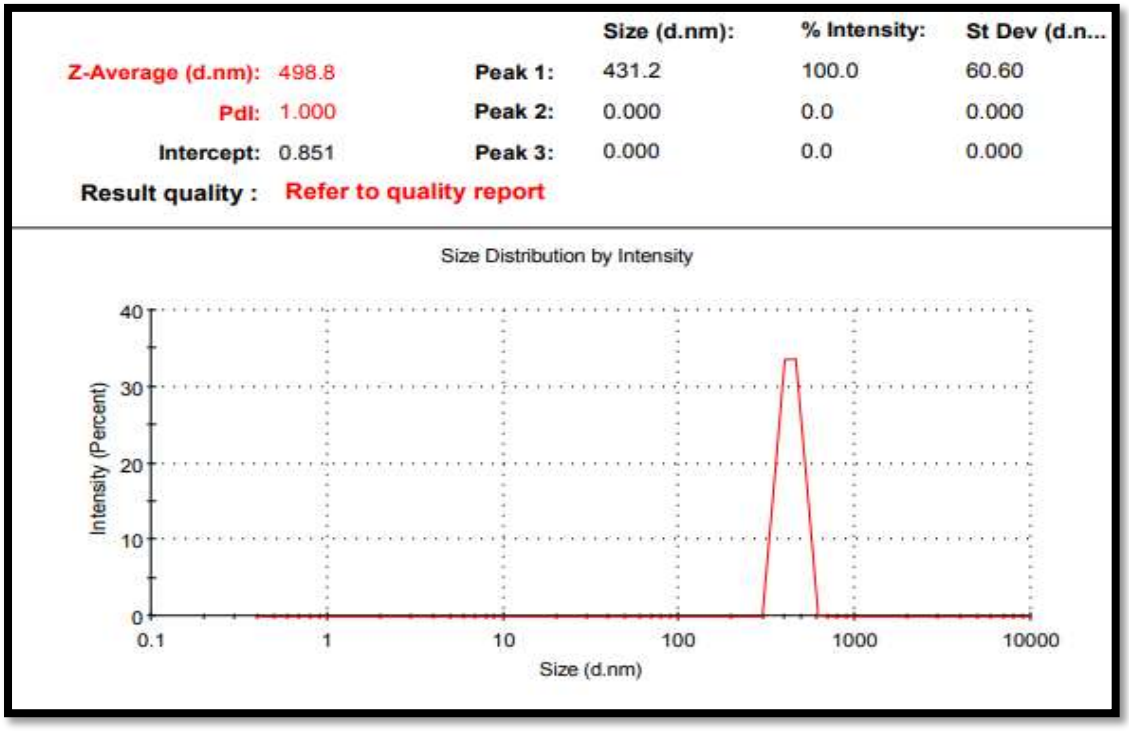

Figure 16: Particle size distribution of RT SLN using poloxamer 188 and tween 80 (combination)

Screening of HSH rpm and time

The HSH time was selected here on the basis of particle size and PDI value. SLN was prepared with poloxamer 188 as surfactant on using GMS as lipid and were evaluated for particle size and PDI. The results obtained are as shown in table 14 and figure 17

HSH speed (rpm)	HSH time (min)	Particle size (nm)	PDI
15000	5	158.0	0.375
	10	246.40	0.389
	15	277.53	0.397

Table 14: Selection of HSH time on the basis of Particle size and PDI

This study indicates that HSH time with 5 minutes (158.0) having smaller particle size when compared to 10 minutes (246.40) and 15 minutes (277.53)

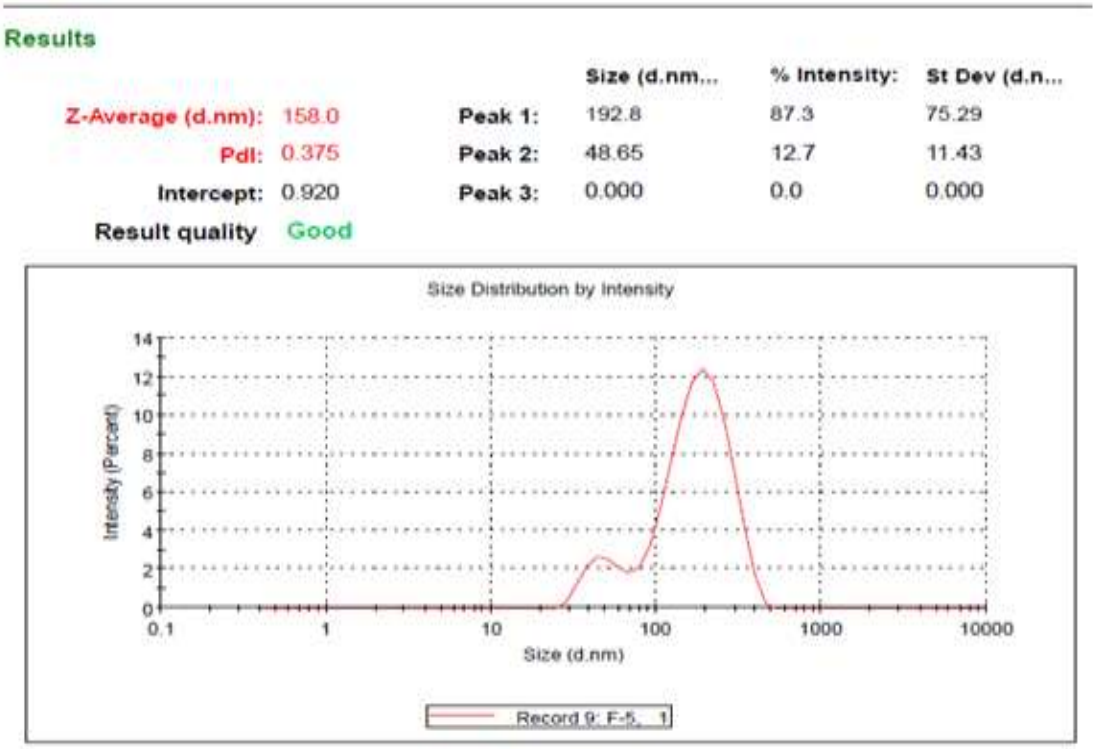

Figure 17: Particle size distribution of RT SLN on HSH 5 minutes

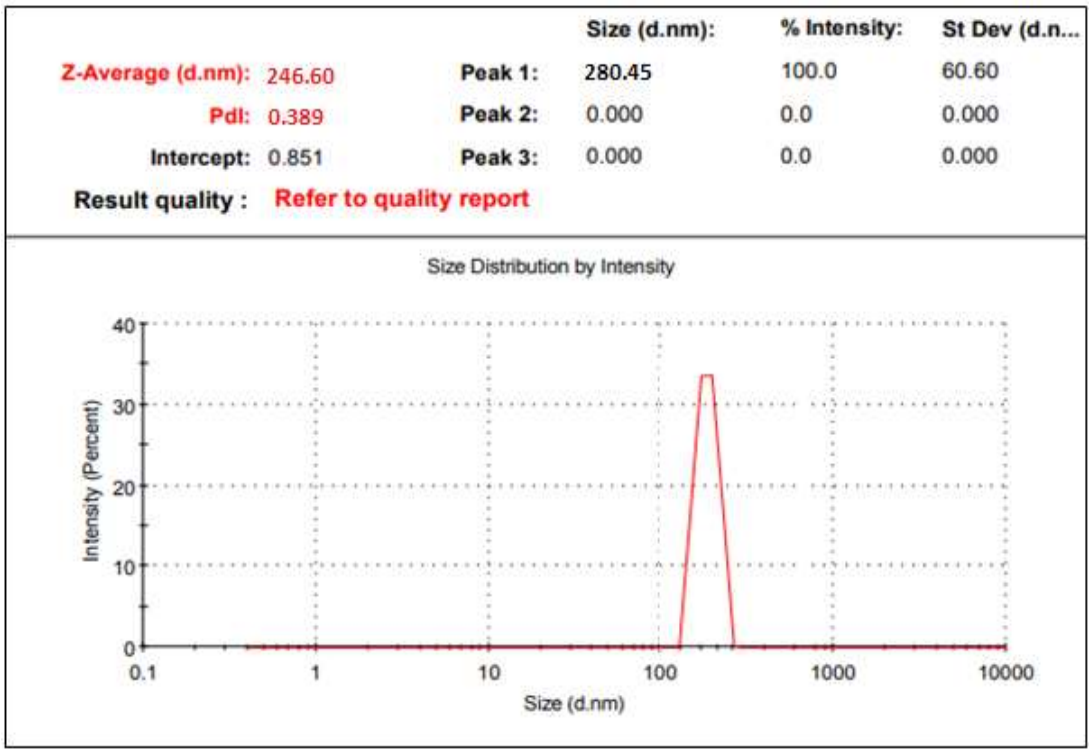

Figure 18: Particle size distribution of RT SLN on HSH 10 minutes

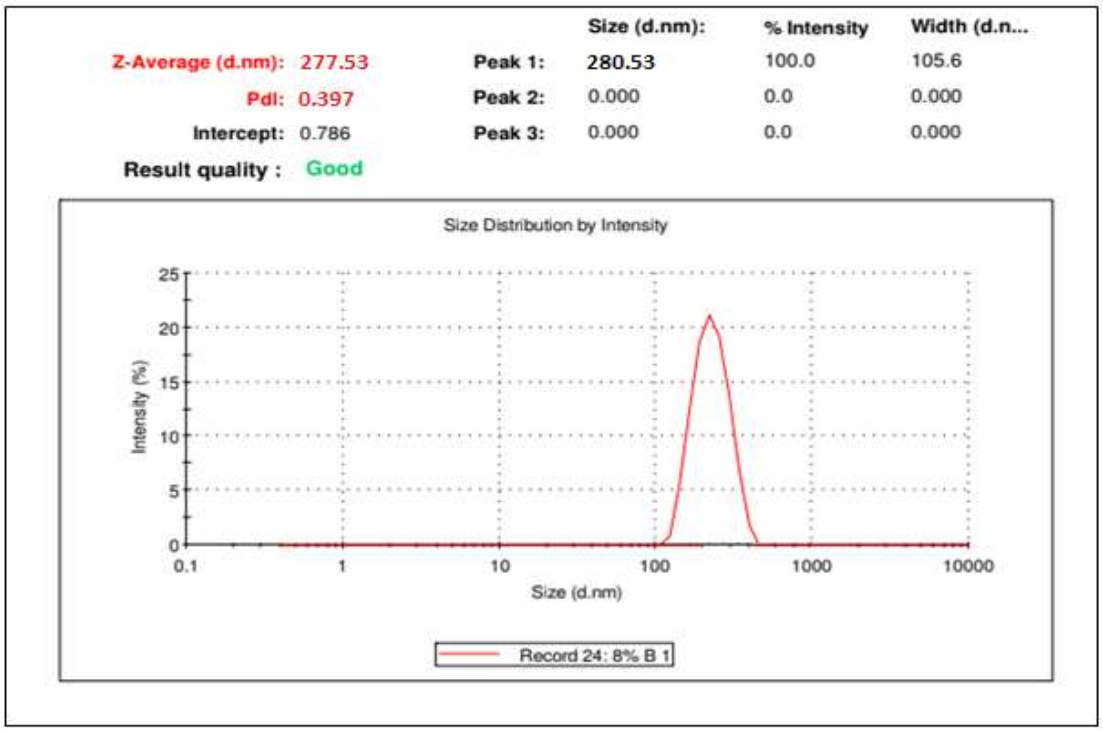

Figure 19: Particle size distribution of RT SLN on HSH 15 minutes

3.3. COMPATIBILITY STUDY OF SELECTED EXCIPIENTS WITH DRUG

FT-IR Spectroscopy

FT-IR spectra of drug, selected lipid, and surfactants were analyzed to check the interactions between them. The spectra and major peaks of individual compounds and their combinations are given in the **Figures (20, 21, 22, 23 and 24).** The wave numbers are given in **Table 15.**

The spectra showed that there is no interaction between the drug, selected lipids and surfactants. Hence, the selected stabilizer was found to be compatible with drug and other components without any mutual interactions.

Sl. No.	Description	Characteristic peaks observed (cm^{-1})
1	Rivastigmine tartrate	3441, 2956, 1616, 1114, 721
2	Glyceryl mono sterate	3176,2916,2533,1729.1180
2	Poloxamer 188	2798.80, 1279.81, 1139
3	Rivastigmine tartrate + Glyceryl mono sterate	3385, 2915, 1688, 1125,668
4	Rivastigmine tartrate + Glyceryl mono sterate + Poloxamer 188	3405, 2914,1471,1115, 668

Table 15: IR wave numbers of drug and excipients

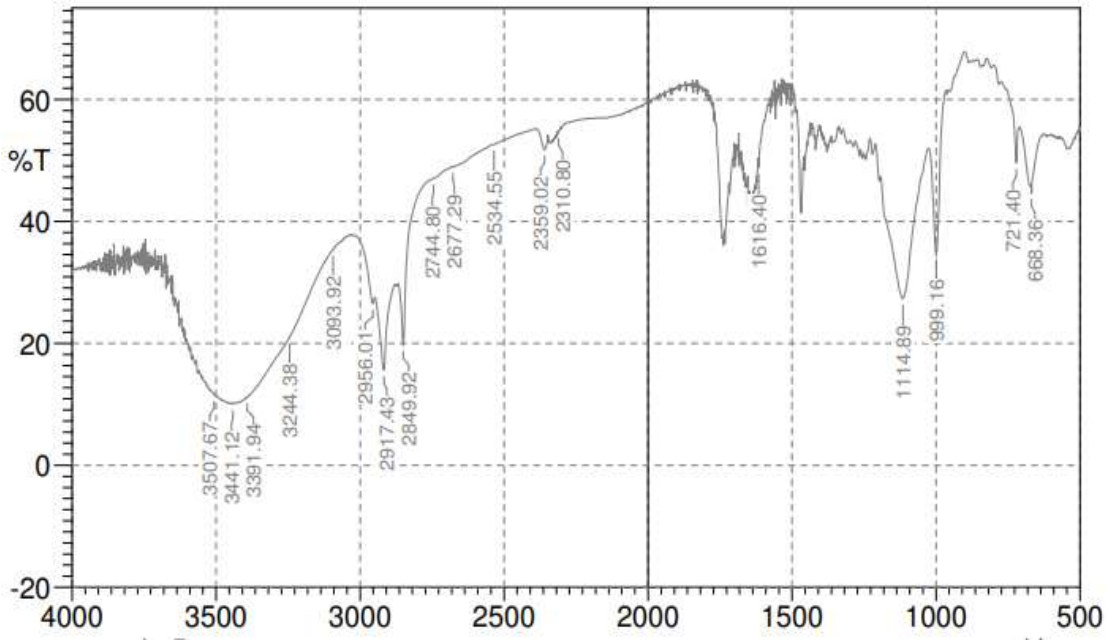

Figure 20: FT-IR spectra of Rivastigmine tartrate

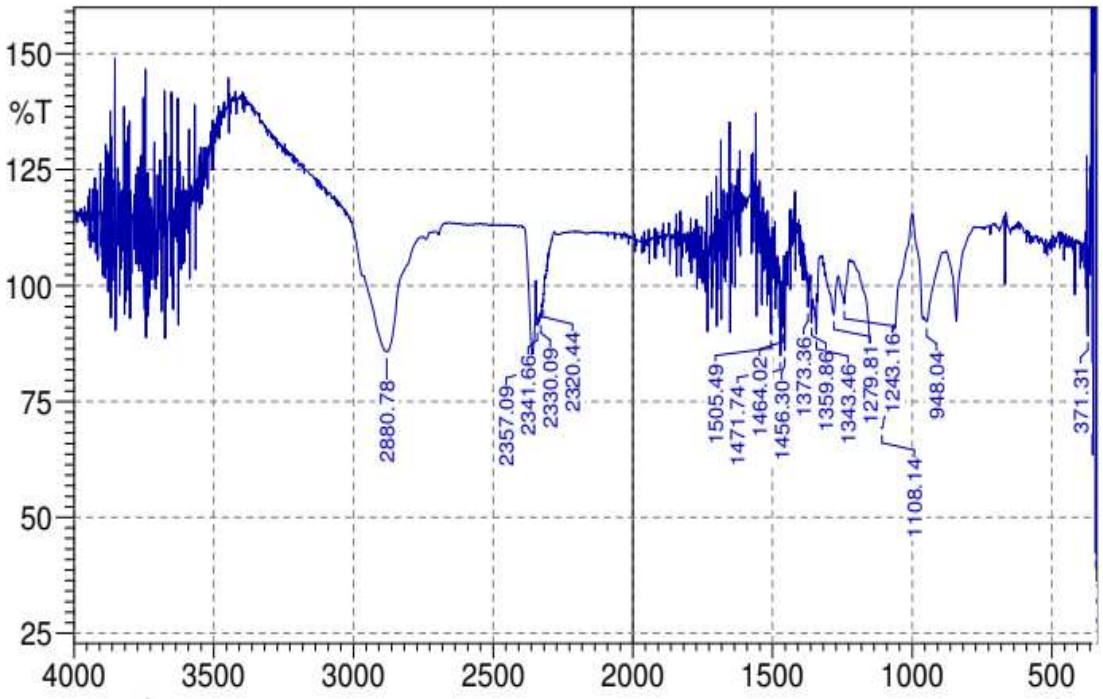

Figure 21: FT-IR spectra of Poloxamer 188

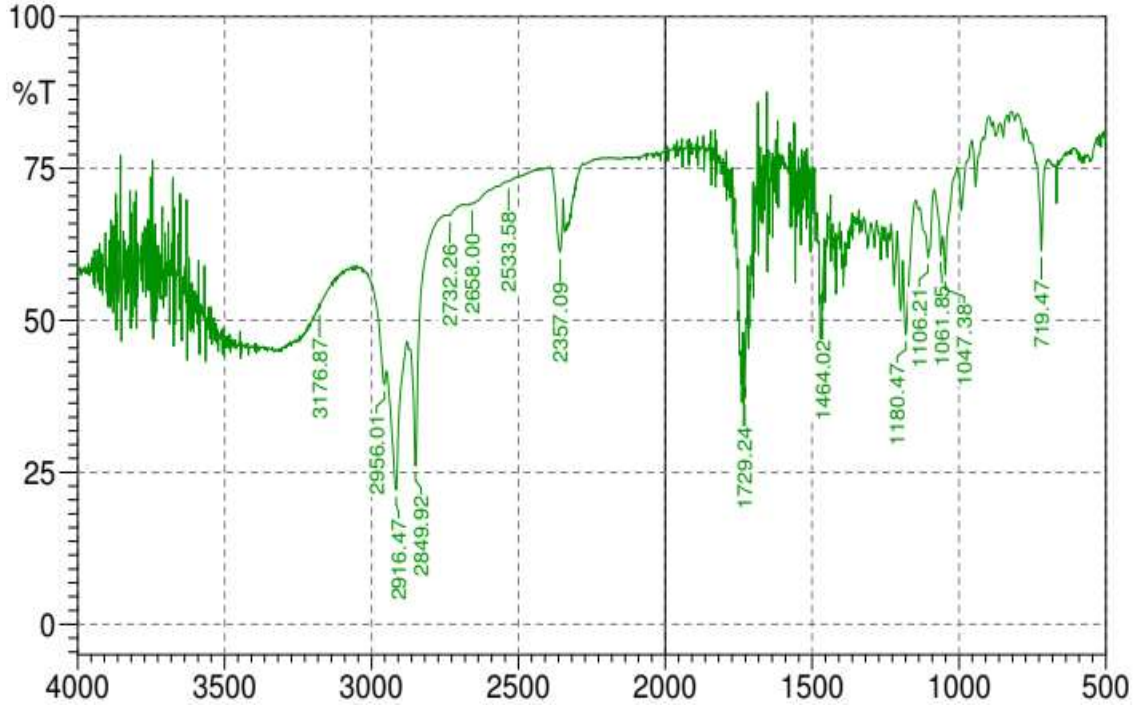

Figure 22: FT-IR spectra of Glyceryl mono sterate

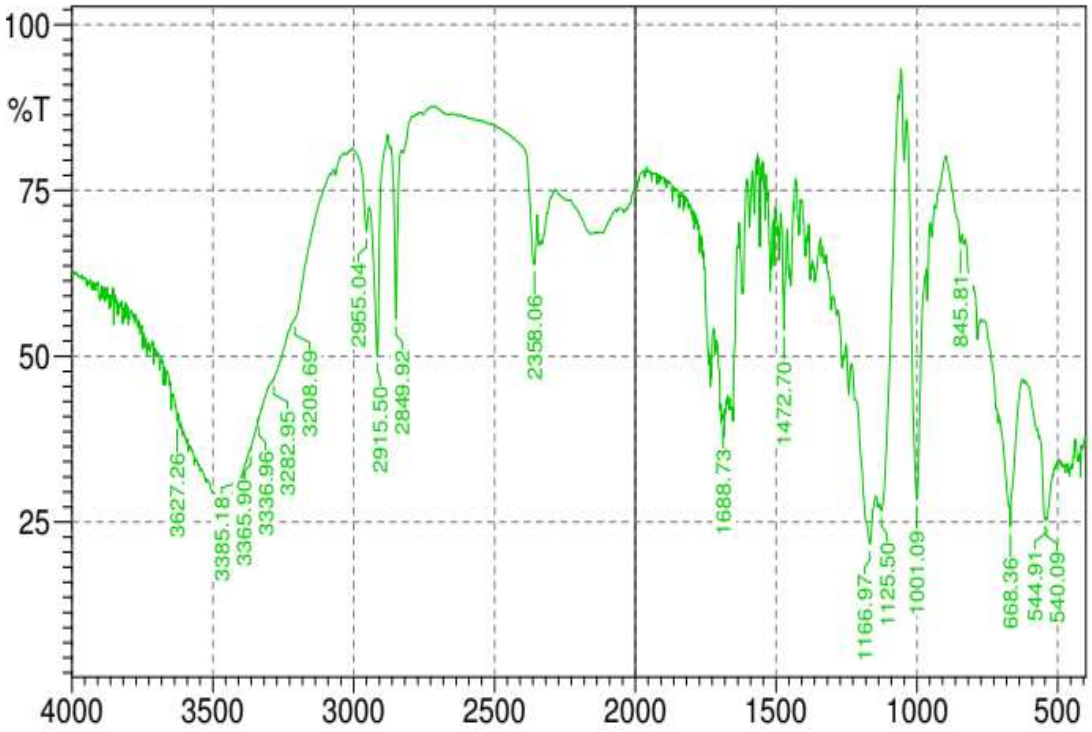

Figure 23: FT-IR spectra of Rivastigmine tartrate and Poloxamer 188

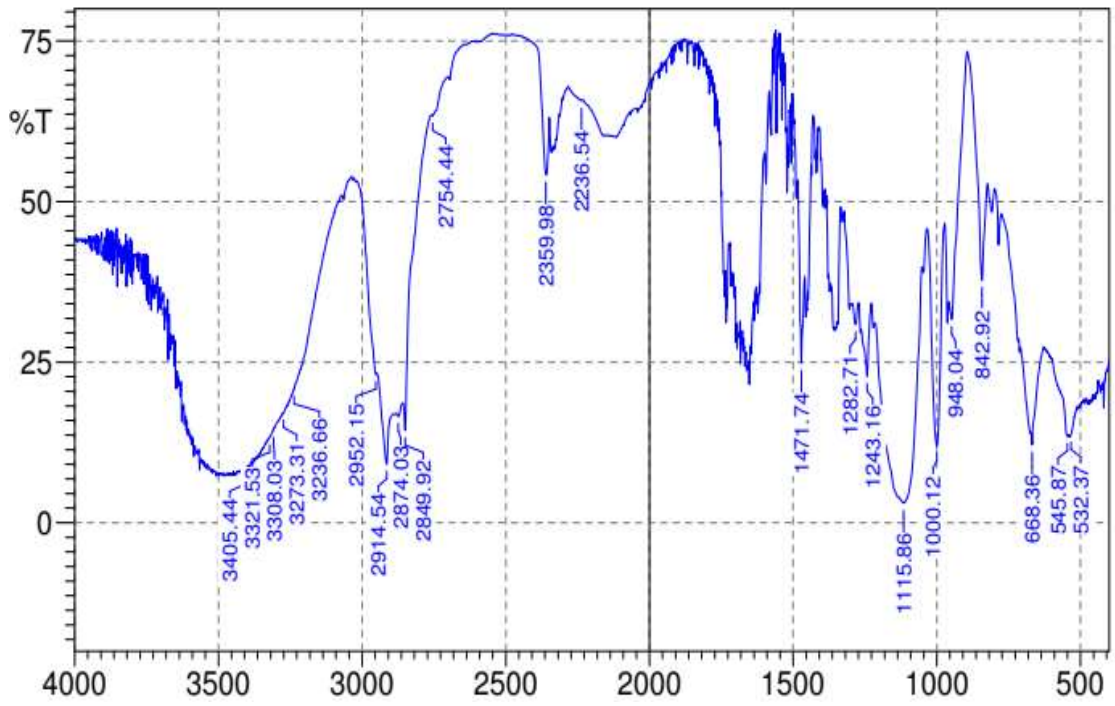

Figure 24: FT-IR spectra of Rivastigmine tartrate, Poloxamer 188 and GMS

4. OPTIMIZATION OF FORMULATION

The design selected was Central composite design by employing design expert software. Two input factors were studied at five different levels including central point 0, +1, -1, ±α throughout the preparation process to determine their effect on two responses, namely mean particle size and encapsulation efficiency. The input factors being selected are the following: Lipid concentration (100,200 and 300), concentration of surfactant (50,100,150) shown in table 16. The response values were subjected to multiple regression analysis to find out the relationship between the input factors used and the response values obtained.

Formulation code	Factor 1	Factor 2
	A:Lipid concentration mg	B:Surfactant concentration Mg
F1	270.711	64.6447
F2	129.289	135.355
F3	200	150
F4	200	100
F5	100	100
F6	200	100
F7	200	100
F8	300	100
F9	270.711	135.355
F10	200	50
F11	129.289	64.6447
F12	200	100
F13	200	100

Table 16: Runs using CCD

Data reported in table 16 provides the 13 runs of experimental design where the compositions of the lipid and surfactant are indicated. Thirteen formulations (F1-F13) were prepared accordingly and analyzed for their physical characteristics.

4.1. DETERMINATION OF PARTICLE SIZE, PDI AND %EE

The results obtained for particle size, PDI and %EE of SLNs are given in table 14 and graphically represented in figure 25 and 26. Particle size of the formulation is found in the range between 121 to 279 nm shown in table 17. Formulation factors were found to influence the particle size significantly. For a successful formulation of safe, stable and effective it requires the preparation of homogenous population of certain size.

Formulation code	Factor 1	Factor 2	Response 1	Response 2
	A:Lipid concentration mg	B:Surfactant concentration mg	Particle Size nm	Encapsulation Efficiency %
F1	270.711	64.6447	279	36.45
F2	129.289	135.355	128.3	68.21
F3	200	150	140.8	73.72
F4	200	100	125.6	76.95
F5	100	100	122.3	70.98
F6	200	100	123	73.26
F7	200	100	126.7	75.11
F8	300	100	226	66.03
F9	270.711	135.355	161	68.31
F10	200	50	257.4	54.03
F11	129.289	64.6447	177.1	63.58
F12	200	100	127.3	75.9
F13	200	100	121	71.62

Table 17: Particle size, and Encapsulation efficiency of all SLNs formulations (F1-F13)

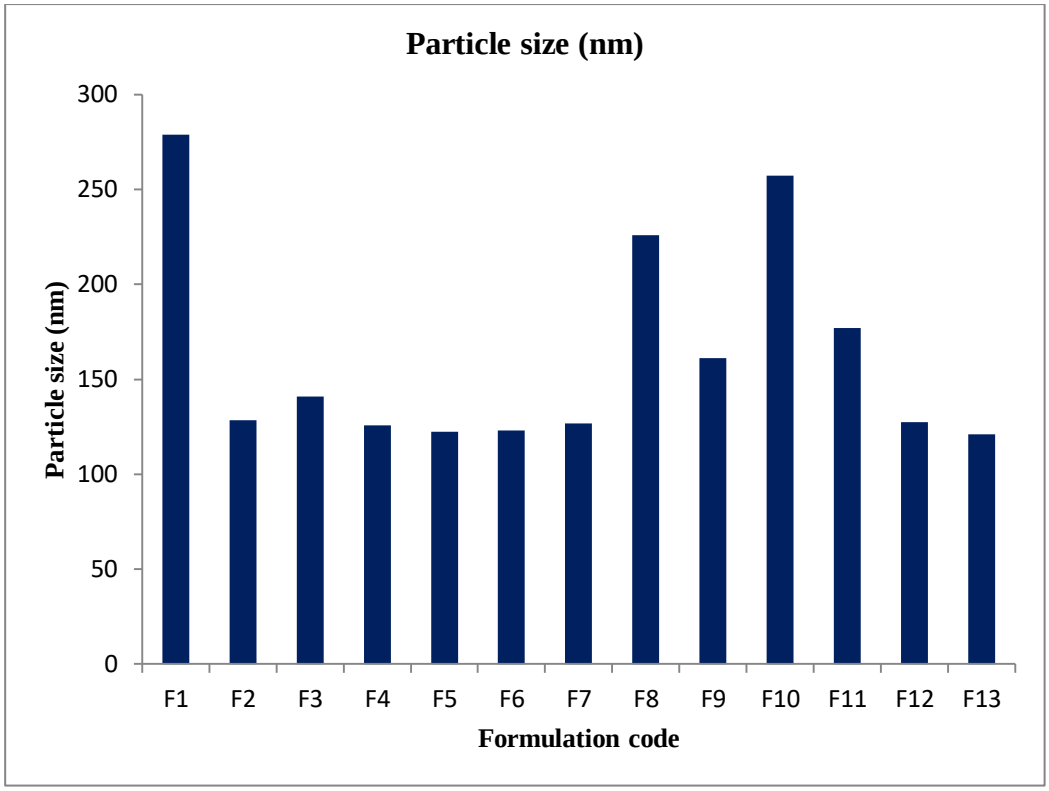

Figure 25: Graphical representation of Particle size for all 13 formulation

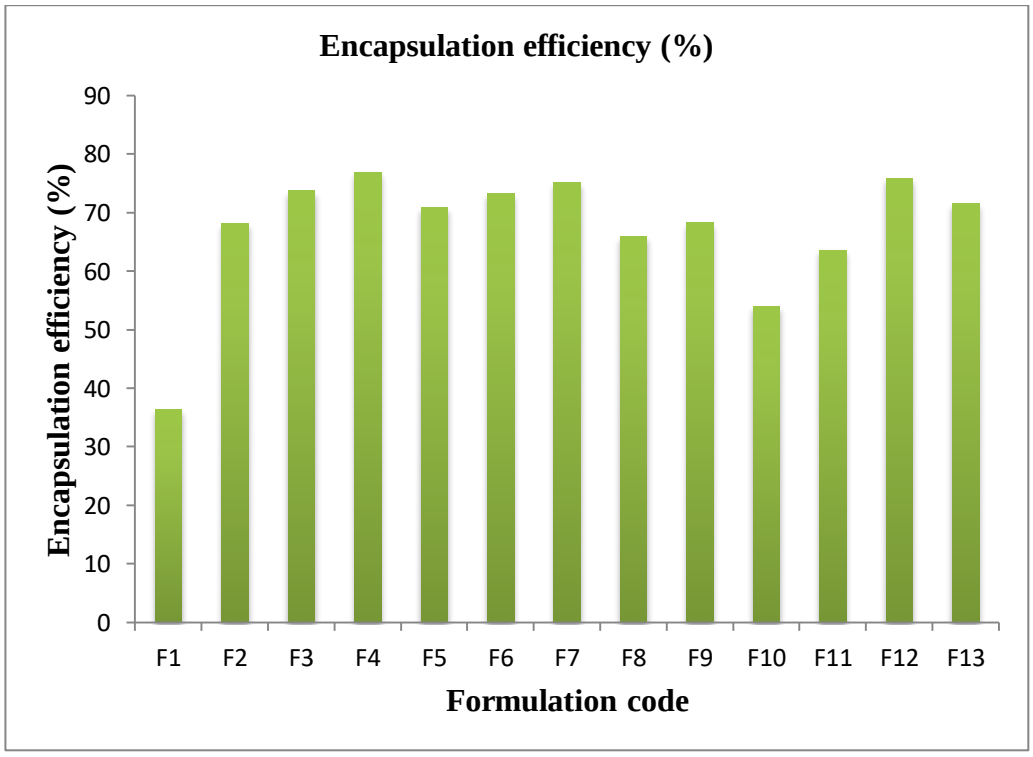

Figure 26: Graphical representation of Encapsulation efficiency for all 13 formulation

4.2. DATA ANALYSIS

The data analysis was carried out using design expert software. The summary of design is described in table 18. This summary describes the overview of entire resultant data for total 32 runs. Summary describes the particle size of the formulation is found in the range between 121 to 279 nm. A mean for size of particle is found 162.73. Similarly encapsulation efficiency size of the formulation is found in the range between 36.45 to 76.95%. The mean value for %EE is 62.74%. Whole analysis was summarised based on the polynomial

Response	Nam-e	Unit	Observation	Minimum	Maximum	Mean	Std. Dev.	Ratio
R1	PS	nm	13.00	121	279	162.73	55.71	2.31
R2	EE	%	13.00	36.45	76.95	67.24	11.11	2.11

Table 18: Result summary from formulation trials (±=SD, n=3)

4.2.1 ANALYSIS OF PARTICLE SIZE

Particle size of all formulation was measured by Malvern particle size analyser. The particle size range in all the formulation was found from 121 nm as minimum size to 279 nm as maximum size.

The result of p-values is indicated for each model. The data presented in table 16 suggest the p-value for all sources i.e.: linear, 2FI, quadratic, and cubic. The p-value was found 0.0065 for linear, 0.3757 for 2FI, <0.0001 for quadric and 0.2826 for cubic model source. From this quadratic model is suggested for study further summary of ANOVA generated from the software is presented in table 20.

Source	Sequential p-value	Lack of Fit p-value	Adjusted R^2	Predicted R^2	
Linear	0.0065	< 0.0001	0.5617	0.3950	
2FI	0.3757	< 0.0001	0.5558	0.2626	
Quadratic	**< 0.0001**	**0.5193**	**0.9978**	**0.9952**	**Suggested**
Cubic	0.2826	0.8905	0.9982	0.9986	Aliased

Table 19: Summary of ANOVA for particle size

Response 1 - PS (Particle Size)						
ANOVA for Response Surface Quadratic Model						
Source	**Sum of Squares**	**Df**	**Mean Square**	**F-value**	**p-value**	
Model	37199.67	5	7439.93	1110.11	< 0.0001	significant
A-Lipid concentration	9887.97	1	9887.97	1475.38	< 0.0001	
B-Surfactant concentration	13752.89	1	13752.89	2052.06	< 0.0001	
AB	1197.16	1	1197.16	178.63	< 0.0001	
A^2	4225.65	1	4225.65	630.51	< 0.0001	
B^2	9586.00	1	9586.00	1430.32	< 0.0001	
Residual	46.91	7	6.70			
Lack of Fit	18.77	3	6.26	0.8889	0.5193	not significant
Pure Error	28.15	4	7.04			
Cor Total	37246.59	12				

Table 20: Response surface quadratic model for particle size

Fit Statistics	
R^2	0.9987
Adjusted R^2	0.9978
Predicted R^2	0.9952
Adeq Precision	88.7632

Table 21: Fit statistics for particle size

Factor coding is **coded**

Sum of square is **TYPE III – Partial**

The **Model F-value** of 1110.11 implies the model is significant. There is only a 0.01% chance that an F-value this large could occur due to noise.

P-values less than 0.0500 indicate model terms are significant. In this case A, B, AB, A^2, B^2 are significant model terms. Values greater than 0.1000 indicate the model terms are not significant.

The **Lack of Fit F-value** of 0.89 implies the Lack of Fit is significant. There is only a 51.93% chance that a Lack of Fit F-value this large could occur due to noise.

The **Predicted R^2** of 0.9952 is in reasonable agreement with the **Adjusted R^2** of 0.9978; i.e. the difference is less than 0.2.

Adeq Precision measures the signal to noise ratio. A ratio greater than 4 is desirable.

Ratio of 88.763 indicates an adequate signal. This model can be used to navigate the design space.

Full model equation for Particle Size in terms of coded factors was obtained as

$PS = +124.72 + 35.16*A – 41.46*B -17.30*AB +24.65 *A^2+37.12*B^2$

PS represents the particle size, and A, B are coded values for the lipid concentration and surfactant concentration, respectively. Terms with p-values of less than 0.0001 were considered as significant. The p-values of all other terms were less than 0.0001 (Table 19); thus they possibly have significant effects on the EE of drug. The coefficient of determination (R^2) and adjusted R^2 were 0.9987 and 0.9978, respectively, which means that there is a good fit between independent variables and the particle size of drug. The statistical analysis of data showed that the obtained model was significant ($p < 0.0001$), which confirms that the coefficient of determination (R^2) and adjusted R^2 are statistically significant. The lack of fit was insignificant ($p = 0.5193$), indicating that the quadratic model accurately explains the variations of experimental data. Since one purpose of this study was to reduce size of SLNs, the terms with positive coefficients are considered favorable for increasing particle size. Conversely, negative coefficients which have a decreasing effect on particle size. The lipid concentration (A) and surfactant concentration (b) have a positive and negative coefficient, respectively. Accordingly, a linear increase in A and B leads to a decreasing and increasing effect on particle size, respectively. The normal probability distribution diagram implies that the residues are mainly located on a straight line and follow a normal distribution, as shown in Fig. 27.

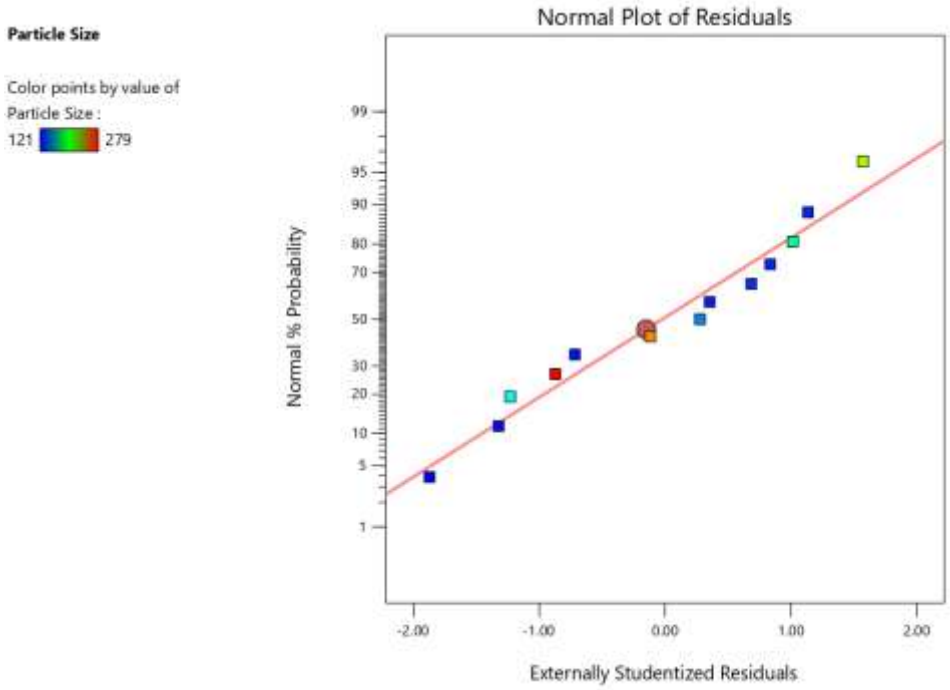

Figure 27: Normal probability distribution plot for particle size

4.2.2 ANALYSIS OF ENCAPSULATION EFFICIENCY

The particle size range in all the formulation was found from 36.45 to 76.95. The result of p-values is indicated for each model. The data presented in table 20 suggest the p-value for all sources i.e.: linear, 2FI, quadratic, and cubic. The p-value was found 0.0518 for linear, 0.1394 for 2FI, 0.0115 for quadric and 0.3594 for cubic model source. From this quadratic model is suggested for study further summary of ANOVA generated from the software is presented in table 22.

Source	Sequential p-value	Lack of Fit p-value	Adjusted R^2	Predicted R^2	
Linear	0.0518	0.0029	0.3361	-0.0214	
2FI	0.1394	0.0035	0.4291	-0.4122	
Quadratic	**0.0115**	**0.0190**	**0.7951**	**0.2182**	**Suggested**
Cubic	0.3594	0.0094	0.8095	-3.3147	Aliased

Table 22: Summary of ANOVA for encapsulation efficiency

Response 1 - EE (Encapsulation efficiency)						
ANOVA for Response Surface Quadratic Model						
Source	**Sum of Squares**	**Df**	**Mean Square**	**F-value**	**p-value**	
Model	1304.99	5	261.00	10.32	0.0040	significant
A-Lipid concentration	144.76	1	144.76	5.72	0.0480	
B-Surfactant concentration	517.39	1	517.39	20.45	0.0027	
AB	185.37	1	185.37	7.33	0.0303	
A^2	159.92	1	159.92	6.32	0.0402	
B^2	351.63	1	351.63	13.90	0.0074	
Residual	177.11	7	25.30			
Lack of Fit	158.96	3	52.99	11.68	0.0190	significant
Pure Error	18.14	4	4.54			
Cor Total	1482.09	12				

Table 23: Response surface quadratic model for encapsulation efficiency

Fit Statistics	
R^2	0.8805
Adjusted R^2	0.7951
Predicted R^2	0.2182
Adeq Precision	9.0739

Table 24: Fit statistics for encapsulation efficiency

Factor coding is **coded**

Sum of square is **TYPE III – Partial**

The **Model F-value** of 10.32 implies the model is significant. There is only a 0.40% chance that an F-value this large could occur due to noise.

P-values less than 0.0500 indicate model terms are significant. In this case A, B, AB, A^2, B^2 are significant model terms. Values greater than 0.1000 indicate the model terms are not significant.

The **Lack of Fit F-value** of 11.68 implies the Lack of Fit is significant. There is only a 1.90% chance that a Lack of Fit F-value this large could occur due to noise.

The **Predicted R^2** of 0.2182 is not as close to the **Adjusted R^2** of 0.7951 as one might normally expect; i.e. the difference is more than 0.2.

Adeq Precision measures the signal to noise ratio. A ratio greater than 4 is desirable. Ratio of 9.074 indicates an adequate signal. This model can be used to navigate the design space

According to the statistical analysis, the quadratic equation of entrapment efficiency is significantly fitted to the experimental data and presented in the following equation:

$$EE = +74.57 - 4.25 * A + 8.04 * B + 6.81 * AB - 4.79 * A^2 - 7.11 * B^2$$

EE represents the entrapment efficiency, A and B are coded values for the lipid concentration and surfactant concentration, respectively. Terms with p-values of less than 0.0040 were considered as significant. Except for the main term of Lipid concentration (A), all other terms were less than 0.0040 (Table 20); The coefficient of determination (R^2) and adjusted R^2 were 0.8805 and 0.7951, respectively, which means that there is a good fit between independent variables and the EE of drug. The statistical analysis of data showed that the obtained model was significant ($p < 0.0040$), which confirms that the coefficient of determination (R^2) and adjusted R^2 are statistically significant. Since one purpose of this study was to increase the amount of entrapped drug in SLNs, the terms with positive coefficients are considered favorable for increasing entrapment efficiency. Conversely, negative coefficients which have a decreasing effect on entrapment efficiency must be kept at lower levels. The Lipid concentration (A) and surfactant concentration (B) have a negative and positive coefficient, respectively. Accordingly, a linear increase in A and B leads to a decreasing and increasing effect on entrapment efficiency, respectively. The normal probability distribution diagram implies that the residues are mainly located on a straight line and follow a normal distribution, as shown in Fig. 28 .Describes the healthy correlation for the data in of predicted results and actual results. Each value points are located closer to the center line which indicates the relations with strong prediction.

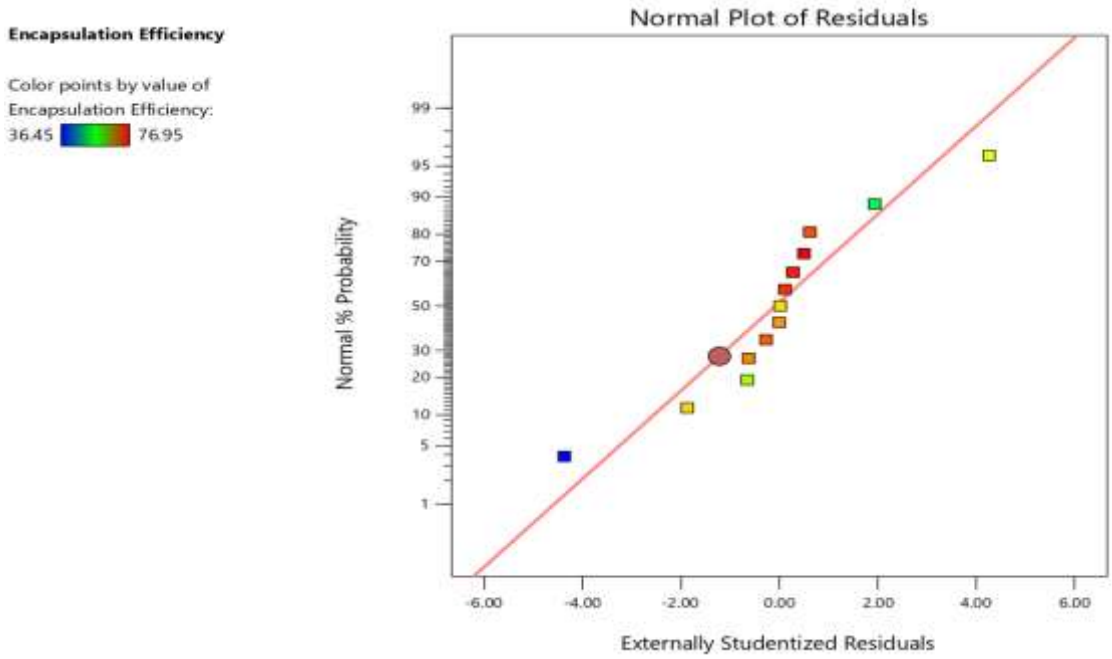

Figure 28: Normal probability distribution plot for encapsulation efficiency

4.3. RESPONSE SURFACE ANALYSIS

The effect of the formulation variables on a response was assessed by studying the three-dimensional response surface plots.

4.3.1. EFFECT ON PARTICLE SIZE

The three-dimensional response surface plots and contour plots for particle size are presented in Figure 29, 30. As shown in Figure particle size increased with increasing in lipid concentration. Furthermore, increasing the particle size as a result of higher content of lipid might occur due to increased collision and aggregation of the nanoparticles, or relatively lack of enough surfactant for covering the surface of the particles. However, as indicated in Table 17, B (surfactant concentration) showed negative effect on particle size and by increasing B, particle size decreased, while increasing the concentration of surfactant.

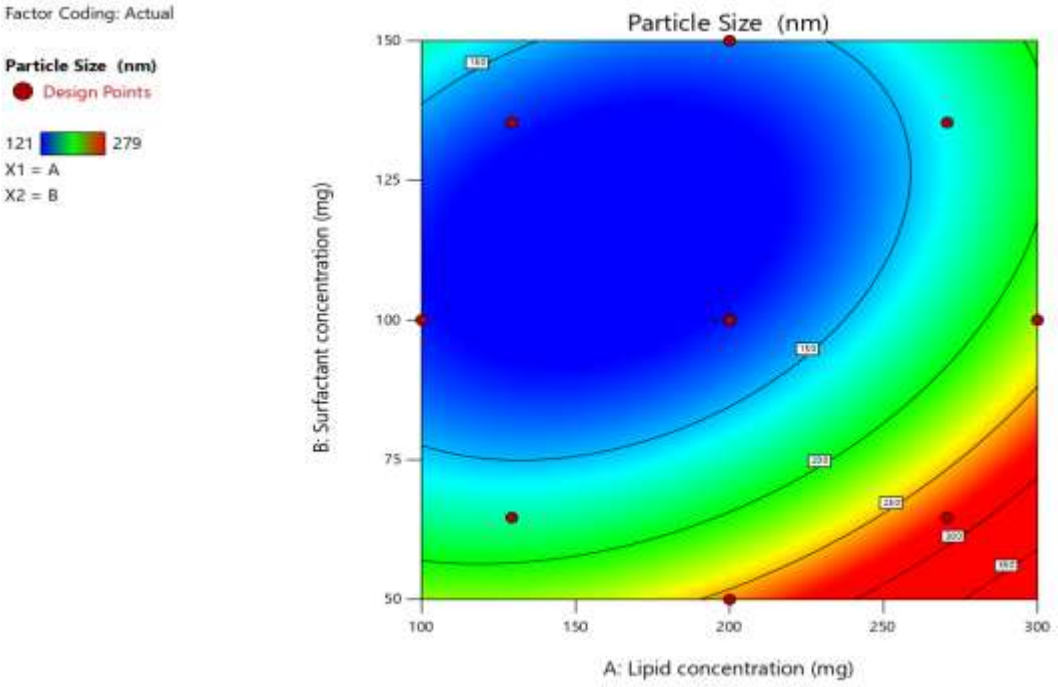

Figure 29: Contour plot for particle size analysis

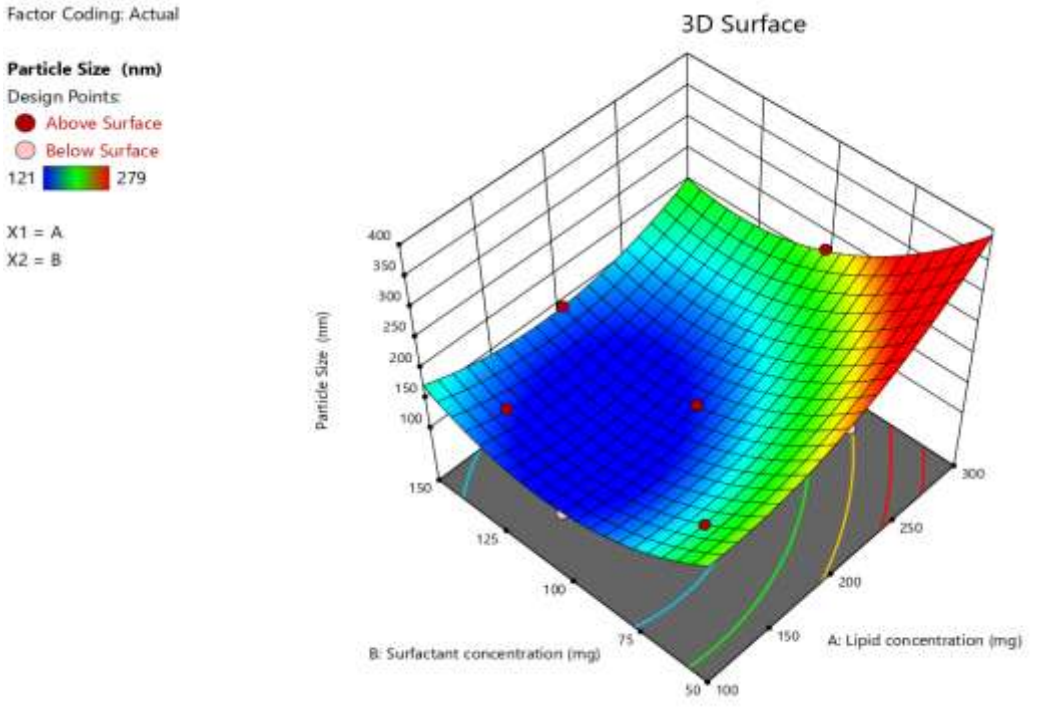

Figure 30: 3D plot for particle size analysis

4.3.2. EFFECT ON ENCAPSULATION EFFICIENCY

Figure 31, 32 describes the response surface model and contour plots for EE in response to the investigated variables. As shown in Figure 31, 32 EE improved with increases in lipid and surfactant concentration to an optimal maximum value. The possible reason could be that higher content of lipid afforded more space to accommodate the drug.

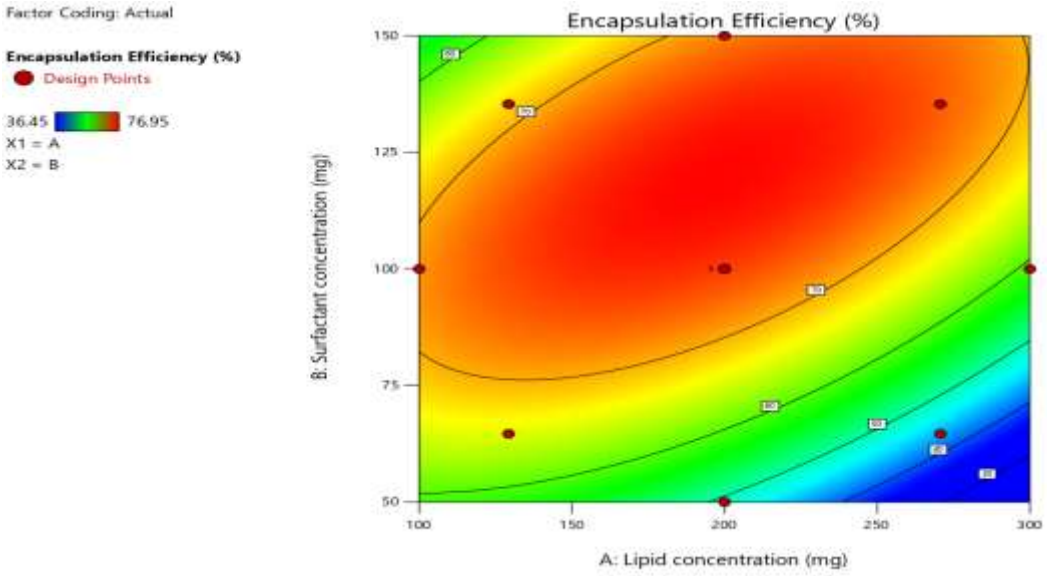

Figure 31: Contour plot for particle size analysis

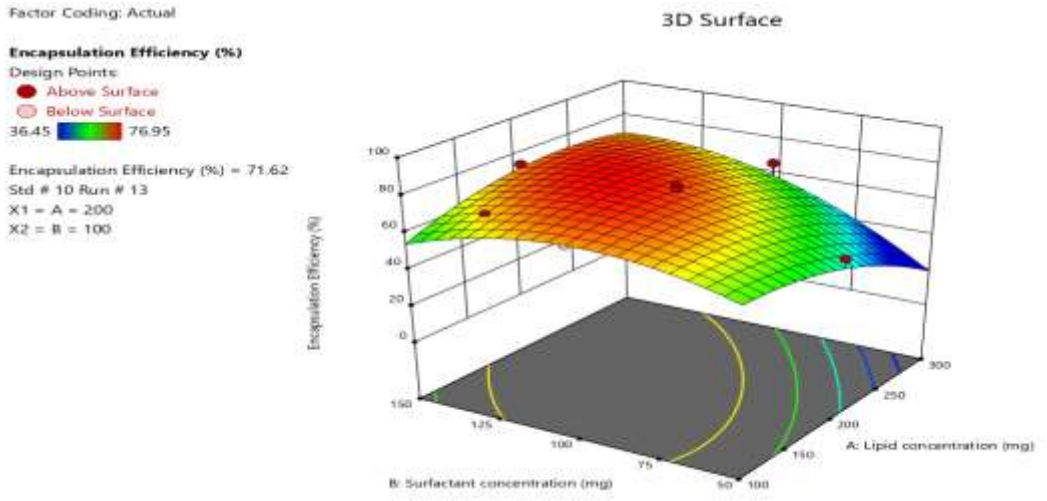

Figure 32: Contour plot for particle size analysis

4.4. EXPERIMENTAL VALIDATION OF DESIGN SPACE

The overlay plot has suggested a maximum possibility for predicted response values and concluded the possible values of responsible factors for it. Based on this conclusion, the trial run was carried out by taking the values reference from overlay plot. Overlay plot for optimization is given in figure 33. The predicted values for respective factors are 111.633 and 76.885 for particle size and %EE respectively

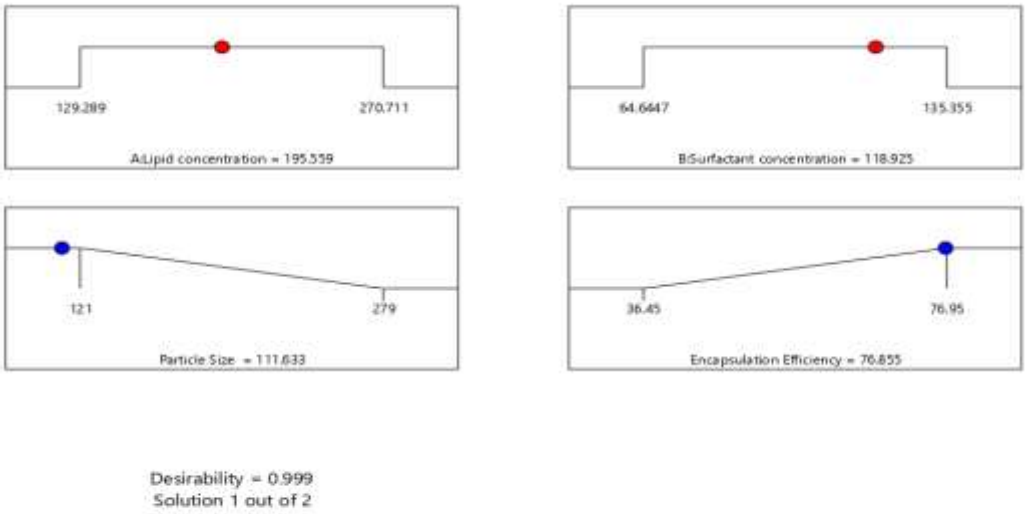

Figure 33: Ramp model of optimized formulation

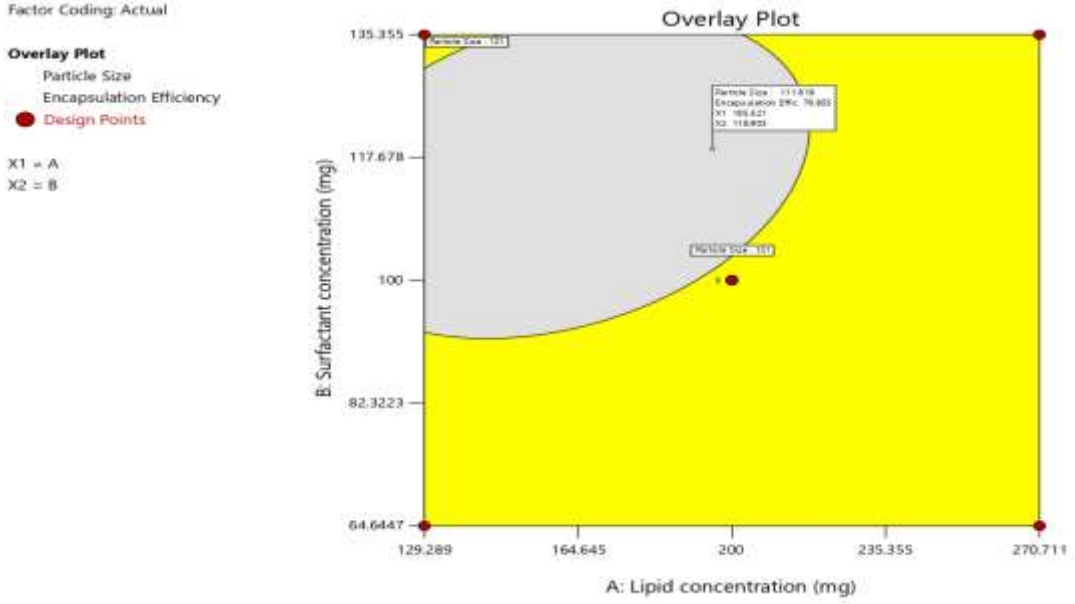

Figure 34: Over lay plot for optimized formulation

5. Characterization of Rivastigmine tartrate SLN

5.1. Particle size, PDI and Zeta potential analysis

The average particle size and the poly dispersity index of optimized formulations were analysed using Malvern zeta sizer is found to be 152.4nm

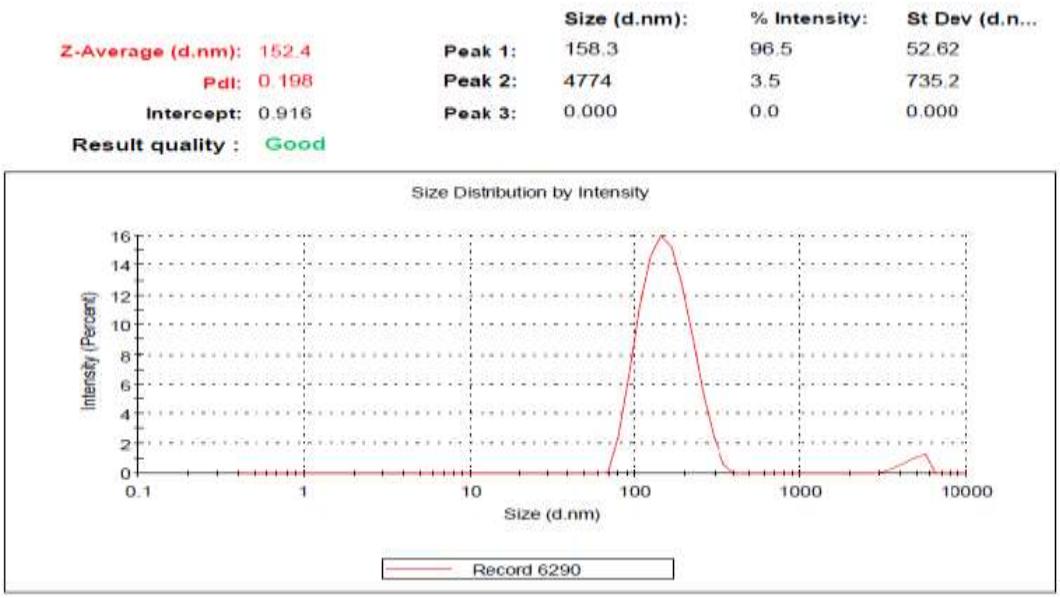

Figure 35: Particle size distribution of Optimized RT SLN

The most important characterization parameter, also called Polydispersity Index (PI) which governs the physical stability of nanoparticles and should be as low as possible for the long term stability of nanoparticles.

a) PI value of 0.1–0.25 indicates a fairly narrow size distribution
b) PI value greater than 0.5 indicates a very broad distribution

Polydispersity index of optimized formulation is 0.198 and it indicates fairly narrow size distribution. Zeta potential is affected by the charge of the groups present on the MWCNTs. Nanoparticles with a zeta potential above ±30 mV have been shown to be stable, as the surface charge prevents aggregation of the particles. Optimized formulation with zeta potential -31.4 mV was found to be stable.

.

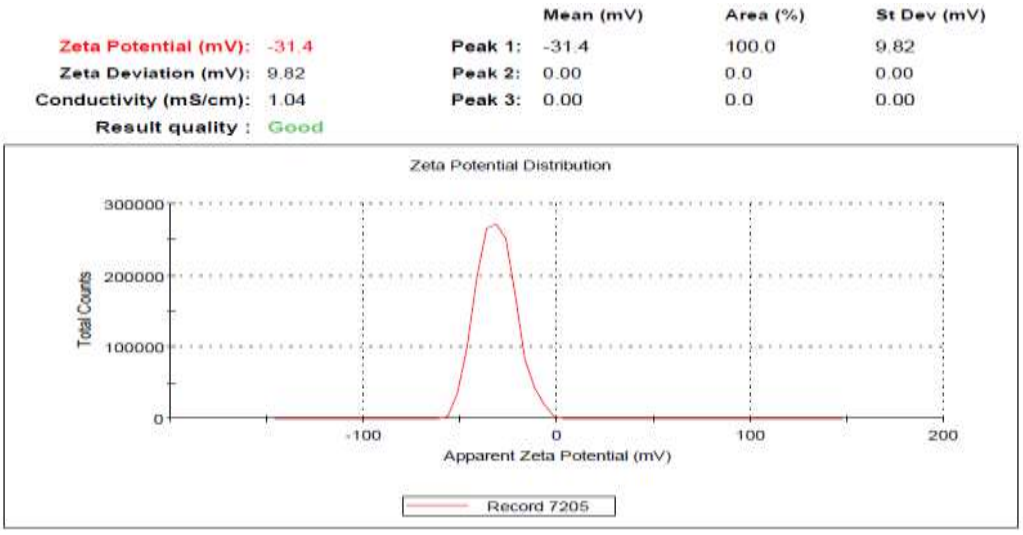

Figure 36: Zeta potential of Optimized RT SLN

5.2. Encapsulation efficiency

The result of entrapment efficiency of optimized formulation is 76.1%. This condition has shown an improved response values in comparison with the previously optimized formulation.

5.3.Scanning electron microscopy (SEM)

SEM image describes that the particles have uniform loose aggregates, spherical in shape with a smooth surface and they are uniformly distributed.

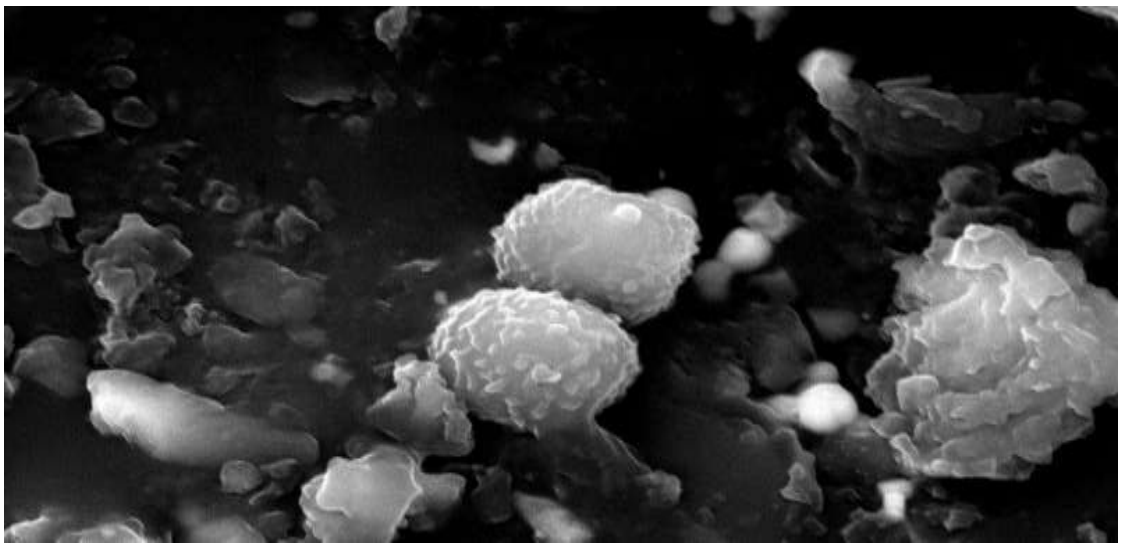

Figure 37: SEM image of Optimized RT SLN

5.4. Differential scanning calorimetry (DSC)

Analysis was carried as described in procedure. This thermal property analysis was carried out on optimized SLN formulation, Rivastigmine tartrate, Glyceryl mono sterate, Blank SLN and physical mixture thermal property was evaluated.

For RT sharp peak was obtained at 128.5˚C which indicates the melting point of RT. DSC peak for GMS alone was obtained at 59 ˚C.DSC analysis shows a peak at 57.3˚C and 130.1 ˚C which indicates the melting peak of drug and lipid. Physical mixture of drug and lipid gives two peaks indicating an individual melting point. The peak point of Blank SLN and RT SLN remain similar level while comparing with drug and lipid.

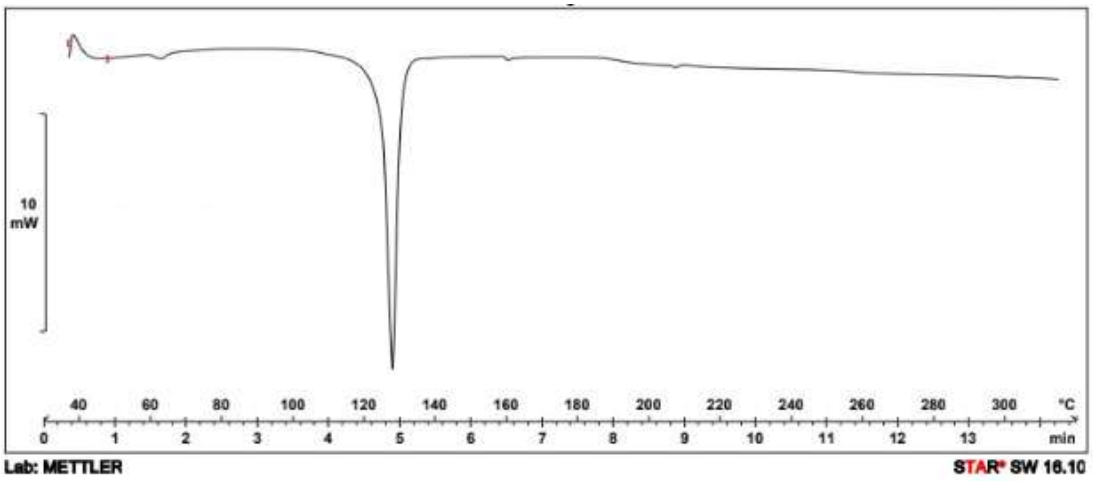

Figure 38: DSC of Rivastigmine tartrate

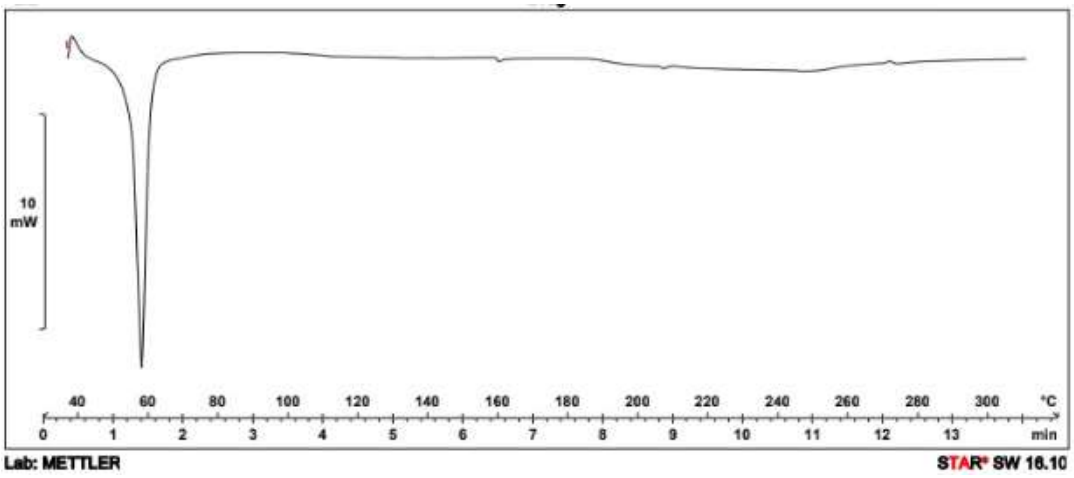

Figure 39: DSC of GMS

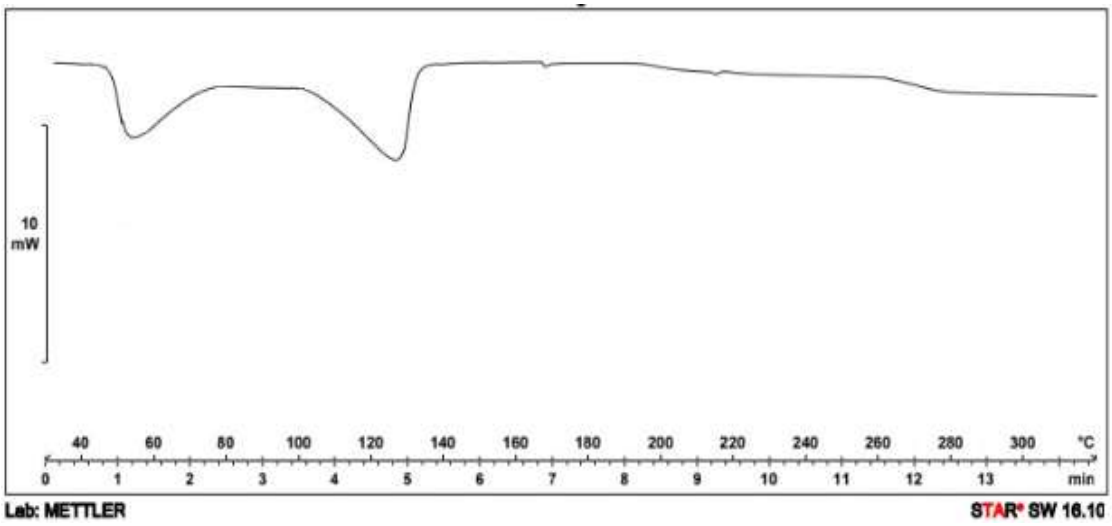

Figure 40: DSC of Physical mixture

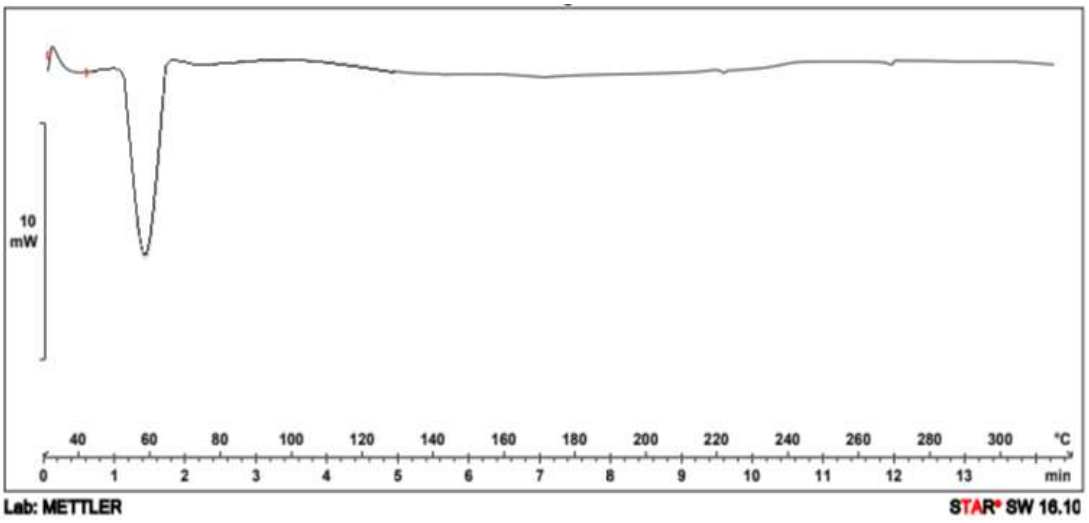

Figure 41: DSC of Blank SLN

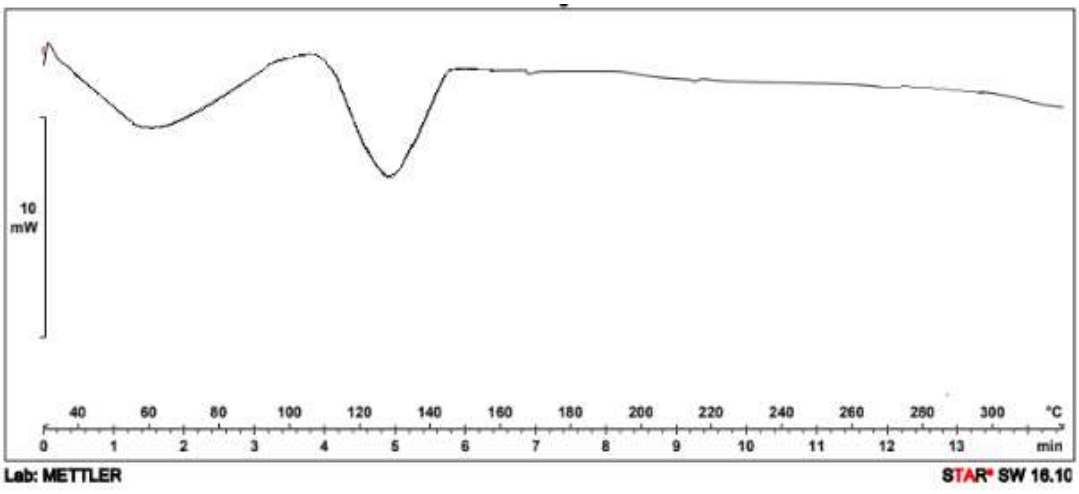

Figure 42: DSC of RT SLN

5.5. In vitro drug release studies

The *in vitro* release of RT-SLN and RT solution was studied by the dialysis bag technique. The release study was performed in Phosphate buffer pH 7.4. The results are shown in table 25**.** The results showed that the during initial time points, slight increase in percentage drug release in drug solution because of high aqueous solubility of RT in aqueous medium. But in case of RT SLN, the time required for drug to leach out from lipid core was high compared to RT solution. Later increase in drug release is due to decrease in particle size. The drug release was plotted in a graph and given in figure 42

.Time (h)	Cumulative drug release (%)	
	RT solution	RT SLN
0	0	0
0.5	21.51	17.81
1	28.3	26.64
2	30.88	38.87
4	35.91	47.15
6	39.81	60.57
8	43.38	68.38
10	53.65	75.93
12	61.59	87.74

Table 25: *In vitro* drug release of RT solution and RT SLN

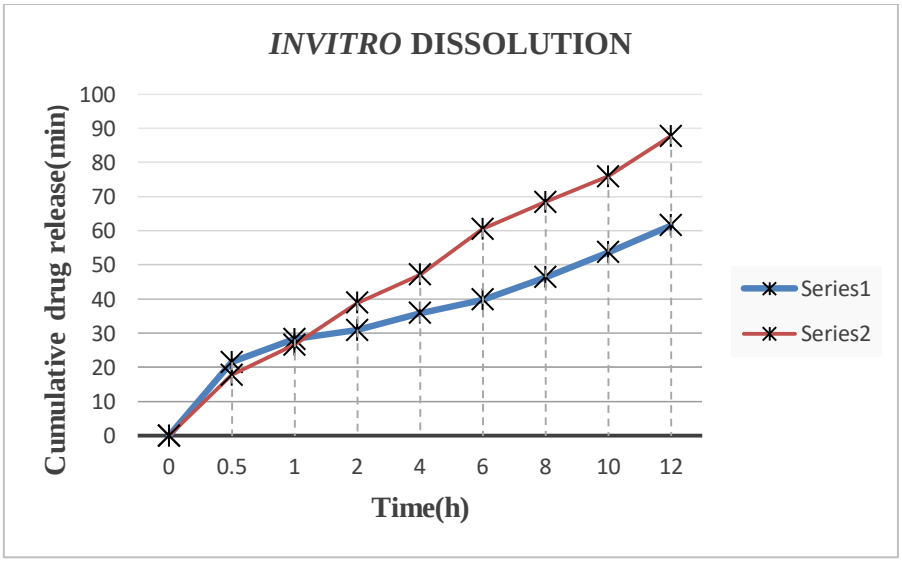

Figure 43: *In vitro* drug release of RT solution and RT SLN

Series 1 – RT solution

Series 2 – RT SLN solution

5.6. *In vitro* release kinetics

The kinetics and mechanism of drug release were studied by release kinetics, r^2 and n values are indicated in the table 26. Results shows Higuchi model have high linearity compared to first and zero order.

The exact mechanism of the release kinetics was determined by korsemeyer peppas model. Results indicated that the SLN formulations followed Non-fikian model of release kinetics

Code	Zero order	First order	Higuchi	Korsemeyer peppas	
	r^2	r^2	r^2	n	r^2
Formulation	0.9627	0.9853	0.9946	0.481	0..9976

Table 26:Release kinetics of Optimized RT SLN

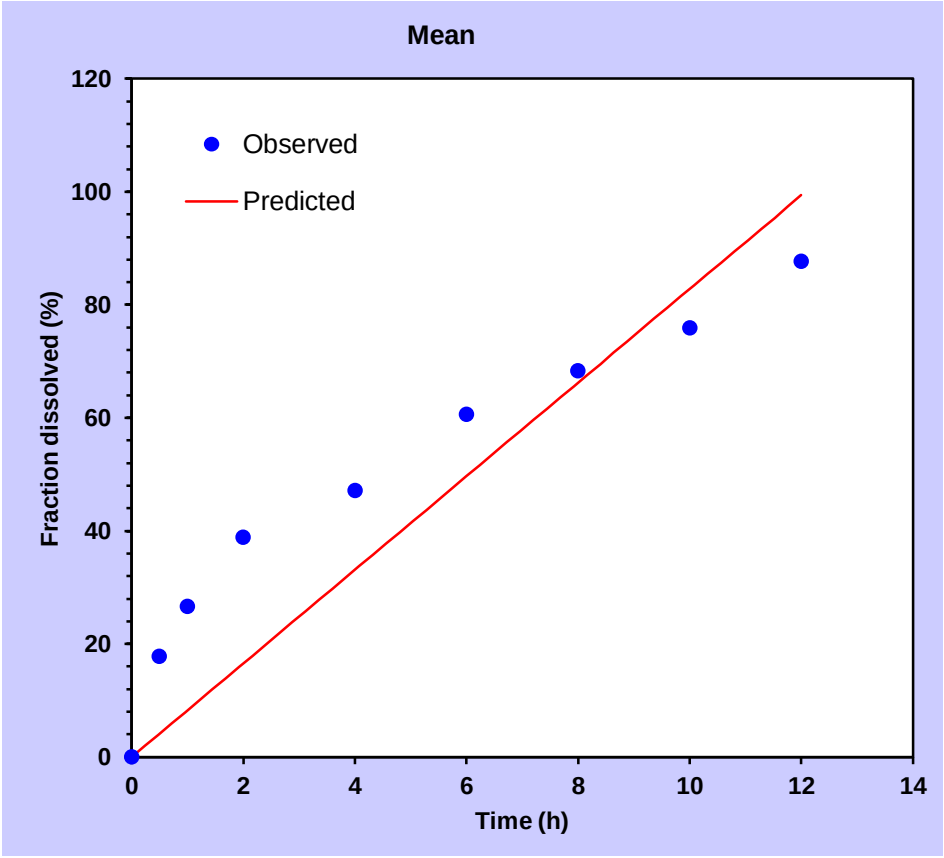

Figure 44: Zero order of drug release

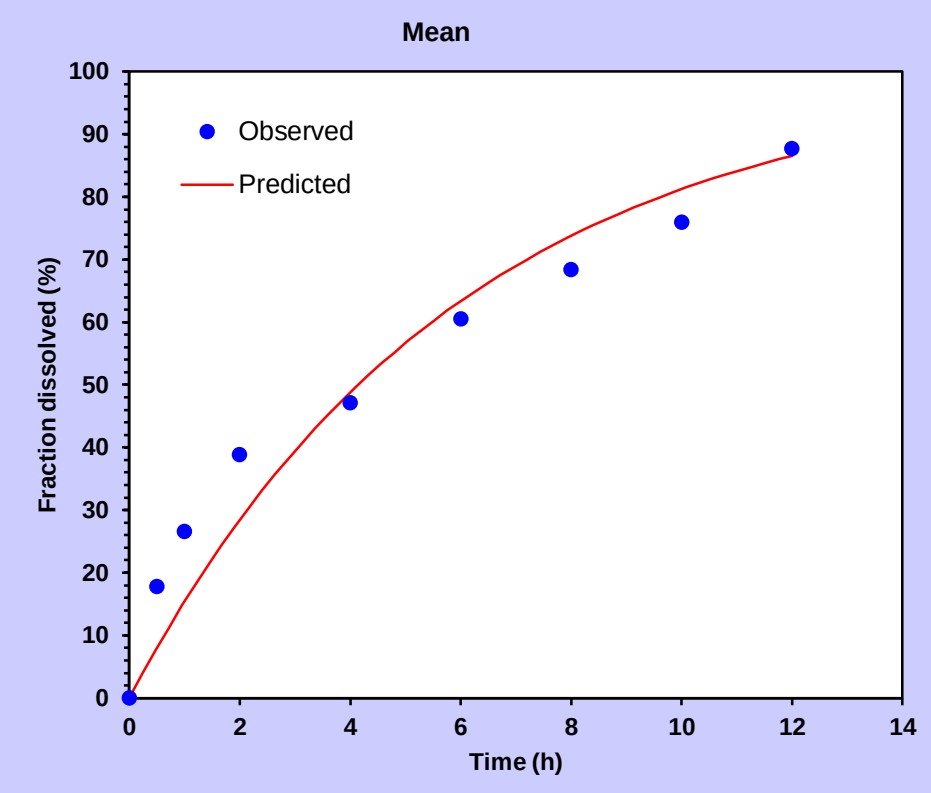

Figure 45: First order of drug release

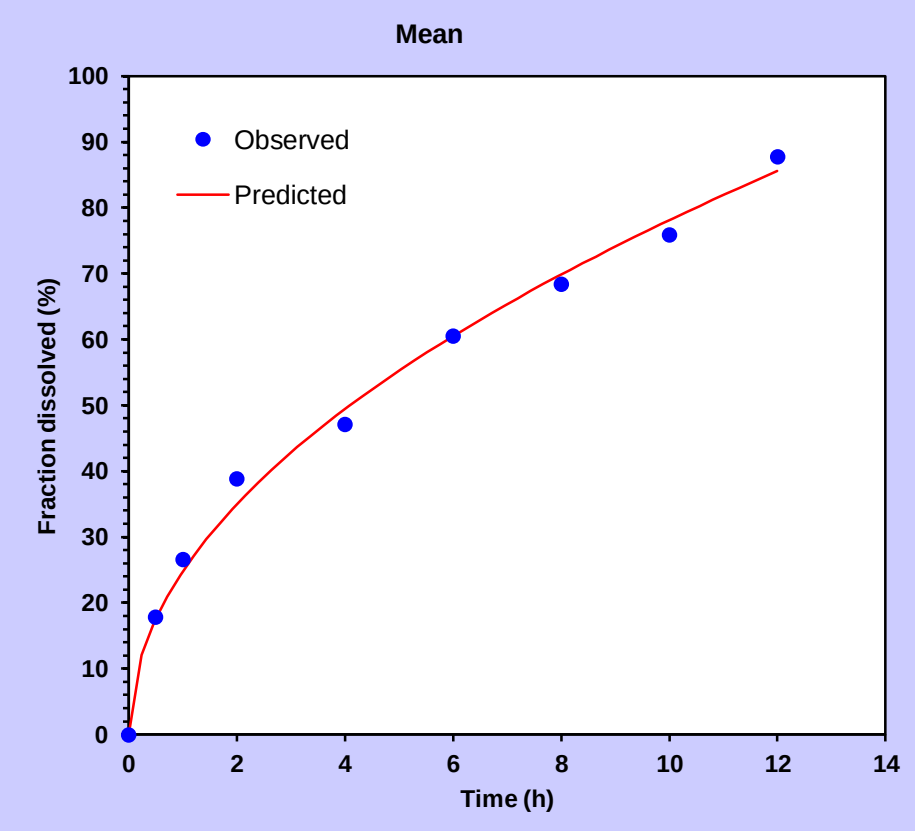

Figure 46: Higuchi model of drug release

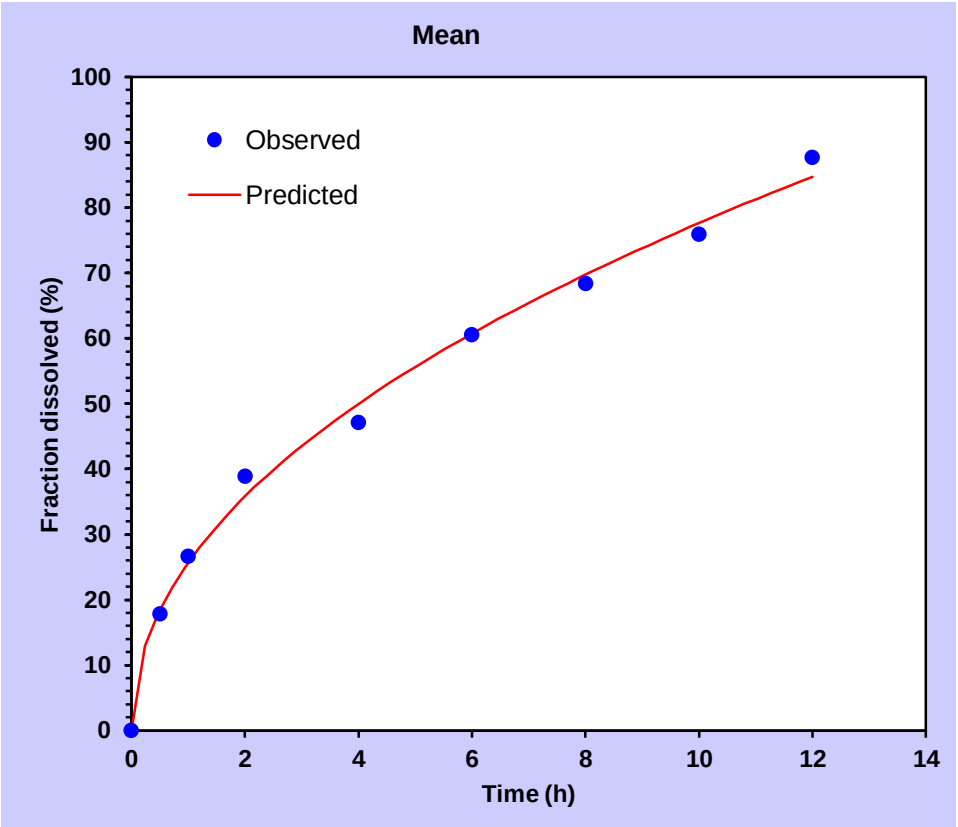

Figure 47: Korsemeyer peppas model of drug release

SUMMARY AND CONCLUSION

The objective of present investigation was to develop, optimize and evaluate rivastigmine tartrate loaded solid lipid nanoparticle (RT SLN) by using central composite design. SLN were prepared by microemulsion method using a systemic approach of design of experiments and evaluated. From the characterization of active drug it was concluded that the drug sample Rivastigmine tartrate was authentic, pure and confirming to the standards. The sample showed maximum absorbance at wavelength 263 nm. The concentrations of RT (10-60 µg/ml) showed good linearity with R2 value of 0.999 which suggests that it obey Beer-Lamberts law. Various preliminary experiments were performed for selection of suitable excipients. Various lipids and surfactant are selected on the basis of solubility and particle size and thus glyceryl monosterate selected as lipid, and poloxamer 188 as surfactant. Further High speed homogenizer stirring speed and time was optimized HSH is operated at 15000 rpm for 5minutes.

The design selected was Central composite design by employing design expert software. Two input factors were studied at five different levels including central point 0, +1, -1, ±α throughout the preparation process to determine their effect on two responses, namely mean particle size and encapsulation efficiency. The input factors being selected are the following: Lipid concentration (100, 200 and 300 mg), concentration of surfactant (50, 100, 150 mg). Characterization of all formulation particle size found to be in range of 121 to 279 nm and encapsulation efficiency in range of 36.45 to 76.95%. The overlay plot has suggested a maximum possibility for predicted response values and concluded the possible values of responsible factors for it. Based on this conclusion, the trial run was carried out by taking the values reference from overlay plot. The predicted values for respective factors are 111.633 and 76.885 for particle size and %EE respectively.

Characterization of optimized RT SLN particle size found to be 152.4nm and particle distribution index value is 0.198 indicates fairly narrow distribution. Optimized formulation with zeta potential -31.4 mV was found to be stable. SEM photographs of RT SLN indicate particles have uniform loose aggregates, spherical in shape with a smooth surface and they are uniformly distributed. On comparison of *in vitro* drug release studies of RT solution and RT SLN shows that RT SLN has higher

release 87.74% at 12hrs compared to RT Solution 61.59%. From the obtained results it was concluded that the Rivastigmine tartrate SLNs can be employed for controlled delivery of drug in the treatment of Alzheimer's disease.

BIBLIOGRAPHY

1. Wong KH, Riaz MK, Xie Y, Zhang X, Liu Q, Chen H, Bian Z, Chen X, Lu A, Yang Z. Review of current strategies for delivering Alzheimer's disease drugs across the blood-brain barrier. International journal of molecular sciences. 2019 Jan;20(2):381.
2. Banks WA. Drug delivery to the brain in Alzheimer's disease: Consideration of the blood–brain barrier. Advanced drug delivery reviews. 2012 May 15;64(7):629-39.
3. Mancini S, Minniti S, Gregori M, Sancini G, Cagnotto A, Couraud PO, Ordóñez-Gutiérrez L, Wandosell F, Salmona M, Re F. The hunt for brain Aβ oligomers by peripherally circulating multi-functional nanoparticles: Potential therapeutic approach for Alzheimer disease. Nanomedicine: Nanotechnology, Biology and Medicine. 2016 Jan 1;12(1):43-52
4. Dementia India report [Internet]. [Cited 2019 Dec 03] Available from: https://www.researchgate.net/publication/291246599_Dementia_in_India
5. Alzheimers association [Internet]. [Cited 2019 Dec 03] Available from http://ardsi.org/SymptomsofAlzheimersDisease.aspx
6. FDA approved treatments for Alzheimers disease https://www.alz.org/media/documents/fda-approved-treatments-alzheimers-ts.pdf
7. Bassil N, Grossberg GT. Novel regimens and delivery systems in the pharmacological treatment of Alzheimer's disease. CNS drugs. 2009 Apr 1;23(4):293-307.
8. Barratt G. Colloidal drug carriers: achievements and perspectives. Cellular and Molecular Life Sciences CMLS. 2003 Jan 1;60(1):21-37.
9. Mara Mainardes R, Cristina Cocenza Urban M, Oliveira Cinto P, Vinicius Chaud M, Cesar Evangelista R, Palmira Daflon Gremiao M. Liposomes and micro/nanoparticles as colloidal carriers for nasal drug delivery. Current drug delivery. 2006 Jul 1;3(3):275-85.
10. Mudshinge SR, Deore AB, Patil S, Bhalgat CM. Nanoparticles: emerging carriers for drug delivery. Saudi pharmaceutical journal. 2011 Jul 1;19(3):129-41.

11. Karthivashan G, Ganesan P, Park SY, Kim JS, Choi DK. Therapeutic strategies and nano-drug delivery applications in management of ageing Alzheimer's disease. Drug delivery. 2018 Jan 1;25(1):307-20.
12. Mishra V, Bansal KK, Verma A, Yadav N, Thakur S, Sudhakar K, Rosenholm JM. Solid lipid nanoparticles: Emerging colloidal nano drug delivery systems. Pharmaceutics. 2018 Dec;10(4):191.
13. Garud A, Singh D, Garud N. Solid lipid nanoparticles (SLN): method, characterization and applications. International Current Pharmaceutical Journal. 2012 Oct 3;1(11):384-93.
14. Ramteke KH, Joshi SA, Dhole SN. Solid lipid nanoparticle: a review. IOSR Journal of pharmacy. 2012 Nov;2(6):34-44.
15. Mishra V, Bansal KK, Verma A, Yadav N, Thakur S, Sudhakar K, Rosenholm JM. Solid lipid nanoparticles: Emerging colloidal nano drug delivery systems. Pharmaceutics. 2018 Dec;10(4):191.
16. Teixeira MI, Lopes CM, Amaral MH, Costa PC. Current insights on lipid nanocarrier-assisted drug delivery in the treatment of neurodegenerative diseases. European Journal of Pharmaceutics and Biopharmaceutics. 2020 Jan 23.
17. Derakhshankhah H, Sajadimajd S, Jafari S, Izadi Z, Sarvari S, Sharifi M, Falahati M, Moakedi F, Muganda WC, Müller M, Raoufi M. Novel therapeutic strategies for Alzheimer's disease: Implications from cell-based therapy and Nanotherapy. Nanomedicine: Nanotechnology, Biology and Medicine. 2020 Jan 10:102149.
18. Chauhan MK, Sharma PK. Optimization and characterization of rivastigmine nanolipid carrier loaded transdermal patches for the treatment of dementia. Chemistry and physics of lipids. 2019 Nov 1;224:104794.
19. Dara T, Vatanara A, Sharifzadeh M, Khani S, Vakilinezhad MA, Vakhshiteh F, Meybodi MN, Malvajerd SS, Hassani S, Mosaddegh MH. Improvement of memory deficits in the rat model of Alzheimer's disease by erythropoietin-loaded solid lipid nanoparticles. Neurobiology of learning and memory. 2019 Dec 1;166:107082.
20. Oehlke K, Keppler JK, Milsmann J, Mayer-Miebach E, Greiner R, Steffen-Heins A. Adsorption of β-lactoglobulin to solid lipid nanoparticles (SLN)

depends on encapsulated compounds. Journal of food engineering. 2019 Apr 1;247:144-51.

21. Anand A, Arya M, Kaithwas G, Singh G, Saraf SA. Sucrose stearate as a biosurfactant for development of rivastigmine containing nanostructured lipid carriers and assessment of its activity against dementia in C. elegans model. Journal of Drug Delivery Science and Technology. 2019 Feb 1;49:219-26.
22. Haider MF, Khan S, Gaba B, Alam T, Baboota S, Ali J, Ali A. Optimization of rivastigmine nanoemulsion for enhanced brain delivery: in-vivo and toxicity evaluation. Journal of Molecular Liquids. 2018 Apr 1;255:384-96.
23. Montoto SS, Sbaraglini ML, Talevi A, Couyoupetrou M, Di Ianni M, Pesce GO, Alvarez VA, Bruno-Blanch LE, Castro GR, Ruiz ME, Islan GA. Carbamazepine-loaded solid lipid nanoparticles and nanostructured lipid carriers: physicochemical characterization and in vitro/in vivo evaluation. Colloids and Surfaces B: Biointerfaces. 2018 Jul 1;167:73-81.
24. Youssef NA, Kassem AA, Farid RM, Ismail FA, EL-Massik MA, Boraie NA. A novel nasal almotriptan loaded solid lipid nanoparticles in mucoadhesive in situ gel formulation for brain targeting: preparation, characterization and in vivo evaluation. International journal of pharmaceutics. 2018 Sep 5;548(1):609-24.
25. Graverini G, Piazzini V, Landucci E, Pantano D, Nardiello P, Casamenti F, Pellegrini-Giampietro DE, Bilia AR, Bergonzi MC. Solid lipid nanoparticles for delivery of andrographolide across the blood-brain barrier: In vitro and in vivo evaluation. Colloids and Surfaces B: Biointerfaces. 2018 Jan 1;161:302-13.
26. Ding Y, Nielsen KA, Nielsen BP, Bøje NW, Müller RH, Pyo SM. Lipid-drug-conjugate (LDC) solid lipid nanoparticles (SLN) for the delivery of nicotine to the oral cavity–optimization of nicotine loading efficiency. European Journal of Pharmaceutics and Biopharmaceutics. 2018 Jul 1;128:10-7.
27. Shtay R, Tan CP, Schwarz K. Development and characterization of solid lipid nanoparticles (SLNs) made of cocoa butter: A factorial design study. Journal of Food Engineering. 2018 Aug 1;231:30-41.
28. Zielińska A, Martins-Gomes C, Ferreira NR, Silva AM, Nowak I, Souto EB. Anti-inflammatory and anti-cancer activity of citral: Optimization of citral-loaded solid lipid nanoparticles (SLN) using experimental factorial design and LUMiSizer®. International journal of pharmaceutics. 2018 Dec 20;553(1-2):428-40.

29. Yokaichiya F, Schmidt C, Storsberg J, Vollrath MK, de Araujo DR, Kent B, Clemens D, Wingert F, Franco MK. Effects of doxorubicin on the structural and morphological characterization of solid lipid nanoparticles (SLN) using small angle neutron scattering (SANS) and small angle X-ray scattering (SAXS). Physica B: Condensed Matter. 2018 Dec 15;551:191-6.
30. Patel M, Sawant K. A quality by design concept on lipid based nanoformulation containing antipsychotic drug: screening design and optimization using response surface methodology. J Nanomed Nanotechnol. 2017;8(3):1-1.
31. Tapeinos C, Battaglini M, Ciofani G. Advances in the design of solid lipid nanoparticles and nanostructured lipid carriers for targeting brain diseases. Journal of Controlled Release. 2017 Oct 28;264:306-32.
32. Abouhussein DM, Khattab A, Bayoumi NA, Mahmoud AF, Sakr TM. Brain targeted rivastigmine mucoadhesive thermosensitive In situ gel: Optimization, in vitro evaluation, radiolabeling, in vivo pharmacokinetics and biodistribution. Journal of Drug Delivery Science and Technology. 2018 Feb 1;43:129-40.
33. Wavikar P, Pai R, Vavia P. Nose to brain delivery of rivastigmine by in situ gelling cationic nanostructured lipid carriers: enhanced brain distribution and pharmacodynamics. Journal of pharmaceutical sciences. 2017 Dec 1;106(12):3613-22.
34. Severino P, Silveira EF, Loureiro K, Chaud MV, Antonini D, Lancellotti M, Sarmento VH, da Silva CF, Santana MH, Souto EB. Antimicrobial activity of polymyxin-loaded solid lipid nanoparticles (PLX-SLN): Characterization of physicochemical properties and in vitro efficacy. European Journal of Pharmaceutical Sciences. 2017 Aug 30;106:177-84.
35. Fatouh AM, Elshafeey AH, Abdelbary A. Intranasal agomelatine solid lipid nanoparticles to enhance brain delivery: formulation, optimization and in vivo pharmacokinetics. Drug design, development and therapy. 2017;11:1815.
36. Kuo YC, Cheng SJ. Brain targeted delivery of carmustine using solid lipid nanoparticles modified with tamoxifen and lactoferrin for antitumor proliferation. International journal of pharmaceutics. 2016 Feb 29;499(1-2):10-9.
37. Muntimadugu E, Dhommati R, Jain A, Challa VG, Shaheen M, Khan W. Intranasal delivery of nanoparticle encapsulated tarenflurbil: A potential brain

targeting strategy for Alzheimer's disease. European journal of pharmaceutical sciences. 2016 Sep 20;92:224-34.

38. Nagpal K, Singh SK, Mishra DN. Optimization of brain targeted chitosan nanoparticles of Rivastigmine for improved efficacy and safety. International journal of biological macromolecules. 2015 Aug 1;59:72-83.
39. Laserra S, Basit A, Sozio P, Marinelli L, Fornasari E, Cacciatore I, Ciulla M, Türkez H, Geyikoglu F, Di Stefano A. Solid lipid nanoparticles loaded with lipoyl–memantine codrug: preparation and characterization. International journal of pharmaceutics. 2015 May 15;485(1-2):183-91.
40. Shah B, Khunt D, Bhatt H, Misra M, Padh H. Application of quality by design approach for intranasal delivery of rivastigmine loaded solid lipid nanoparticles: effect on formulation and characterization parameters. European journal of pharmaceutical sciences. 2015 Oct 12;78:54-66.
41. Baig MS, Ahad A, Aslam M, Imam SS, Aqil M, Ali A. Application of Box–Behnken design for preparation of levofloxacin-loaded stearic acid solid lipid nanoparticles for ocular delivery: optimization, in vitro release, ocular tolerance, and antibacterial activity. International journal of biological macromolecules. 2016 Apr 1;85:258-70.
42. Gajra B, Patel RR, Dalwadi C. Formulation, optimization and characterization of cationic polymeric nanoparticles of mast cell stabilizing agent using the Box–Behnken experimental design. Drug development and industrial pharmacy. 2016 May 3;42(5):747-57.
43. Kovačević AB, Müller RH, Savić SD, Vuleta GM, Keck CM. Solid lipid nanoparticles (SLN) stabilized with polyhydroxy surfactants: preparation, characterization and physical stability investigation. Colloids and Surfaces A: Physicochemical and Engineering Aspects. 2014 Mar 5;444:15-25.
44. Kakkar V, Mishra AK, Chuttani K, Kaur IP. Proof of concept studies to confirm the delivery of curcumin loaded solid lipid nanoparticles (C-SLNs) to brain. International journal of pharmaceutics. 2013 May 20;448(2):354-9.
45. Negi JS, Chattopadhyay P, Sharma AK, Ram V. Development of solid lipid nanoparticles (SLNs) of lopinavir using hot self nano-emulsification (SNE) technique. European Journal of Pharmaceutical Sciences. 2013 Jan 23;48(1-2):231-9.

46. Kumar PP, Gayatri P, Sunil R, Jaganmohan S, Rao YM. Atorvastatin loaded solid lipid nanoparticles: formulation, optimization, and in vitro characterization. IOSR J Pharm. 2012;2(5):23-32.
47. Fazil M, Md S, Haque S, Kumar M, Baboota S, kaur Sahni J, Ali J. Development and evaluation of rivastigmine loaded chitosan nanoparticles for brain targeting. European journal of pharmaceutical sciences. 2012 Aug 30;47(1):6-15.
48. Vitorino C, Carvalho FA, Almeida AJ, Sousa JJ, Pais AA. The size of solid lipid nanoparticles: an interpretation from experimental design. Colloids and surfaces B: biointerfaces. 2011 May 1;84(1):117-30.
49. Dhawan S, Kapil R, Singh B. Formulation development and systematic optimization of solid lipid nanoparticles of quercetin for improved brain delivery. Journal of Pharmacy and Pharmacology. 2011 Mar;63(3):342-51.
50. Singh S, Dobhal AK, Jain A, Pandit JK, Chakraborty S. Formulation and evaluation of solid lipid nanoparticles of a water soluble drug: zidovudine. Chemical and pharmaceutical bulletin. 2010 May 1;58(5):650-5.
51. Bondì ML, Craparo EF, Giammona G, Drago F. Brain-targeted solid lipid nanoparticles containing riluzole: preparation, characterization and biodistribution. Nanomedicine. 2010 Jan;5(1):25-32.
52. Mandawgade SD, Sharma S, Pathak S, Patravale VB. Development of SMEDDS using natural lipophile: application to β-artemether delivery. International journal of pharmaceutics. 2008 Oct 1;362(1-2):179-83.
53. Roney C, Kulkarni P, Arora V, Antich P, Bonte F, Wu A, Mallikarjuana NN, Manohar S, Liang HF, Kulkarni AR, Sung HW. Targeted nanoparticles for drug delivery through the blood–brain barrier for Alzheimer's disease. Journal of controlled release. 2005 Nov 28;108(2-3):193-214.
54. Rivastigmine tartrate [Internet]. [Cited 2019 Nov 17] Available from: https://www.webmd.com/drugs/2/drug-18190-8218/rivastigmine-tartrate-oral/rivastigmine-oral/details
55. Rivastigmine tartrate [Internet].US national library for medicine [Cited 2019 Nov 17] Available from: https://pubchem.ncbi.nlm.nih.gov/compound/Rivastigmine-tartrate
56. Rivastigmine tartrate [Internet]. [Cited 2019 Nov 25] Available from: https://www.drugbank.ca/salts/DBSALT001252

57. FDA Rivastigmine tartrate [Internet] Exelon. [Cited 2019 Nov 25] Available from:https://www.accessdata.fda.gov/drugsatfda_docs/label/2000/21025lbl.pdf
58. Poloxamer 188 [Internet]. National Center for Biotechnology Information. PubChem Compound Database. U.S. National Library of Medicine; [Cited 2019Dec03].
Available from: https://pubchem.ncbi.nlm.nih.gov/compound/Poloxamer-188
59. Poloxamer 188 [Internet]. DrugBank. [Cited 2019Dec03]. Available from: https://www.drugbank.ca/drugs/DB11333
60. Tween 80 [Internet]. National Center for Biotechnology Information. PubChem Compound Database. U.S. National Library of Medicine. [Cited 2019Dec03]. Available from: https://pubchem.ncbi.nlm.nih.gov/compound/tween-80
61. Tween 80 [Internet]. DrugBank. [Cited 2019Dec03]. Available from: https://www.drugbank.ca/drugs/DB11063
62. Glyceryl mono sterate [Internet]. National Center for Biotechnology Information. PubChem Compound Database. U.S. National Library of Medicine. [Cited 2019Dec03]. Available from:
https://pubchem.ncbi.nlm.nih.gov/compound/Glyceryl-monostearate#section=Other-CAS
63. Glyceryl mono sterate [Internet]. DrugBank. [Cited 2019Dec03]. Available from: https://www.drugbank.ca/drugs/DB11250
64. Stearic acid [Internet]. National Center for Biotechnology Information. PubChem Compound Database. U.S. National Library of Medicine. [Cited 2019Dec03]. Available from:
https://pubchem.ncbi.nlm.nih.gov/compound/stearic_acid#section=Uses
65. Glyceryl tri sterate [Internet]. National Center for Biotechnology Information. PubChem Compound Database. U.S. National Library of Medicine. [Cited 2019Dec03]. Available from:
https://pubchem.ncbi.nlm.nih.gov/compound/Tristearin#section=2D-Structure
66. Coco mono ethanolamide [Internet]. National Center for Biotechnology Information. PubChem Compound Database. U.S. National Library of Medicine. [Cited 2019Dec03]. Available from
https://pubchem.ncbi.nlm.nih.gov/compound/coco mono ethanolamide

67. M Avachat A, M Oswal Y, N Gujar K, D Shah R. Preparation and characterization of rivastigmine loaded human serum albumin (HSA) nanoparticles. Current drug delivery. 2014 Jun 1;11(3):359-70.
68. N. Politis S, Colombo P, Colombo G, M. Rekkas D. Design of experiments (DoE) in pharmaceutical development. Drug development and industrial pharmacy. 2017 Jun 3;43(6):889-901.
69. Chowdary KP, Shankar KR, Kumar PS. Recent research on QbD approach in formulation development: A review. Int. J. Chem. Sci. & Tech. 2014;4(1):282-92.
70. Sangshetti JN, Deshpande M, Zaheer Z, Shinde DB, Arote R. Quality by design approach: Regulatory need. Arabian Journal of Chemistry. 2017 May 1;10:S3412-25.
71. Booka IA, Rao PB, Hamuli CP. Rajanrajan (2016) Design, Development and Optimization of Topotecan Hydrochloride Solid Lipid Nanoparticles for Oral Chemotherapy. J Nanomed Res.;3(1):00044.
72. Das S, Ng WK, Kanaujia P, Kim S, Tan RB. Formulation design, preparation and physicochemical characterizations of solid lipid nanoparticles containing a hydrophobic drug: effects of process variables. Colloids and surfaces B: biointerfaces. 2011 Nov 1;88(1):483-9.
73. Dhillon P, Mirza M, Anwer M, Alshetaili AS, Alshahrani SM, Iqbal Z. Development and optimization of erythromycin-loaded lipid-based gel by Taguchi design: In vitro characterization and antimicrobial evaluation. Brazilian Journal of Pharmaceutical Sciences. 2019;55.
74. Behbahani ES, Ghaedi M, Abbaspour M, Rostamizadeh K. Optimization and characterization of ultrasound assisted preparation of curcumin-loaded solid lipid nanoparticles: Application of central composite design, thermal analysis and X-ray diffraction techniques. Ultrasonics sonochemistry. 2017 Sep 1;38:271-80.
75. Patel M, Sawant K. A quality by design concept on lipid based nanoformulation containing antipsychotic drug: screening design and optimization using response surface methodology. J Nanomed Nanotechnol. 2017;8(3):1-1.
76. López-García R, Ganem-Rondero A. Solid lipid nanoparticles (SLN) and nanostructured lipid carriers (NLC): occlusive effect and penetration

enhancement ability. Journal of Cosmetics, Dermatological Sciences and Applications. 2015 Mar 20;5(02):62.

77. Joshi SA, Chavhan SS, Sawant KK. Rivastigmine-loaded PLGA and PBCA nanoparticles: preparation, optimization, characterization, in vitro and pharmacodynamic studies. European Journal of Pharmaceutics and Biopharmaceutics. 2010 Oct 1;76(2):189-99.
78. Kotikalapudi LS, Adepu L, VijayaRatna J, Diwan PV. Formulation and in vitro characterization of domperidone loaded solid lipid nanoparticles. Int J Pharm Biomed Res. 2012;3(1):22-9.
79. Vijaykumar O, Joe VF, Vishwanath BA. Formulation and evaluation of rivastigmine loaded polymeric nanoparticles. J Chem Pharm Res. 2014;6:556.
80. Ahmad I, Pandit J, Sultana Y, Mishra AK, Hazari PP, Aqil M. Optimization by design of etoposide loaded solid lipid nanoparticles for ocular delivery: Characterization, pharmacokinetic and deposition study. Materials Science and Engineering: C. 2019 Jul 1;100:959-70

ABSTRACT

Solid lipid nanoparticle (SLN) having an attracting importance for drug developer to produce intellectual property through innovations in drug delivery. The objective of present investigation was to develop, optimize and evaluate Rivastigmine tartrate loaded solid lipid nanoparticle (RT SLN) by using central composite design. SLN were prepared by microemulsion method using a systemic approach of design of experiments and evaluated. Various preliminary experiments were performed for selection of suitable excipients. Various lipids and surfactant are selected on the basis of solubility and particle size and thus glyceryl monosterate selected as lipid, and poloxamer 188 as surfactant. Further High speed homogenizer stirring speed and time was optimized HSH is operated at 15000 rpm for 5minutes.Characterization of RT SLN was carried out by infrared spectroscopy (FTIR), scanning electron microscopy (SEM), particle size and zeta potential, differential scanning calorimetry (DSC), entrapment efficiency, *in vitro* drug release and kinetics. Particle size of optimized formulation is 152.4 nm and PDI value 0.198 indicates mono dispersion. Optimized formulation with zeta potential -31.4 mV was found to be stable. Entrapment efficiency of optimized formulation is 76.1%. This condition has shown an improved response values in comparison with the previously optimized formulation. SEM photographs of RT SLN indicate particles have uniform loose aggregates, spherical in shape with a smooth surface and they are uniformly distributed. On comparison of *in vitro* drug release studies of RT solution and RT SLN shows that RT SLN has higher release 87.74% at 12 hrs compared to RT solution RT Solution 61.59%. From the obtained results it was concluded that the Rivastigmine Tartrate SLNs can be employed for controlled delivery of drug in the treatment of Alzheimer's disease.